

Rb-Sr GEOCHRONOLOGY AND Sr ISOTOPE SYSTEMATICS OF SOME  
MAJOR LITHOLOGIES IN CHANDOS TOWNSHIP, ONTARIO



By

LARRY M. HEAMAN, Hons. B.Sc.

A Thesis

Submitted to the School of Graduate Studies  
in Partial Fulfilment of the Requirements

for the Degree

Master of Science

McMaster University

November 1980

MASTER OF SCIENCE (1980)  
(GEOLOGY)

McMaster University  
Hamilton, Ontario

TITLE: Rb-Sr Geochronology and Sr Isotope  
Systematics of Some Major Lithologies  
in Chandos Township, Ontario.

AUTHOR: Larry M. Heaman, Hons. B.Sc. (University  
of Western Ontario)

SUPERVISORS: Dr. D.M. Shaw and Dr. R.H. McNutt

NUMBER OF PAGES: x; 141.

## ABSTRACT

The strontium isotopic composition of three major units in Chandos Township was investigated to determine the age of each unit and attempt to discern some geological enigmas associated with these rocks.

The Loon Lake pluton is composed of a monzonite core gradational to a quartz monzonite rim with subordinate isolated outcrops of diorite-gabbro and granodiorite gneiss. Separate Rb-Sr whole rock isochrons were determined for the monzonite ( $t=1052\pm 21$  Ma.;  $R_i=0.7036\pm 6$ ) and quartz monzonite ( $t=1071\pm 17$  Ma.;  $R_i=0.7034\pm 5$ ). Since these ages and initial strontium ratios ( $R_i$ ) are indistinguishable, the data from both units were combined to form a Loon Lake composite isochron ( $t=1065\pm 13$  Ma.;  $R_i=0.7034\pm 4$ ). The age determined from the composite isochron is interpreted as the time of emplacement of this pluton. The overlap in  $R_i$  favours a cogenetic relationship for these two units dominated by fractional crystallization but the extreme Rb enrichment in the quartz monzonites and the significant hiatus in the average  $\delta^{18}O_{WR}$  values (monzonite - 9.5 ‰; quartz monzonite - 11.0 ‰) are difficult to explain by this model. The relatively high range of  $\delta^{18}O_{WR}$  values for this pluton (8.8 to 12.0 ‰) and the low  $R_i$  reflect a source in the lower crust.

The Tallan Lake sill consists of an upper 180 meters of amphibolite which is transitional to a lower 80 meters of well foliated syenite. Strontium isotope results for samples from both horizons were combined in the regression treatment to yield a McIntyre III errorchron age of  $1225 \pm 50$  Ma. Although there is some uncertainty associated with this errorchron age, this data is interpreted to indicate the time of intrusion of the sill. This data is consistent with the contention that these rocks represent a consanguineous sequence which now forms part of a large scale nappe structure. A mantle derivation for this sill is supported by the low  $R_i$  ( $0.7031 \pm 7$ ).

A detailed strontium isotope study of the Apsley biotite gneiss indicated contrasting systematics between the "sodic" and "potassic" suites. The results from a regression treatment of five "sodic" Apsley gneiss samples indicated an isochron age of  $1402 \pm 57$  Ma. This age is interpreted as an average depositional age for the volcanic and sedimentary components of this unit thus the Apsley gneiss represents the oldest known rocks in this part of the Grenville Province. The low  $R_i$  for the sodic samples ( $0.7022 \pm 12$ ) provides additional evidence that the isotopic composition of this unit was not severely affected by Grenville metamorphism. On the other hand, the "potassic" Apsley gneiss shows open system behaviour.

## ACKNOWLEDGEMENTS

I wish to express my appreciation to Denis Shaw and Bob McNutt who provided guidance throughout this research and offered constructive criticism on earlier drafts of this dissertation. I am indebted to Denis Shaw for initiating the study, introducing me to the geology of Chandos Twp., and financial support for field work. I am equally indebted to Bob McNutt for introducing me to the "art" of solid source mass spectrometry and the arduous chemical procedure for separating strontium.

I would also like to thank Yuch-Ning Shieh who willingly analysed several samples for oxygen isotopes.

Various aspects of this thesis have benefited from discussions with Gary Beakhouse and Carlos Rapela: especially on the intricacies and limitations of trace element modeling and Rb-Sr geochronology.

Other members of the geology department contributed in various ways to the final form of this dissertation but special recognition should be given to Bob Bowins whose electronics and mass spectrometer expertise proved invaluable on many occasions.

Finally, I wish to express my gratitude to Marian Peirce for her continual encouragement and typing assistance.

## TABLE OF CONTENTS

		Page
CHAPTER I	INTRODUCTION	
	1.1 Location	1
	1.2 General Geology	1
	1.3 Previous Isotope Studies	4
CHAPTER II	ANALYTICAL PROCEDURES	
	2.1 Sample Collection and Crushing	10
	2.2 X-ray Fluorescence Spectroscopy	12
	2.3 Sample Dissolution and Cation Exchange Chemistry	12
	2.4 Mass Spectrometry	13
	2.5 Isotope Dilution	17
	2.6 Blanks	19
	2.7 Analytical Errors	21
	2.7.1 Accuracy	21
	2.7.2 Reproducibility	25
	2.8 Isochron Errors	28
CHAPTER III	SR AND O ISOTOPIC RESULTS FROM CHANDOS TOWNSHIP	
	3.1 Introduction to the Geology of Chandos Township	34
	3.1.1 Country Rocks	34
	3.1.2 Tallan Lake Sill	37
	3.1.3 Loon Lake Pluton	38
	3.1.4 Dikes	40
	3.2 Sr Isotopic Composition of the Apsley Biotite Gneiss	40
	3.2.1 Sodid Apsley Gneiss	41
	3.2.2 Potassic Apsley Gneiss	44
	3.2.3 Mineral Isochrons	49
	3.3 Rb-Sr Whole Rock Study of the Tallan Lake Sill	54
	3.4 Sr and O Isotopic Composition of the Loon Lake Pluton	57
	3.4.1 Rb-Sr Whole Rock Study	57
	3.4.2 Oxygen Isotope Data	62
CHAPTER IV	DISCUSSION	
	4.1 Introduction	66

4.2	Initial Strontium Ratios	66
4.2.1	Partial Melting in the Mantle	67
4.2.2	Partial Melting of Low Rb/Sr Crustal Rocks	68
4.2.3	Short Crustal Residence Histories	69
4.2.4	Disequilibrium Partial Melting	69
4.3	Initial Strontium Ratios From Chandos Township	74
4.4	Monzonite - Quartz Monzonite Association	77
4.4.1	Silica Metasomatism	78
4.4.2	Mixing - Assimilation	80
4.4.3	Separate Intrusions	83
4.4.4	Fractional Crystallization	85
4.5	Origin of the Loon Lake Pluton	91
CHAPTER V	SUMMARY	95
REFERENCES		98
APPENDIX A	DETAILED CHEMISTRY	
A.1	Sample Dissolution	111
A.2	Cation Exchange Columns	113
APPENDIX B	MAJOR AND TRACE ELEMENT DATA FOR THE LOON LAKE PLUTON	116
APPENDIX C	TRS-80 MICRO-PROCESSOR PROGRAMS	119

LIST OF TABLES

Table	Page
1.1 Previous Geochronological Studies Near Chandos Township	5
1.2 Stable Isotope Data From Chandos Twp. And Vicinity	8
2.1 Operating Conditions For The Mass Spectrometer, AAS, and XRF	11
2.2 Composition of Spikes and Shelf Solutions	14
2.3 Blanks Analysed During This Study	20
2.4 Trace Element Data For Standards Determined By XRF and Isotope Dilution	23
2.5 Accuracy of the Sr Isotopic Analyses	24
2.6 Precision of the Trace Element Data	26
2.7 Duplicates Analysed on the Mass Spectrometer	27
2.8 Two-Error Regression Parameters	29
2.9 Age and $R_i$ Calculations From Each Model For Units Which Indicate Geologic Error	32
3.1 Rb-Sr Data For the Apsley Gneiss	42
3.2 Rb-Sr Data For the Tallan Lake Sill	55
3.3 Sr and O Isotopic Data For the Loon Lake Pluton	59
4.1 Initial Strontium Ratio Calculations For Disequilibrium Partial Melting	73
4.2 Trace Element Partition Coefficients Used in Model Calculations	89
4.3 Trace Element Concentrations (ppm) in Melt and Cumulates	90
4.4 Granitoid Classification	92



## LIST OF FIGURES

Figure	Page
1.1 Location Map	2
3.1 Geology Map of Chandos Township	35
3.2 Rb-Sr Whole Rock Isochron Diagram For the Sodic Apsley Gneiss	43
3.3 Rb-Sr Whole Rock Isochron Diagram For the Potassic Apsley Gneiss	45
3.4 Apsley Gneiss Samples Selected For Slab Analyses	47
3.5 Rb-Sr Whole Rock Isochron Diagram For Slab Sections From the Apsley Gneiss	48
3.6 Mineral Isochron Diagram For the Sodic Apsley Gneiss	51
3.7 Mineral Isochron Diagram For Whole Rock Slabs of Potassic Apsley Gneiss	52
3.8 Rb-Sr Whole Rock Isochron Diagram For the Tallan Lake Sill	56
3.9 Rb-Sr Whole Rock Isochron Diagrams For the Loon Lake Monzonite and Quartz Monzonite	60
3.10 Composite Rb-Sr Whole Rock Isochron Diagram For the Loon Lake Pluton	61
3.11 Rb-Sr Whole Rock Isochron Diagram For the Granodiorite Gneiss	63
3.12 Oxygen Isotope Data For the Loon Lake Pluton, Apsley Gneiss, and Normal Granitoids	65
4.1 The Effect Of Non-Modal Partial Melting On $R_i$ Values	72
4.2 Strontium Evolution Diagram For the Apsley Gneiss, Tallan Lake Sill, and Loon Lake Pluton	75
4.3 K-Rb Variation Diagram For the Loon Lake Monzonites and Quartz Monzonites	81

Figure

4.4	TiO <sub>2</sub> -Zr Variation Diagram For the Loon Lake Monzonites and Quartz Monzonites	84
4.5	Log Rb - Log Sr Variation Diagram For the Loon Lake Suite	87
4.6	Evolution Of the Loon Lake Monzonites In the "Granite" Quaternary System	88
5.1	Summary Of Ages Obtained From Rock Units In the Hastings Basin and Vicinity	96
A.1	Sample Location Map	141

CHAPTER I  
INTRODUCTION

1.1 Location

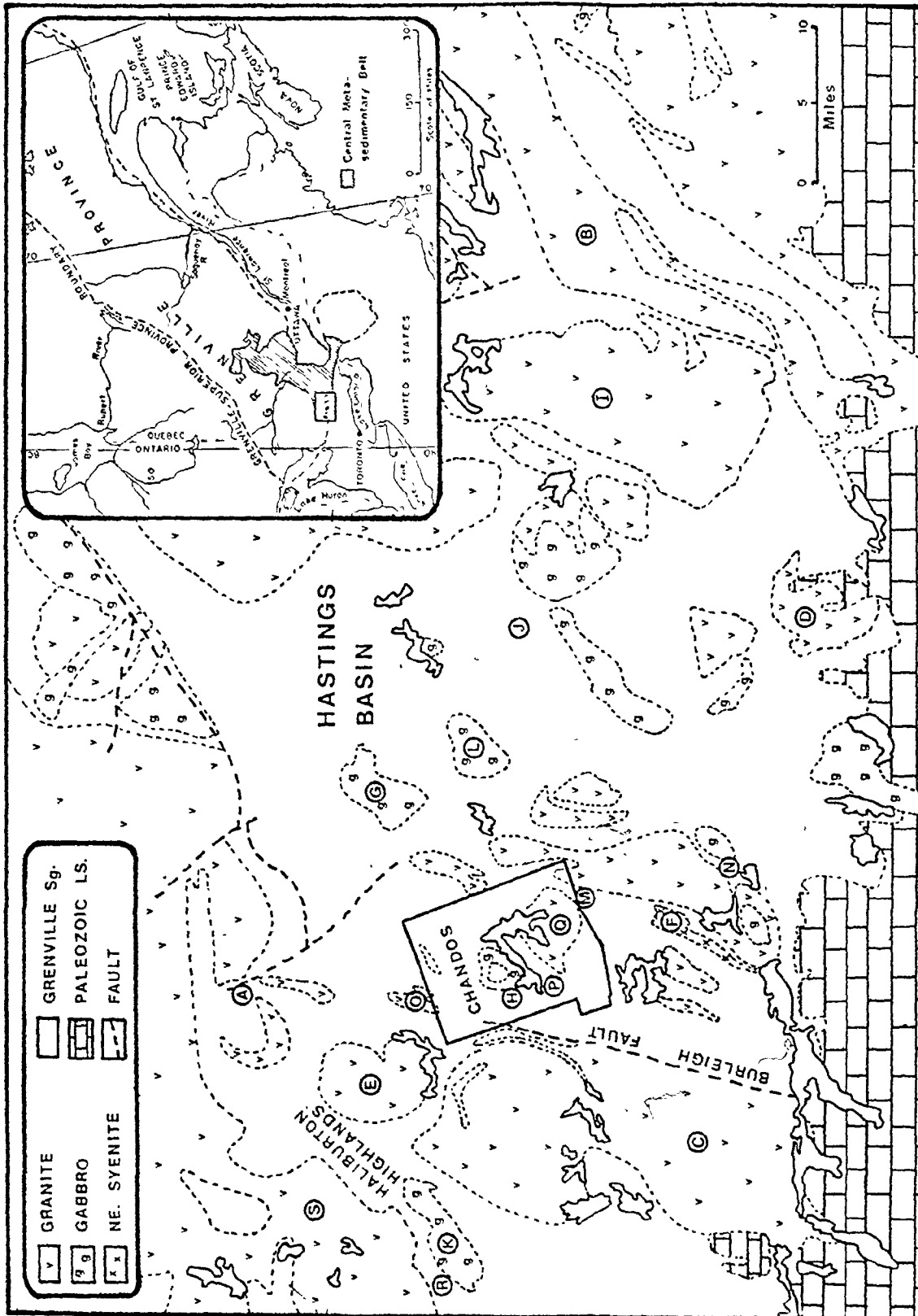
The area chosen for study is located within Chandos Township, Peterborough County, Ontario (Fig. 1.1). Most of the local relief is gentle undulating terrain with a maximum elevation contrast of 75 meters. Low lying regions are often occupied by swamps or lakes, hence the best outcrop exposures are along lakeshores and roadcuts.

1.2 General Geology

The rocks of Chandos Twp. constitute a small portion of the Central Metasedimentary Belt in the Grenville Structural Province (Wynne-Edwards, 1972). This belt can be traced for approximately 400 kilometers in a SSW-NNE direction (Fig. 1.1, inset) and consists primarily of intercalated marbles, calc-silicates, quartzo-feldspathic gneisses, and amphibolites of the Grenville Supergroup. This supracrustal sequence has been subsequently invaded by numerous igneous bodies of various composition and geometry (Wynne-Edwards, 1972).

Previous reconnaissance studies in the SW portion of the belt (Hewitt, 1956; Lumbers, 1967; Wynne-Edwards, 1972) have distinguished two types of terrain:

- (a) Haliburton Highlands - a high grade meta-



MODIFIED AFTER HEWITT (1956)

FIG. 1.1

morphic terrain dominated by mantled gneiss domes. It is bounded to the east by the Burleigh fault (Fig. 1.1).

- (b) Hastings Basin - this region consists predominantly of greenschist facies supracrustal rocks corresponding to the Grenville Supergroup. The grade of metamorphism increases to middle amphibolite facies near the fault controlled NW margin.

Stratigraphic correlation within the Hastings Basin is complicated by the lack of recognizable marker horizons, absence of sedimentary structures in the high grade domains, and complex folding (Lumbers, 1967; Shaw, 1972). A regional correlation has been attempted by Lumbers (1967) but in view of the limitations mentioned above, this correlation is quite tenuous.

The two prevailing stratigraphic units in the vicinity of Chandos Twp. are the Hermon and Mayo Groups. The former is characterized by abundant metavolcanic members which are believed to be lower in the stratigraphic sequence than the metasedimentary members of the Mayo Group (Lumbers, 1967).

Detailed descriptions of individual formations have been published elsewhere (Adams and Barlow, 1910; Hewitt, 1956; 1957; 1961; Simony, 1960; Shaw, 1962; Lumbers, 1967; Laasko, 1968; and Jennings, 1970) and the relevant

information from these studies will be discussed in the following chapters.

### 1.3 Previous Isotopic Studies

Many of the early isotopic studies in the Grenville Province, initiated by the Geological Survey of Canada, employed the K-Ar mineral technique for age determinations (Aldrich et al., 1958; Lowdon, 1960; MacIntyre et al., 1967). Eventually, it was recognized that this data did not record the age of intrusive events but represented the time when a particular mineral phase passed through its "blocking temperature" (Hurley et al., 1962). Furthermore, other radiometric studies using the U-Pb zircon and Rb-Sr whole rock methods indicated that the corresponding K-Ar ages were ca. 200 Ma. lower.

Harper (1967) attempted to synthesize all the K-Ar data by contouring the ages obtained from biotite separates. He interpreted the increase in K-Ar biotite ages towards the Grenville front to represent the progressive uplift of the Grenville craton through an isothermal plane.

Subsequently, there have been numerous radiogenic isotope studies in the Grenville Province and a summary of the geochronological studies near Chandos Twp. (excluding the K-Ar age determinations) is presented in Table 1.1. The location of specific studies are delineated in Figure 1.1 by letters corresponding to the results in Table 1.1.

Table 1.1 Previous geochronological studies near Chandos Township

Rb-Sr Whole Rock

<u>Map Code</u> *	<u>Location</u>	<u>Rock Type</u>	<u>Age (Ma)</u>	<u>Initial Ratio</u>	<u>Reference</u>
A	Bicroft Mine	Pegmatite	959±15	0.7054	1,8
B	Kaladar	Granite Gneiss	1013±60	0.7110	2
C	Burleigh Falls	Granite Gneiss	1080±39	0.7046	2
D	Deloro	Granite	1096±48	0.7036	3,7
E	Cheddar	Granite	1181±51	0.6909	1,8
F	Blue Mountain	Ne. Syenite	1258±41	0.7041	2
G	Umfraville	Gabbro		0.7025	2
H	Tallan Lake	Marble (skarn)		0.7056	4

U-Pb Zircon

<u>Map Code</u> *	<u>Location</u>	<u>Rock Type</u>	<u>Age (Ma)</u>	<u>Reference</u>
G	Umfraville	Syenite	1157±20	5,9
I	Elzevir	Granite	1226±25	5,7
J	Burnt Lake	Metarhyolite	1226±25	10,11
J	Tudor	Metarhyolite	1286±15	5,7

<sup>40</sup>Ar-<sup>39</sup>Ar

<u>Map Code</u> *	<u>Location</u>	<u>Rock Type</u>	<u>Age (Ma)</u>	<u>Reference</u>
K	Glamorgan	Gabbro(Hb)**	980	6
L	Thanet	Gabbro(Hb,Bio)**	1200,1090	6

Note: Ages are re-calculated using the revised decay constants (Steiger and Jäger, 1977)

\* See Fig. 1.1

\*\* (Hb) - Hornblende separate; (Bio) - Biotite separate

## References

- 1 Fowler and Doig (1979)
- 2 Krogh and Hurley (1968)
- 3 Wanless and Loveridge (1972)
- 4 Gittins et al. (1969)
- 5 Silver and Lumbers (1965)
- 6 York (1979)
- 7 Davidson et al. (1979)
- 8 Fowler (1980)
- 9 Syrons (1978)
- 10 Baer (1976)
- 11 Lumbers (1967)

To facilitate comparison of data from previous studies with the results from this thesis, all Rb-Sr whole rock and U-Pb zircon age determinations in Table 1.1 have been recalculated using the revised decay constants for  $^{87}\text{Rb}$  ( $\lambda=1.42 \times 10^{-11} \text{ yr.}^{-1}$ ) and U ( $\lambda_{238}=1.55125 \times 10^{-10} \text{ yr.}^{-1}$  and  $\lambda_{235}=9.8485 \times 10^{-10} \text{ yr.}^{-1}$ ). These decay constants were approved by the I.U.G.S. Subcommittee on Geochronology for interlaboratory standardization (Steiger and Jager, 1977).

Most of the U-Pb zircon age determinations in the Hastings Basin have been summarized by Silver and Lumbers (1965). They distinguished two major periods of igneous activity ca. 1240 and 1115 Ma. (revised ages) which they suggest coincide with two major pulses of the Grenville orogeny. There is only one published age determination for the Grenville Supergroup in the Hastings Basin, a U-Pb zircon age of  $1286 \pm 15$  Ma. for a metarhyolite flow from a lower section of the Tudor volcanics (Silver and Lumbers, 1965).

The grouping of igneous activity defined by U-Pb zircon ages is supported by Rb-Sr whole rock studies east of the Elzevir batholith (J.M. Moore, personal communication). However, the Rb-Sr data indicates a period of younger activity with emplacement of small plutons and dikes ca. 950-1050 Ma. (Krogh and Hurley, 1968; Wanless and Loveridge, 1972). Some of the Rb-Sr whole rock studies which lack sufficient isotopic data (ie. the two point isochron



for the Ridge granite; Krogh and Hurley, 1968) or show a significant scatter in the data (e.g. the Rb-Sr whole rock errorchron for the Deloro pluton; Wanless and Loveridge, 1972) should be interpreted with extreme caution.

Rb-Sr whole rock analyses of marbles from the Grenville Supergroup (Gast, 1960; Krogh and Hurley, 1968; Gittins et al., 1969) indicate a range of initial strontium ratios from 0.7048 to 0.7084. There is some evidence that marbles in contact with intrusive bodies are enriched in radiogenic strontium (Gittins et al., 1969) so only the lower values are considered representative of Precambrian carbonates deposited ca. 1300 Ma. (Veizer and Compston, 1976a).

Stable isotope studies in the Hastings Basin encompass a reconnaissance oxygen and carbon isotope study of marbles (Sheppard, 1966; Sheppard and Schwarcz, 1970), a regional oxygen isotope study of granites and migmatites (Shieh and Schwarcz, 1974; Shieh, 1980), and a more detailed oxygen and carbon isotope investigation in Chandos Twp. (Shieh et al., 1976). A compilation of this data is presented in Table 1.2 and can be summarized as follows:

- (a) The average oxygen and carbon isotopic compositions of Grenville marbles in Chandos Twp. ( $\delta^{18}\text{O} = 26.6 \text{ ‰}$ ;  $\delta^{13}\text{C} = 3.0 \text{ ‰}$ ) are in the upper range of marine carbonates (Shieh et al., 1976). Samples which show a

Table 1.2 Stable isotope data from Chandos Township and vicinity

Map Code†	Location	Rock Type	WR	Ct	Dol	$\frac{18O(^{18}O)}{QZ}$	Bio	Feld	Mt	$\frac{13C(^{13}C)}{Dol}$	Reference
M	Lasswade	Marble		17.7	17.6					4.55	1
H	Lasswade	Marble		25.2-27.8						2.4-3.7	3
N	Methuen	Marble		18.5						0.64	1
C	Burleigh Falls	Granite Gneiss	8.8			8.9-11.0	8.0-10.0				2
O	Silent Lake	Trondhjemite	12.3					12.5	3.1		2
		Quartz Monzonite				13.2					2
P	Apsey	Paragneiss	8.3-16.9*			11.2-16.5	6.0-11.5		3.8-6.4		3
Q	Chandos Lake	Quartz Monzonite	8.9-13.9*			9.9-14.4	4.9-8.7	11.7-15.4	0.4-3.9		3
Q	Chandos Lake	Monzonite	8.9- 9.7*			11.7	5.5-6.8	9.9-10.7	1.4-2.8		3
R	Glamorgan	Paragneiss	6.8- 7.8			8.5-9.7	3.9-5.0		0.1-0.9		2
S	Glamorgan	Granite Gneiss	6.9- 7.9			7.8-11.0	2.2-6.3		-0.9-1.3		2

WR = whole rock Ct = calcite Dol = dolomite Qtz = quartz Bio = biotite Feld = feldspar Mt = magnetite

† See Fig 11

\* whole rock values estimated

References

- 1 Sheppard and Schwarz (1970)
- 2 Shieh and Schwarz (1974)
- 3 Shieh et al. (1976)

depletion in the heavy isotopes were collected near or within intrusive bodies and may have suffered decarbonation reactions or isotopic exchange with the intrusion.

- (b) The oxygen isotopic composition of igneous rocks in the Hastings Basin is more variable (7.0 to 16.5 ‰; Shieh, 1980) than the range for intrusive rocks from the Haliburton Highlands (6.0 to 9.0 ‰; Shieh and Schwarcz, 1974).

CHAPTER II  
ANALYTICAL PROCEDURES

2.1 Sample Collection and Crushing

Fresh hand samples or composite chip samples weighing between 5 and 20 kilograms were collected from outcrops that were visibly devoid of veins, extreme weathering, or faulting. A suite of samples were collected from each unit to obtain a variable range in the Rb/Sr ratio.

The samples were prepared for crushing by removing all weathered surfaces with a hammer. Approximately one half of the sample was retained for thin sectioning while the remainder was passed through three pulverizing stages:

- (1) Jaw Crusher - hand samples reduced to 2-4 cm<sup>3</sup> chips
- (2) Ceramic Disk Grinder - sample reduced to 1 cm<sup>3</sup> chips
- (3) Tungsten-Carbide Beuler - sample reduced to a fine powder

The samples were stored in clean 250 ml. polypropylene containers. All metal parts of the jaw crusher were cleaned with a wire brush and subsequently rinsed with acetone after each sample. The other crushing equipment was cleaned with air and acetone.

Table 2.1 Operating conditions for mass spectrometer, AAS, and XRF

	<u>Sr</u>	<u>Rb</u>
<u>Mass Spectrometer</u>		
Ionization current (amps)		
Wide Ta filament(0.03x0.001mm)	2.5	
Narrow Ta filament(0.02x0.001mm)	1.8	1.0
Ionization voltage (volts)		
	ca. 1.0	ca. 0.3
Accelerating voltage (mass 88)		
	5540	5580
Magnetic field strength (gauss)		
	4015	4015
Range on VRE (volts)		
	1	0.300-3
Input resistor (ohms)		
	10 <sup>11</sup>	10 <sup>11</sup>
Count/delay time (seconds)		
	10/5	1/3
<u>Atomic Absorbtion Spectroscopy</u>		
Wavelength (nm)		
	230	390
Slit setting (nm)		
	1.4	4.0
Light source		
	electrodeless discharge	hollow cathode
Flame		
	air-C <sub>2</sub> H <sub>2</sub>	air-C <sub>2</sub> H <sub>2</sub>
Burner head		
	3-slot	3-slot
Fuel/oxidant <sup>†</sup>		
	45/70	45/70
Filter		
	-	red
Na buffer		
	no	no
<u>X-ray Fluorescence Spectroscopy</u>		
Program		
	Rb-Sr	Rb-Sr-Y-Zr-Nb
Voltage (Kv)		
	80	50
Current (mA)		
	30	50
Target		
	Mo tube	W tube
Crystal		
	LiF 200	LiF 200
Collimnator		
	fine(15mm)	fine(15mm)
Counter		
	scintillation	scintillation
Count time (seconds)		
	40	20
Spinner		
	on	on
PHA		
	yes	yes

† Acetylene/Oxygen

## 2.2 X-ray Fluorescence Spectroscopy

Trace element concentrations were determined for each sample using a Phillips PW 1450 automated XRF. The operating conditions for each program used in this study are outlined in Table 2.1.

All trace element analyses were obtained on powder pellets. These pellets were prepared by combining the sample powder (3 to 4 grams) with 3 drops of Mowiol binding solution in a 5 dram glass vial. This mixture was loaded into chemplex aluminium pellet cups and compressed to 20 tons pressure in a Spex 30 ton press.

Preliminary analyses for Rb, Sr, Y, Nb, and Zr (Table 2.1) were used to select 6 to 12 samples from each unit with sufficient Rb/Sr variation for isochron analysis. Triplicate powder pellets were prepared for each selected sample and analysed for Rb and Sr concentrations following the Mo-Compton peak method (Rb-Sr program; Table 2.1) described by Reynolds (1963; 1967) and Turek et al. (1977). The Rb/Sr ratios were determined as ratios of the total corrected peak counts (Doering, 1968; Marchand, 1973).

## 2.3 Sample Dissolution and Cation Exchange

The samples selected for isotopic analyses were prepared for strontium isolation following the procedure outlined in Appendix A (see Beakhouse and Heaman, 1980). This procedure is similar to that of Gibbins (1972) and

includes the modifications described by Birk (1977). New acid digestion bombs with metal retaining jackets (Parr model #4745) allowed sample dissolution at higher temperatures (135 °C) without loss of vapor.

Samples prepared for isotope dilution analyses were double spiked with isotopically enriched  $^{87}\text{Rb}$  and  $^{84}\text{Sr}$  solutions and then processed following the procedure in Appendix A. The isotopic composition and concentration of the spike solutions are presented in Table 2.2.

The relative concentrations of Rb and Sr in the cation exchange column discharge was determined by atomic absorption spectroscopy (AAS). The operating conditions for the analysis of Rb and Sr by AAS are tabulated in Table 2.1.

#### 2.4 Mass Spectrometry

Strontium isotopic ratios plus Rb and Sr concentrations for whole rock samples and mineral separates were determined using a single filament, 10 inch, 90° sector, Nier-type mass spectrometer (SS-2 McMaster Geochronology Lab). A detailed description of the hardware and loading procedures for this mass spectrometer has been presented by Wolff (1977a; b).

Prior to loading the sample onto a pre-conditioned button, the tantalum filament was etched with one drop of 1.0 M  $\text{H}_3\text{PO}_4$ . The sample was dissolved in double distilled

Table 2.2 Composition of spikes and shelf solutions

 $^{84}\text{Sr}$  spike

Sr concentration	9.80 $\mu\text{g}/\text{ml}$
Atomic fraction <sup>1</sup>	$^{84}\text{Sr} = 0.99892$ ; $^{86}\text{Sr} = 0.00059$ $^{87}\text{Sr} = 0.00010$ ; $^{88}\text{Sr} = 0.00039$

Sr shelf solution

Sr concentration	40.78 $\mu\text{g}/\text{ml}$
Atomic fraction <sup>2</sup>	$^{84}\text{Sr} = 0.0056$ ; $^{86}\text{Sr} = 0.0997$ $^{87}\text{Sr} = 0.0704$ ; $^{88}\text{Sr} = 0.8253$

 $^{87}\text{Rb}$  spike

Rb concentration	16.27 $\mu\text{g}/\text{ml}$
Atomic fraction <sup>3</sup>	$^{87}\text{Rb} = 0.99151$ ; $^{85}\text{Rb} = 0.00849$

Rb shelf solution

Rb concentration	26.86 $\mu\text{g}/\text{ml}$
Atomic fraction <sup>2</sup>	$^{87}\text{Rb} = 0.2783$ ; $^{85}\text{Rb} = 0.7217$

- 1 NBS certificate for reference material 988
- 2 Faure (1977)
- 3 Measured in this study



H<sub>2</sub>O then three successive drops of this solution were loaded onto the filament and allowed to dry under an infra-red heat lamp. The button was loaded into the mass spectrometer following the procedure outlined by Wolff (1977a) then degassed at a current of 1.0 ampere when the vacuum was less than 10<sup>-5</sup> torr. Degassing under poor vacuum (<10<sup>-5</sup> torr) is not recommended as extreme oxidation weakens the filament and it may deform at higher temperatures.

To prepare for normal strontium isotope data collection, the Sr beam was located on the 10 mvolt range of the vibrating reed electrometer (VRE) and allowed to stabilize for 0.5 to 1.0 hour. If there was any peak detected at mass 85 then these conditions were maintained until all the Rb had been vaporized. The ionization current was then gradually increased until the <sup>88</sup>Sr peak registered on the 1 volt range of the VRE.

The operating conditions for the two filament sizes used in this study are outlined in Table 2.1. For most analyses, wide tantalum filaments were used and individual runs routinely consisted of 150 to 200 scans over three strontium peaks (mass 88,87,86). Most of the data reported in this study were collected when the strontium beam was growing at a slow and steady rate (ie. ~ 200 counts/sec. for the <sup>88</sup>Sr peak). Whole rock samples with less than 50 ppm strontium and samples to be analysed

by isotope dilution were loaded onto narrow tantalum filaments to increase the run duration.

Isotopic analyses during the winter months were very stable and operating vacuums between 5 and  $8 \times 10^{-8}$  torr could be achieved consistently by "baking" the source with heating coils between runs. Analyses during the summer months were hindered by the high humidity conditions in the laboratory.

The source was cleaned with methanol every 4 to 6 weeks during continuous operation and not disassembled in order to preserve the source plate geometry.

Two major modifications on the mass spectrometer were made during this study. The first involved interfacing a TRS-80 (Radio Shack Corp.) micro-processor to facilitate automated magnetic field strength switching and on-line data calculations. A copy of the raw data and calculations were recorded on a teletype which allowed the operator to monitor the emission behaviour of the sample at the end of each data block (10 to 30 scans). Four programs were written for the micro-processor in Level II basic (Appendix C):

- (1) Strontium isotope data collection and ratio calculations
- (2) Strontium isotope data collection for isotope dilution (ID) analyses
- (3) Strontium ratio and concentration calculations

for ID data

- (4) Rubidium isotope data collection and calculations for ID analyses

A brief explanation of each program is included in Appendix C.

The second modification eliminated the abundant high frequency voltage surges in the main power line which were detected on the VRE and digital voltmeter. A separate main power supply line was installed which was free of any extraneous signals.

## 2.5 Isotope Dilution

In many geochronological studies, isotope dilution analyses have been replaced by the more rapid XRF method for determining the Rb/Sr ratio of a sample. However, isotope dilution is very useful for determining precisely the trace element concentrations in small sample aliquots (ie. mineral separates) or in samples with extremely low or high Rb and Sr concentrations. The theory of isotope dilution is covered by Faure and Powell (1972) and Faure (1977) and will not be developed here.

To analyse Sr by isotope dilution, data was collected at five mass positions (88 to 84 inclusive) on  $^{84}\text{Sr}$  spike - sample mixtures using program 2 (Appendix C). This data was stored on cassette tapes and later reloaded into program 3 (Appendix C) to simultaneously calculate the

strontium concentration and isotopic ratio for each sample. Programs 2 and 3 were not combined so as to maximize the amount of data collected per sample.

Rubidium analyses were determined on  $^{87}\text{Rb}$  spike-sample mixtures using a single tantalum filament assembly (see Table 2.1 for operating conditions). To monitor extreme fractionation effects, the Rb data was collected at three ionization temperatures (300 mV, 1 V, and 3 V range on the VRE) but the measured ratios did not vary by more than  $\pm 2\%$ .

The  $^{84}\text{Sr}$  and  $^{87}\text{Rb}$  spikes used in this study were obtained from the Oak Ridge National Laboratory. The isotopic composition of the  $^{84}\text{Sr}$  spike used in the ratio calculations is that reported by the National Bureau of Standards for reference material 988 (Table 2.2). The isotopic composition of the  $^{87}\text{Rb}$  spike reported in Table 2.2 was measured directly on the mass spectrometer.

Rubidium and strontium shelf solutions, for calibration of the spikes, were prepared by dissolving known quantities of Johnson Matthey "specpure"  $\text{RbCl}$  and  $\text{Sr}(\text{NO}_3)_2$  in 50 ml of 2.5 N  $\text{HCl}$ . These shelf solutions were quantitatively combined with the corresponding spike solution and the isotopic composition of the mixtures analysed on the mass spectrometer. The concentration of the spike solutions (Table 2.2) were calculated from the expression:

$$S = \left[ \frac{N \times W_n \times C_n}{W_s} \right] \times \left[ \frac{(Ab_n^B \times R_m) - Ab_n^A}{Ab_n^A - (R_m \times Ab_n^B)} \right] / WR$$

Where: N = weight of shelf solution  
 C<sub>n</sub> = concentration of shelf solution  
 W<sub>n</sub> = atomic weight of an element in the shelf solution  
 W<sub>s</sub> = atomic weight of an element in the spike solution  
 R<sub>m</sub> = measured isotopic ratio (A/B)  
 WR = weight of spike solution  
 Ab<sub>n</sub><sup>A</sup> = abundance of isotope A in the shelf solution  
 Ab<sub>s</sub><sup>A</sup> = abundance of isotope A in the spike solution

## 2.6 Blanks

Total blanks for the complete analytical procedure were determined by processing a measured quantity of spike solution in place of a sample. The total Sr blanks determined in this study (Table 2.3) are comparable to values previously reported for 100 mg samples by this laboratory (e.g. Gibbins, 1973 - 16 ng; Wolff, 1977b - 15 ng; and Birk, 1977 - 33 ng). These relatively low total Sr blanks do not significantly alter the strontium isotopic ratios determined for whole rock samples with greater than 10 ppm Sr so a Sr blank correction was not necessary.

Individual reagent blanks for Sr were also determined (Table 2.3) and collectively account for most of the total Sr blank.

One total Rb blank (Table 2.3) determined in this study is relatively high compared to other laboratories

Table 2.3 Blanks analysed during this study

<u>Total Blanks</u> <sup>1</sup>	<u>Sr</u>	<u>Rb</u>
6/05/79	32 ng	
21/09/79	6 ng	
8/02/80		85 ng

Reagent Blanks<sup>2</sup>

HF	1.6 ng
H <sub>2</sub> O	0.7 ng
HCl*	1.1 ng
HNO <sub>3</sub> *	3.2 ng

<sup>1</sup> Total blanks determined for 250 mg samples

<sup>2</sup> Values reported per ml

\* Analysed by G. Beakhouse

(e.g. Peterman et al., 1967 - 20 ng; Chappell et al., 1969 - 11 ng; Menzies et al., 1978 - 0.1 ng; and Wooden and Goodwin, 1980 - 1.0 ng) but the source of this Rb contamination is uncertain. Therefore, a Rb blank correction was applied to all the Rb analyses reported in chapter 3.

## 2.7 Analytical Errors

In order to evaluate the error associated with a particular analytical method it is essential to determine the accuracy and reproducibility (precision) of the total procedure. In the following discussion the error associated with the Rb and Sr elemental data includes the accuracy and precision of the XRF analyses plus sample inhomogeneity. The error in the isotopic analyses include the reproducibility of the total chemical procedure and the mass spectrometer analyses.

### 2.7.1 Accuracy

Detailed analyses of several U.S.G.S. standards determined by isotope dilution (Compston et al., 1969; De Laeter and Abercrombie, 1970; Fairburn and Hurley, 1971; Pankhurst and O'Nions, 1973) and a compilation of XRF analyses (Abbey, 1977) provide the best references for evaluating the accuracy of trace element and isotopic analyses. A comparison of trace element data determined by XRF in this study for two U.S.G.S. standards (G-2 and GSP-1) with the corresponding values reported by Abbey (1977) is

presented in Table 2.4. The Rb and Sr data from this study agree within 2% of the values reported by Abbey (1977). The Rb/Sr ratios, determined by the Mo-Compton peak method deviate by less than 1% from Abbey's data (Table 2.4).

Rubidium and strontium concentrations determined for these same two standards by isotope dilution (Table 2.4) are not as accurate as the XRF results. If these isotope dilution results are compared to the analyses of Pankhurst and O'Nions (1973), the error in the Sr data is less than 2%. The isotope dilution data for Rb on standard G-2 is very close to the value reported by Pankhurst and O'Nions (1973) but the Rb data for GSP-1 deviates by more than 8%. This large deviation may reflect the poor control on fractionation of Rb isotopes using a single filament assembly.

The accuracy of the strontium isotopic analyses was determined on three analyses of the Eimer and Amend  $\text{SrCO}_3$  standard (Table 2.5). The average value of these three analyses ( $0.70806 \pm 5$ ) agrees within 0.01% of the value assigned to this standard (0.70800). These analyses plus the results for the NBS 987 standard ( $\pm 0.03\%$ ) reflects only the accuracy of the mass spectrometer analyses. To determine the accuracy of the total procedure for isotopic analyses, two standards (G-2 and GSP-1) were passed through all stages of the procedure. The results for GSP-1 (Table 2.5) are in close agreement ( $\pm 0.01\%$ ) with the data



Table 2.4 Trace element data for standards determined by XRF and isotope dilution

<u>XRF</u>	<u>Rb</u>	<u>Sr</u>	<u>Rb/Sr</u>	<u>Reference</u>
G-2*	167	473	0.3536	
	170	480	0.3542	1
GSP-1	247	229	1.0815	
	250	230	1.0869	1
<u>Isotope Dilution</u>				
G-2	170	484	0.3512	
	169	475	0.3558	2
GSP-1	268	238	1.1261	
	255	235	1.0910	2

\* Average of three analyses

1 Abbey (1977)

2 Pankhurst and O'Nions (1973)

Table 2.5 Accuracy of the Sr isotopic analyses

<u>Date</u>	<u>Standard</u>	$^{87}\text{Sr}/^{86}\text{Sr}^*$	<u>1<math>\sigma</math></u>	<u>Peak Scans</u>	<u>Published Values</u>
27/01/79	E + A	0.70795	0.00024	90	
13/03/79	E + A	0.70813	0.00017	90	
21/06/79	E + A	0.70809	0.00014	90	0.70800
		Mean 0.70806 $\pm$ 0.00005			
09/11/79	NBS 987	0.71036	0.00013	110	0.71014 <sup>1</sup>
					0.71039 <sup>2</sup>
02/02/80	GSP-1	0.76874	0.00011	130	0.7688 <sup>2</sup>
11/02/80	G2	0.71028	0.00020	80	0.7097 <sup>2</sup>

\* All  $^{87}\text{Sr}/^{86}\text{Sr}$  data normalized to 0.1194.

1 NBS certificate

2 Pankhurst and O'Nions (1973)

published by Pankhurst and O'Nions (1973) but the isotopic data for G-2 has a much greater deviation ( $\pm 0.08\%$ ). Only one analyses of G-2 was attempted so the large error may reflect a poor mass spectrometer run and/or contamination of the standard.

### 2.7.2 Reproducibility

The precision of the Rb and Sr data reported in Appendix B was calculated on three analyses of the standard G-2 (Table 2.6) using the Rb-Sr XRF program. These results indicate that the precision of the Rb, Sr, and Rb/Sr data using the Mo-Compton peak method (Turek et al., 1977) is better than  $\pm 1.0\%$ . The precision for the total analytical procedure to determine the Rb/Sr ratios was determined from an average of all samples analysed in triplicate. A blanket error of 1.0% for all Rb/Sr ratios was considered a generous estimate and hence used in the isochron error calculations (section 2.8).

Two standards (G-2 and JG-1) were repeatedly analysed with the Rb-Sr-Y-Zr-Nb program (Table 2.6) and the error in the Y, Zr, and Nb data is generally less than 15%.

A total of eight samples were analysed in duplicate for the strontium isotopic ratio on the mass spectrometer SS-2 in the period 1978 - 1980 by three separate analysts (Table 2.7). The average error for these analyses is

Table 2.6 Precision of trace element data

	<u>Analyses</u>				<u>Mean</u>	<u>% Error<sup>a</sup></u>	<u>Published Values<sup>b</sup></u>
	<u>1</u>	<u>2</u>	<u>3</u>	<u>4</u>			
G-2*							
Rb	167	168	166		167	0.6	170
Sr	469	475	474		473	0.7	480
Rb/Sr	0.35548	0.35471	0.35064		0.35361	0.7	
Date	22/02/79	13/12/79	13/12/79				
G-2							
Y	12	12	15	11	13	14.0	12
Zr	311	306	323	326	317	3.0	300
Nb	17	17	16	20	18	10.1	19
Date	02/08/79	02/08/79	20/08/79	20/08/79			
JG-1							
Y	27	35	27		30	15.4	31
Zr	174	112	179		155	24.1	110
Nb	10	14	17		14	25.3	-

\* Using Mo-Compton peak program  
 b Abbey (1977)

$$^a \text{ \% Error} = \left[ \left[ \frac{\sum (x - \bar{x})^2}{N - 1} \right]^{1/2} \right] \div \bar{x} \times 100$$

Table 2.7 Duplicates analysed on the mass spectrometer

<u>Analyst</u>	<u>Sample</u>	<u>(<sup>87</sup>Sr/<sup>86</sup>Sr)*</u>	<u>1σ</u>	<u>Scans</u>	<u>(<sup>87</sup>Sr/<sup>86</sup>Sr)</u>	<u>% Error</u>
1	LL8	0.73474	0.00026	100	0.73454	0.027
		0.73434	0.00015	130		
1	LL27	0.72029	0.00022	80	0.72052	0.032
		0.72075	0.00013	170		
1	TL12	0.74639	0.00007	120	0.74654	0.019
		0.74668	0.00009	120		
1	D1	0.76161	0.00019	200	0.76138	0.030
		0.76115	0.00020	140		
2	R-5	0.71411	0.00008	240	0.71388	0.032
		0.71364	0.00015	200		
2	R-52	0.72733	0.00016	60	0.72316	0.004
		0.72739	0.00013	130		
2	R-70	0.72327	0.00011	200	0.72316	0.015
		0.72305	0.00008	130		
3	CR	0.70855	0.00007	130	0.70863	0.011
		0.70870	0.00009	80		

1 - L. Heaman

2 - G. Beakhouse

3 - C. Rapela

\* All ratios normalized to  $^{86}\text{Sr}/^{88}\text{Sr} = 0.1194$ \* Error calculated from  $[((x_1 - x_2)/2)/\bar{x}] \times 100$

$\pm 0.02\%$  and this value was used as a blanket error for all whole rock Sr isotopic ratios.

## 2.8 Isochron Errors

A comprehensive review of the available two-error regression models for isochron error calculations is presented by Brooks et al. (1972). It is important to apply a rigorous statistical treatment to a linear data array on a  $^{87}\text{Sr}/^{86}\text{Sr}$  versus  $^{87}\text{Rb}/^{86}\text{Sr}$  diagram to determine if this array represents the time of some geological event. In the following discussions, the term isochron will refer to a regression line in which the data scatter is not in excess of experimental error. A regression line with data scatter in excess of experimental error is defined as an errorchron (Brooks et al., 1972). The theoretical cutoff between analytical and geological error is obtained from an F-distribution table which combines the number of samples regressed and the number of duplicates used in determining the experimental error. The suggested cutoff level of 2.5 or less (Brooks et al., 1972) was not practical in this study since only eight samples were analysed in duplicate.

A compilation of the two-error regression parameters appropriate for this study are presented in Table 2.8 along with the statistical indices characteristic of each regression model (ie. MSWD, MSUM,  $\Sigma\chi^2$ ). A detailed description of each model and an explanation of the statistical

Table 2.8 Two-error regression parameters

<u>Unit Studied</u>	<u>Samples</u>	<u>F-Variate</u> <sup>a</sup>	<u>MSWD</u> <sup>*</sup>	<u>MSUM</u> <sup>*</sup>	<u><math>\Sigma X^2</math></u> <sup>*</sup>	<u>Regression Line</u> <sup>b</sup>
Loon Lake Pluton						
Monzonite	6	3.84	0.65	0.81	0.81	I
Qtz. Monzonite	8	3.58	3.14	1.77	1.77	I
Composite	14	3.28	2.79	1.69	1.69	I
Diorite	4	4.46	-	0.05	0.05	I
Composite +						
Diorite	18	3.19	2.23	1.49	1.49	I
Granodiorite						
Gneiss	4	4.46	17.40	4.17	4.17	E
Apsley Gneiss	6	3.84	10.48	3.25	3.24	E
Tallan Lake Sill	6	3.84	9.61	3.14	3.14	E

<sup>a</sup> Number of duplicates = 8

<sup>b</sup> I = Isochron    E = Errorchron

Student t-multiplier (2 $\sigma$ ) = 2.366

Blanket error in X = 1.0%; Y = 0.02%

\* MSWD (Mean Square of Weighted Deviates) - McIntyre I Model

MSUM (Modified Residual Sums) - York II Model

$\Sigma X^2$  (Sum of Chi Square) - Wendt II Model

indices mentioned above have been published by McIntyre et al. (1966), York (1966; 1967; 1969), and Wendt (1969). All the calculated indices for the lithologic units of the Loon Lake pluton (except the granodiorite gneiss) are considerably lower than the corresponding theoretical cutoff levels (Table 2.8). Therefore, the data from these units define isochrons *sensu stricto* regardless of the regression model chosen.

The McIntyre I model assumes a constant absolute error in Y ie. a decreasing percentage error with increasing  $^{87}\text{Sr}/^{86}\text{Sr}$  values. This trend is contrary to the observed trend for a large number of duplicates covering a range of  $^{87}\text{Sr}/^{86}\text{Sr}$  ratios between 0.7 and 2.0 (Brooks et al., 1972), hence, the McIntyre I model should be used only if there is a restricted range in the strontium isotopic data (ie. 0.7 to 1.0). Although most Rb-Sr whole rock studies do have a limited range in strontium isotopic composition, all regression lines which result in isochrons (Table 2.8), for consistency, are reported from calculations using the York II model. However, both the York II and Wendt II models yield similar results.

Many studies have used the calculated index MSWD (mean square of the weighted deviates) to distinguish between isochrons and errorchrons (eg. Roddick and Compston, 1977; Verpaelst et al., 1980; Brooks, 1980) without reporting the calculated indices from the other regression models.



In this study, the calculated indices from the York II and Wendt II models are comparable (Table 2.8) but are consistently lower than the MSWD from the McIntyre I model. This discrepancy complicates the detection of geological error in the Apsley gneiss, Tallan Lake sill, and granodiorite gneiss data because not all the indices indicate geological error.

However, geological error is suspected if the calculated index MSWD is greater than the theoretical index obtained from the F-variate table (see Brooks et al., 1972). Once an errorchron has been identified then three geological error models are calculated based on the distribution of error in excess of experimental error. The McIntyre II model assumes the excess error is distributed proportional to the  $^{87}\text{Rb}/^{86}\text{Sr}$  ratio while the McIntyre III model assumes the excess error is independent of this ratio. The third geological error model (McIntyre IV) is a mixture of McIntyre II and III type distribution and is preferred in this study because it assigns the excess error to both the  $^{87}\text{Sr}/^{86}\text{Sr}$  and  $^{87}\text{Rb}/^{86}\text{Sr}$  ratios. Unfortunately, the REGROSS program only advances to the McIntyre IV model if the other two models are not applicable (see Potassic Apsley gneiss, Table 2.9). For normal whole rock analyses, there is no way of determining whether the geologic error should be attributed primarily to the  $^{87}\text{Sr}/^{86}\text{Sr}$  or  $^{87}\text{Rb}/^{86}\text{Sr}$  ratio so the choice of McIntyre II or III is somewhat arbitrary.

Table 2.9 Age and  $R_1$  calculations from each model for units which indicate geologic errorGranodiorite Gneiss (4)<sup>a</sup>

Model		$t$ (Ma) <sup>b</sup>	$R_1$ <sup>c</sup>
McIntyre	I	1296 ± 45	0.7032 ± 5
	II	1286 ± 168	0.7036 ± 14
	III	1331 ± 203	0.7028 ± 27
	IV		
York	I	1293 ± 190	0.7033 ± 21
	II	1295 ± 44	0.7032 ± 7
Wendt	I	1294 ± 44	0.7033 ± 5
	II	1295 ± 43	0.7032 ± 5

Apsley GneissSodic(6)Potassic(5)

Model		$t$ (Ma)	$R_1$	$t$ (Ma)	$R_1$
McIntyre	I	1462 ± 57	0.7012 ± 12	985 ± 53	0.7143 ± 26
	II	1444 ± 172	0.7016 ± 36	978 ± 139	0.7145 ± 76
	III	1475 ± 230	0.7009 ± 54	979 ± 131	0.7143 ± 70
	IV			975 ± 146	0.7145 ± 74
York	I	1462 ± 193	0.7012 ± 39	986 ± 157	0.7140 ± 77
	II	1461 ± 56	0.7012 ± 19	985 ± 50	0.7140 ± 26
Wendt	I	1464 ± 56	0.7011 ± 12	983 ± 52	0.7141 ± 25
	II	1462 ± 55	0.7012 ± 12	985 ± 51	0.7140 ± 25

Tallar Lake SillSyenite Gneiss(5)Composite(7)

Model		$t$ (Ma)	$R_1$	$t$ (Ma)	$R_1$
McIntyre	I	1257 ± 33	0.7026 ± 4	1228 ± 25	0.7031 ± 2
	II	1281 ± 112	0.7023 ± 11	1195 ± 115	0.7033 ± 5
	III	1239 ± 79	0.7029 ± 13	1225 ± 50	0.7031 ± 7
	IV				
York	I	1258 ± 97	0.7026 ± 13	1225 ± 69	0.7031 ± 7
	II	1257 ± 34	0.7026 ± 7	1228 ± 24	0.7031 ± 4
Wendt	I	1259 ± 33	0.7026 ± 4	1225 ± 24	0.7032 ± 2
	II	1258 ± 33	0.7026 ± 4	1228 ± 24	0.7031 ± 2

<sup>a</sup> ( ) - number of samples used in regression

<sup>b</sup> 2σ errors calculated using the student-t multiplier

<sup>c</sup> 2σ errors reported in the third and fourth significant figures

Therefore, the geological error model which yields the lowest isochron errors (Table 2.9) is reported in chapter 3 but this data should not be considered reliable.

CHAPTER III  
SR AND O ISOTOPIC RESULTS  
FROM CHANDOS TOWNSHIP

3.1 Introduction

The rocks from Chandos Twp. and vicinity selected for isotopic analyses include samples from the Apsley biotite gneiss, Tallan Lake sill, and Loon Lake pluton. Specific sample locations are indicated on Map 1. A brief description of the common lithologies in Chandos Twp. is presented below.

3.1.1 Country Rocks

The two most abundant lithologies in Chandos Twp. are the Apsley gneiss, with good exposures near the village of Apsley, and the Dungannon marble which is exposed north of Chandos Lake (Fig. 3.1). Previous studies on the geology and geochemistry of the Apsley gneiss (Simony, 1960; Shaw, 1972) indicated that the most abundant member, a quartz-oligoclase-microcline-biotite rock, could be subdivided into a potassic and a sodic suite. Samples from both units are massive and remarkably fresh in thin section. The former can be distinguished by the presence of anhedral microcline poikiloblasts (0.5 to 2.0 mm.) and a  $K_2O:Na_2O$  ratio greater than 0.5 (Simony, 1960). Otherwise, both

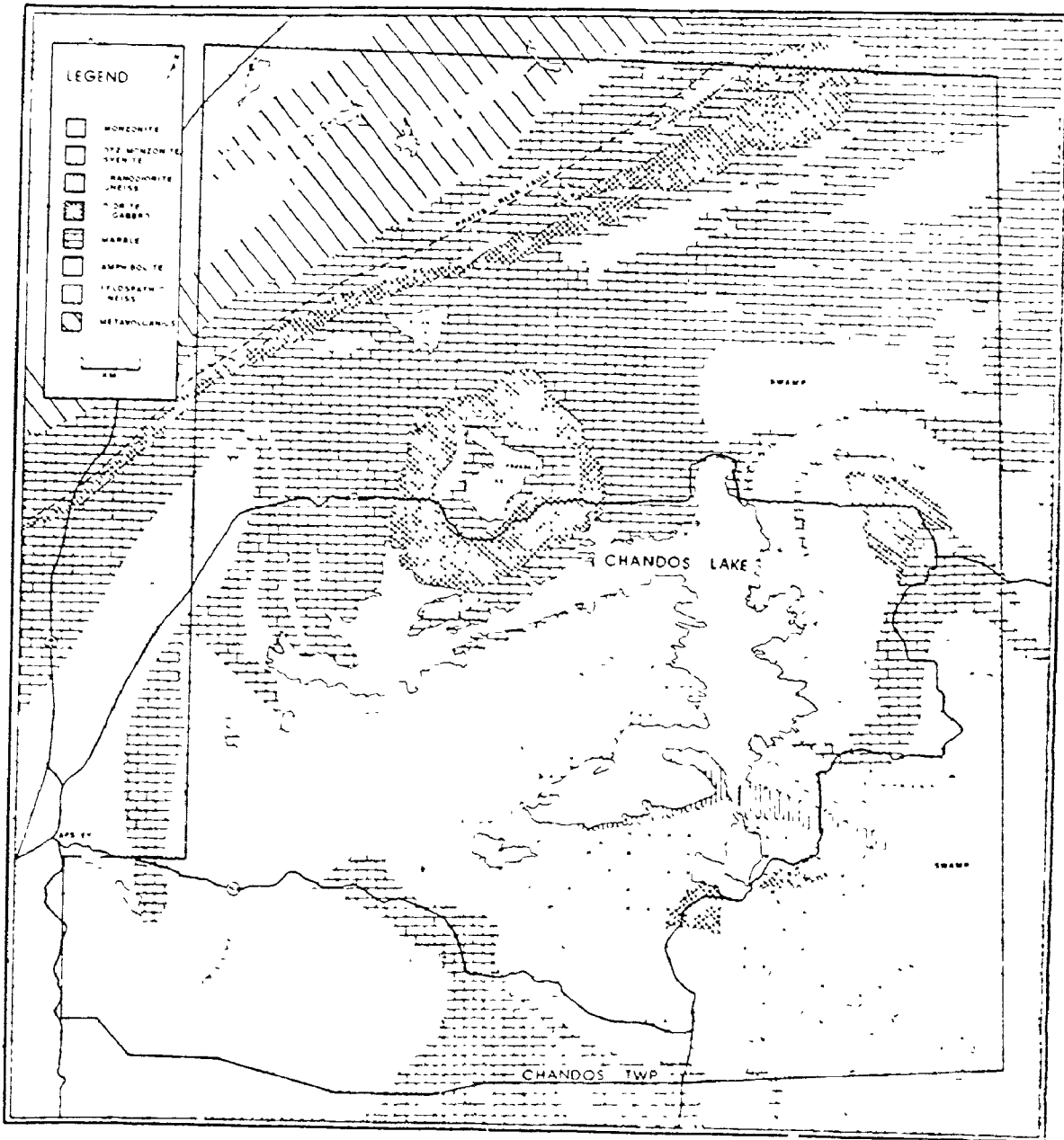


Fig. 3.1 GEOLOGY MAP OF CHANDOS TWP

suites have a fine grained granoblastic texture with polygonal quartz and feldspar intergrown with biotite laths. The biotite laths define a weak foliation parallel to the layering.

The sodic and potassic suites are intercalated with thin (0.5 to 3.0 cm.) biotite rich layers which consist of coarse biotite porphyroblasts (ca. 90%) and microcline poikiloblasts with subordinate garnet and opaques.

It is difficult to determine whether the banding in the Apsley gneiss represents original sedimentary layering or a transposed layering. Simony (1960) interpreted the variation in grain size in one outcrop to represent graded bedding but, in general, sedimentary structures are rare in the Apsley gneiss. In an attempt to distinguish high grade gneisses of sedimentary origin from an igneous precursor, Shaw (1972) used a geochemical discriminant function (DF) to estimate that 60% of the Apsley gneiss was compositionally akin to silicic volcanics (ie. positive DF values).

The Dungannon marble is layered with alternating bands of calcite (white) and calc-silicate minerals (greenish-grey). This marble is commonly associated with feather amphibolite horizons (Shaw, 1962).

### 3.1.2 Tallan Lake Sill

The Tallan Lake sill is exposed in the NW quadrant of Chandos Twp. and occurs as an elongate narrow body (12 km. x 0.3 km.) trending NE-SW and dipping  $60^{\circ}$  -  $70^{\circ}$  SE (Fig. 3.1). A probable extension of this sill occurs in a dome structure centered around Clydesdale Lake. In a detailed petrochemical study, Griep (1975) described the sill as consisting of an upper 180 meters of weakly foliated amphibolite (metagabbro ?) which is transitional to a lower 80 meters of well foliated syenite.

A typical sample of amphibolite from the upper part of the sill contains 55% hornblende, 39% plagioclase, and minor amounts of quartz, biotite, sphene, and ilmenite (sample 120 from Griep, 1975). Below the upper amphibolite zone, garnet and cummingtonite become important phases. The syenite samples contain plagioclase, quartz, alkali feldspar, biotite, and hornblende (in order of decreasing abundance) with subordinate zircon, allanite, and ilmenite.

Most of the samples do not show evidence of extreme alteration, however, the feldspars are often slightly turbid and are occasionally associated with epidote. Griep (1975) reported that several samples contained micro-fractures filled with calcite.

Although the Tallan Lake sill has been metamorphosed to amphibolite facies subsequent to its emplacement the syenite end member has been interpreted as a direct

differentiate from a gabbroic parental magma (Griep,1975). This suggests that the sill has been tectonically inverted and may form part of a large scale nappe structure.

### 3.1.3 Loon Lake Pluton

The felsic igneous rocks exposed on the shores of Chandos (Loon) Lake were initially described by Adams and Barlow (1910) during a reconnaissance mapping project for the Geological Survey of Canada. Subsequently, several noteworthy contributions on the structure (Cloos,1934; Saha,1957; 1959), petrography (Saha,1957; 1959; Shaw,1962; Chiang,1965; Dostal,1973), and geochemistry (Shaw and Kudo, 1965; McCammon,1968; Dostal,1973; 1975; Shieh et al.,1976) have been reported. The salient features of this pluton are summarized below.

At the present erosional level, the Loon Lake pluton has an ovoidal outline (8 km. x 5 km.) with a monzonite core transitional to a quartz monzonite rim (Fig. 3.1). This pluton intrudes the structurally complex sequence of quartzo-feldspathic gneiss, marble, and amphibolite of the Grenville Supergroup.

The average modal composition of the monzonite is 45% K feldspar, 42% plagioclase, 6% biotite, 3% hornblende, 2% quartz, 1% opaques, and minor amounts of sphene, apatite, epidote, calcite, and sericite (Dostal,1973). The quartz content of the monzonite increases to a maximum of 12% near



the margin of the core. There is a sharp increase in the modal quartz content of the quartz monzonites and biotite is the major mafic mineral (ie. 34% plagioclase, 34% K-feldspar, 25% quartz, 5% biotite, 1% opaques, and similar accessory minerals). Samples from both the monzonite and quartz monzonite suite show a weak but pervasive sericitization of plagioclase and a few samples contain slightly chloritized biotite.

In most exposures, the monzonite is massive to slightly foliated (Saha, 1959) and contrasts with the strong "flow" foliation of the quartz monzonite. This "flow" foliation is oriented parallel to the intrusion - wall rock contact and in some areas, clearly intersects the  $S_1$  foliation of the Apsley gneiss. The intrusion - wall rock contact is generally abrupt, varying from a brecciated SW margin to the juxtaposition of monzonite and pyroxene hornfels facies rocks to the south (Chiang, 1965) but locally the contact is migmatitic.

A summary of the trace and major element geochemistry of this pluton was presented by Dostal (1973). The smooth trends on many major and trace element variation diagrams suggest a co-magmatic origin for the monzonite and quartz monzonite suite. These trends allude to the importance of fractional crystallization dominated by feldspar separation in the evolution of the parent magma.

Other major rock types within the pluton include a

band of granodiorite gneiss plus several isolated bodies of diorite - syenodiorite (Fig. 3.1). The former occasionally exhibits a banded to migmatitic structure but generally is weakly foliated with abundant mafic inclusions. In thin section, the granodiorite gneiss shows a pervasive sericitization of the feldspars and is enriched in plagioclase and mafics (biotite and hornblende) compared to the quartz monzonite suite (Dostal, 1973).

Compositionally, the mafic bodies vary from diorite in the core to syeno-diorite near their margins (Dostal, 1973). Saha (1957) concluded that these mafic bodies represent inclusions or roof pendants, a contention which cannot be eliminated with the geochemical data of Dostal (1973).

#### 3.1.4 Dikes

Small dikes and veins are ubiquitous in Chandos Twp. and cross-cut most of the major lithologies. Pegmatite and aplite dikes are especially common around the Loon Lake pluton and many have a modal composition similar to the quartz monzonite suite. A description of their mineralogy, texture, and mode of occurrence has been reported by Shaw (1962).

### 3.2 Sr Isotopic Composition of the Apsley Biotite Gneiss

Preliminary Sr isotopic data for the Apsley biotite

gneiss indicated that the sodic and potassic suites (Simony, 1960) do not exhibit similar Sr isotopic systematics. To understand the strontium isotopic composition of the Apsley gneiss it was necessary to treat the data from each unit separately.

### 3.2.1 "Sodic" Apsley Gneiss

Samples representative of the sodic suite were collected from thick massive bands of the Apsley gneiss. The strontium isotopic results for six samples from this unit are presented in Table 3.1 and plotted on Fig. 3.2. The data scatter in Fig. 3.2 exceeds that expected from analytical error (see Table 2.8) and indicates a model II errorchron age of  $1444 \pm 172$  Ma. with an initial strontium ratio ( $R_i$ ) of  $0.7016 \pm 36$ . It is difficult to determine whether this age has any geological significance but since this low  $R_i$  falls below the range of values accepted for the mantle at this time, the 1444 Ma. age should be suspect. If the data point AG 7 is omitted from the regression analysis then the remaining five samples define a Rb-Sr whole rock isochron age of  $1402 \pm 57$  Ma. with an  $R_i$  of  $0.7022 \pm 12$ . This  $R_i$  lies very close to the mantle growth line (Fig. 4.2) so the 1402 Ma. age is probably a better estimate for the time of volcanism for the protolith of the Apsley gneiss. Closer inspection of AG 7 indicates a thin mafic band along one surface which may be responsible

Table 3.1 Rb-Sr data for the Apsley Gneiss

	Rb <sup>1</sup>	Sr <sup>1</sup>	Rb/Sr	<sup>87</sup> Rb/ <sup>86</sup> Sr <sup>6</sup>	<sup>87</sup> Sr/ <sup>86</sup> Sr <sup>2</sup>	$\sigma$ (x10 <sup>-4</sup> ) <sup>3</sup>
<u>"Sodic" Bands</u>						
AG1	50.3	78.5	0.640	1.860	0.73935	0.8860
AG2	11.2	35.1	0.318	0.921	0.72091	1.2878
AG3	39.3	67.7	0.581	1.687	0.73636	1.3440
AG5	33.9	49.2	0.689	2.003	0.74299	1.2762
AG7	30.9	47.8	0.647	1.880	0.74261	0.6313
AG11	46.1	92.5	0.499	1.447	0.73036	1.5809
<u>"Potassic" Bands</u>						
AG6	82.9	72.3	1.147	3.339	0.76289	1.4310
AG8	90.4	48.5	1.862	5.435	0.79078	1.5452
AG9	58.2	58.4	0.997	2.899	0.75498	1.2849
AG10	66.1	67.2	0.983	2.859	0.75378	1.2822
AG12	51.9	38.4	1.352	3.936	0.76735	1.1299
<u>Slabs<sup>5</sup></u>						
AG8B	182	25.4	7.146	21.216	0.96709	2.3846
AG8C	40.6	29.7	1.364	3.962	0.77069	1.2684 <sup>4</sup>
AG12A	33.1	33.2	0.991	2.876	0.73150	1.2164 <sup>4</sup>
AG12B	26.4	31.1	0.848	2.464	0.74907	2.1030
AG12C	24.8	39.6	0.627	1.818	0.73615	1.5414
AG12D	137	44.4	3.077	9.012	0.81099	2.0000
<u>Mineral Separates<sup>5</sup></u>						
AG1 (feldspar)	9.6	106	0.090	0.262	0.71513	2.3440
AG12C (feldspar)	3.5	56.6	0.057	0.164	0.71285	2.2557
AG12D (feldspar)	26.5	116	0.229	0.664	0.73162	2.2226 <sup>4</sup>
AG12D (biotite)	232	2.5	94.187	352.984	3.71884	2.9915 <sup>4</sup>

1 Rb and Sr concentrations reported at the ppm level

2 <sup>87</sup>Sr/<sup>86</sup>Sr ratios normalized to <sup>86</sup>Sr/<sup>88</sup>Sr = 0.1194

3 1 $\sigma$  error in <sup>87</sup>Sr/<sup>86</sup>Sr ratio

4  $\sigma$  (10<sup>-3</sup>)

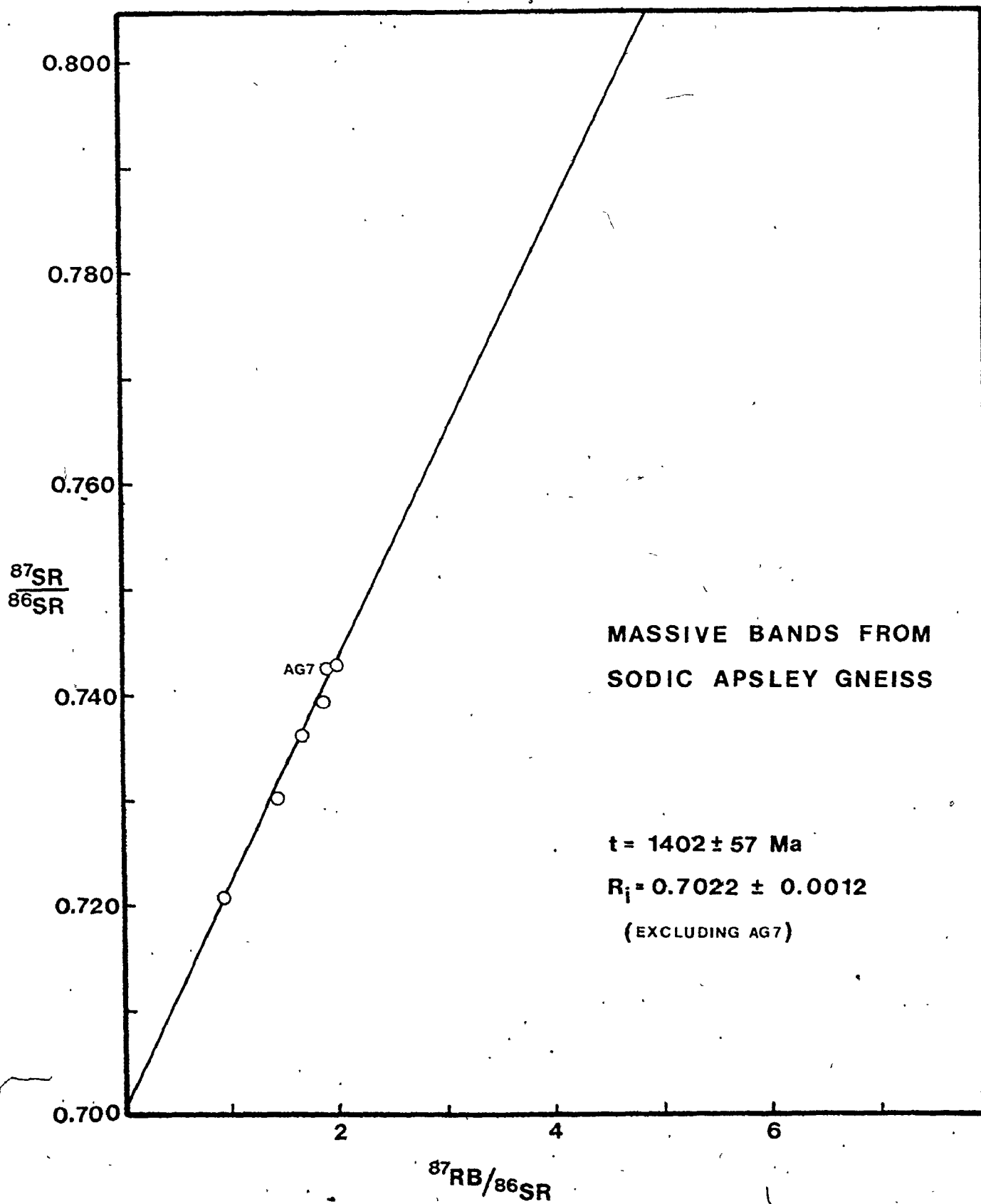
5 Rb and Sr concentrations determined by isotope dilution

6 <sup>87</sup>Rb/<sup>86</sup>Sr calculated from the expression:

$$\left( \frac{{}^{87}\text{Rb}}{{}^{86}\text{Sr}} \right)_{\text{Atomic}} = \left[ \frac{\text{Ab}^{87}_{\text{Rb}} \times \text{At.wt. Sr}}{\text{Ab}^{86}_{\text{Sr}} \times \text{At.wt. Rb}} \right] \times \left[ \frac{\text{Rb}}{\text{Sr}} \right]_{\text{wt}}$$

$$= [2.69454 + (0.28319 \times {}^{87}\text{Sr}/{}^{86}\text{Sr})] \times (\text{Rb}/\text{Sr})_{\text{wt}}$$

FIGURE 3.2 RB-SR ISOCHRON FOR SODIC APSLEY GNEISS SAMPLES



for the apparent discordance of this sample in Fig. 3.2.

The age of the Apsley gneiss is considerably older than the 1298 Ma. U/Pb zircon age for the nearby Tudor volcanics (Silver and Lumbers, 1965). From a regional stratigraphic correlation, Lumbers (1967) suggested that the volcanic members of the Tudor formation are older than the Apsley gneiss which is contrary to the above geochronologic data. Since stratigraphic correlation is difficult in this part of the Grenville (see Section 1.2), the older age for the Apsley gneiss suggests the possibility of structural inversion.

### 3.2.2 "Potassic" Apsley Gneiss

Five samples of potassic Apsley gneiss were selected for strontium isotopic analysis (Table 3.1). All these samples fall below the reference isochron for the sodic Apsley gneiss (Fig. 3.3) and do not form a co-linear array. Regression of these samples indicates a model III errorchron age of  $979 \pm 131$  Ma. ( $R_1 = 0.7143 \pm .70$ ) which implies that some of the potassic bands have not remained closed to Sr and Rb migration during metamorphism.

The complex isotopic characteristics of high grade gneisses has been addressed by many authors (e.g. Krogh and Davis, 1969; 1973; Grauert and Hall, 1973; Steiger et al., 1976; Jacobsen and Heier, 1978; Gray and Compston, 1978; Montgomery and Hurley, 1978; Brooks, 1980; Aftalion and

Figure 3.3 Strontium isotope data for five samples of potassic Apsley gneiss. These samples define an errorchron age of  $979 \pm 131$  Ma ( $R_1 = 0.7143 \pm 70$ ). All of the potassic Apsley gneiss samples plot below the reference isochron defined by the sodic Apsley gneiss.


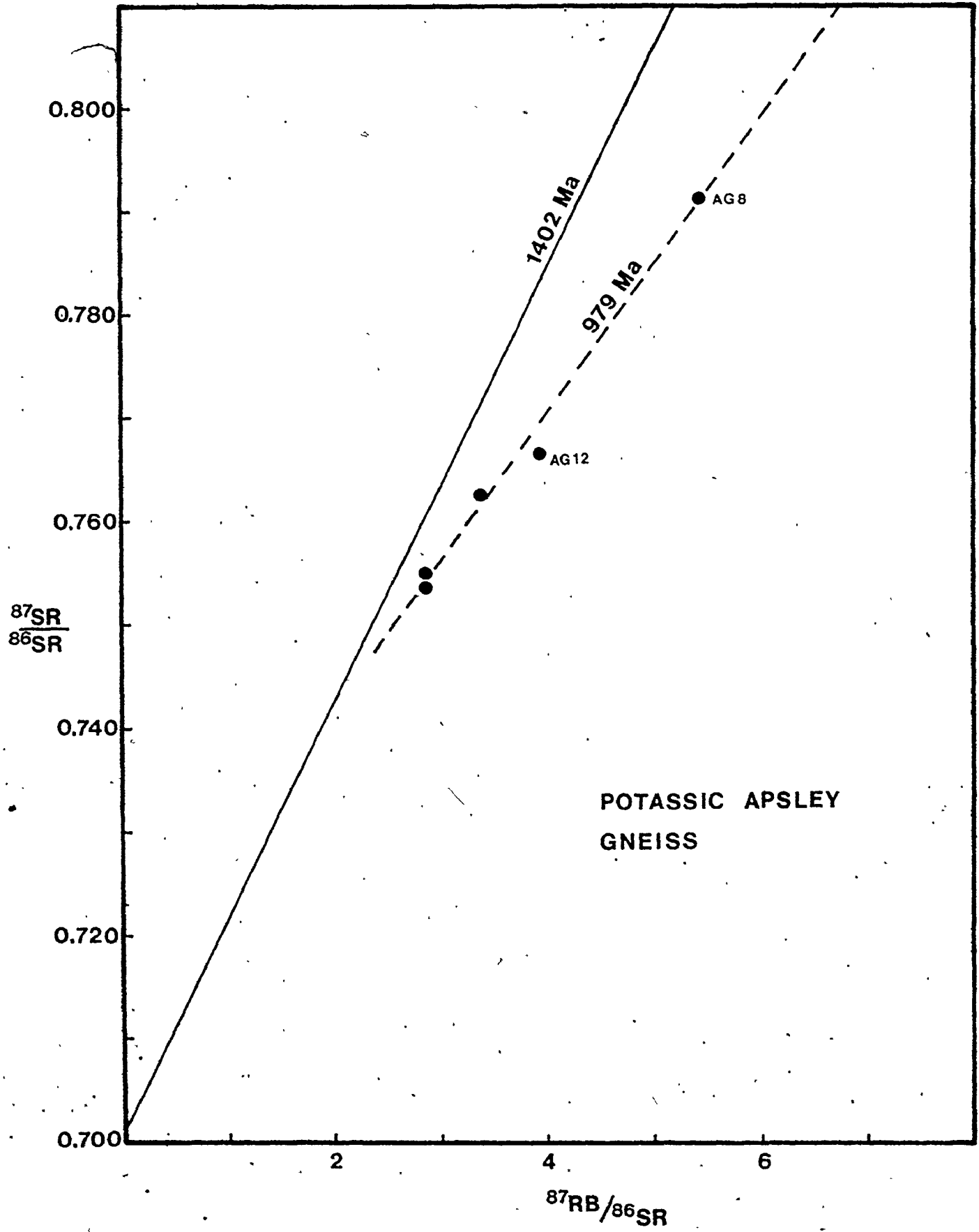


FIGURE 3.3 SR ISOTOPE DATA FOR POTASSIC APSLEY GNEISS SAMPLES





Van Breeman, 1980). Most of these studies employed the slab approach of Krogh and Davis (1969) to discriminate between bands which have remained closed to Sr and Rb migration (on the scale of cm.) from bands which show open system behaviour. As pointed out by Hofmann (1977), the scale of isotopic equilibration is quite variable (cm. to meters) and the slab approach offers a compromise which often reveals the maximum isotopic information about the evolution of a complex system.

Two of the samples analysed from the potassic suite (AG 8 and AG 12) have thin (0.5 to 2.0 cm.) mafic bands (Fig. 3.4) and have the highest Rb/Sr ratios on Fig. 3.3. The other samples have domains enriched in biotite but do not have discrete mafic bands. To determine the scale of strontium isotopic equilibration in the potassic suite, the two banded samples were cut into slabs (Fig. 3.4) similar to the approach of Krogh and Davis (1969). Strontium isotopic results for individual slab sections (Table 3.1; Fig. 3.5) indicate that the mafic bands plus one felsic band with a mafic rich domain (AG 12A) display a greater degree of discordance from the reference isochron than the felsic bands. The two felsic bands from sample AG 12 (B and C) define a trend which is below and at a slight angle to the reference isochron. This trend could be interpreted to represent a relatively undisturbed system with a slightly lower initial strontium ratio than the sodic suite. Hence,

FIGURE 3.4 APSLEY GNEISS SLAB SECTIONS

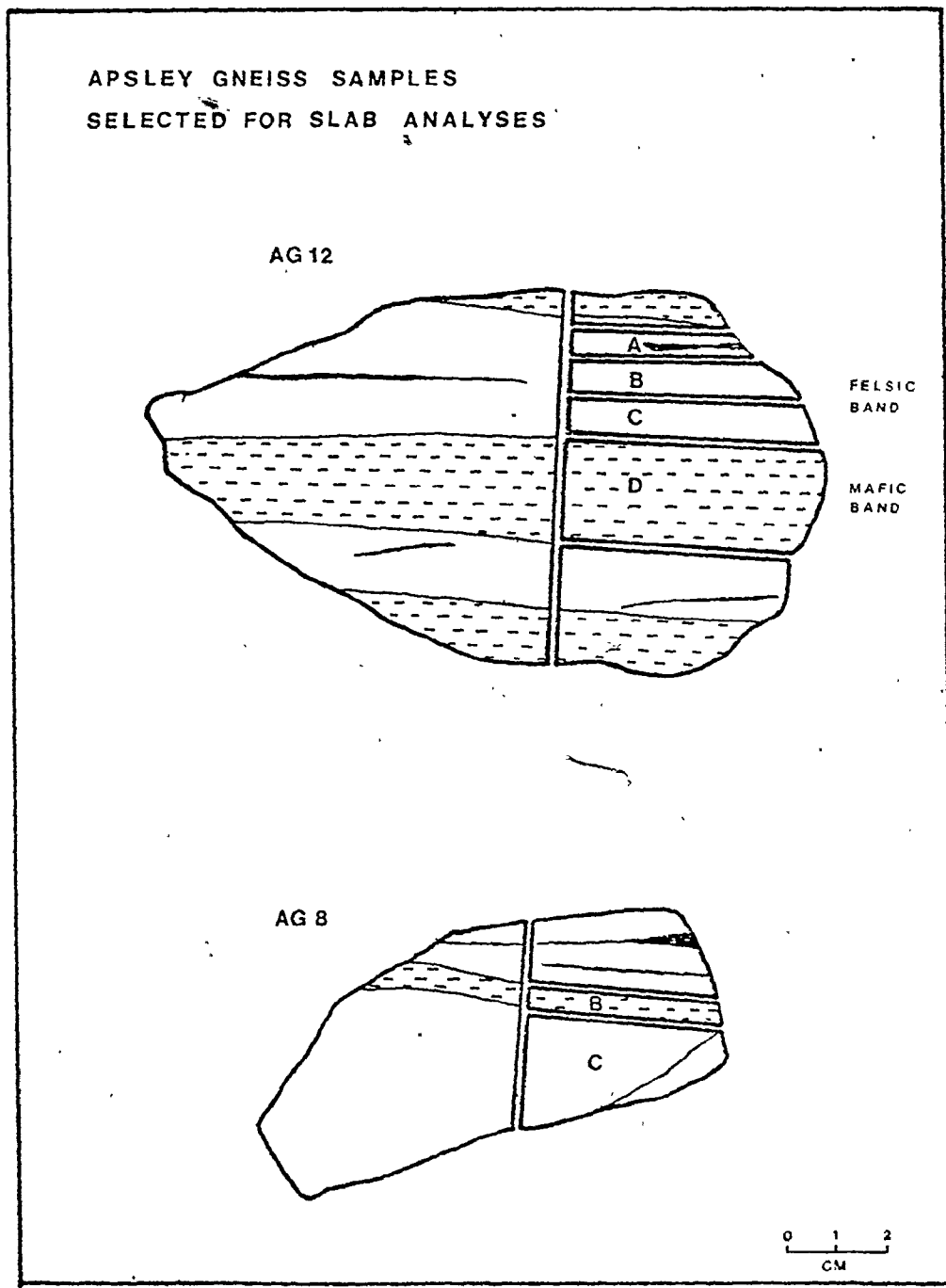
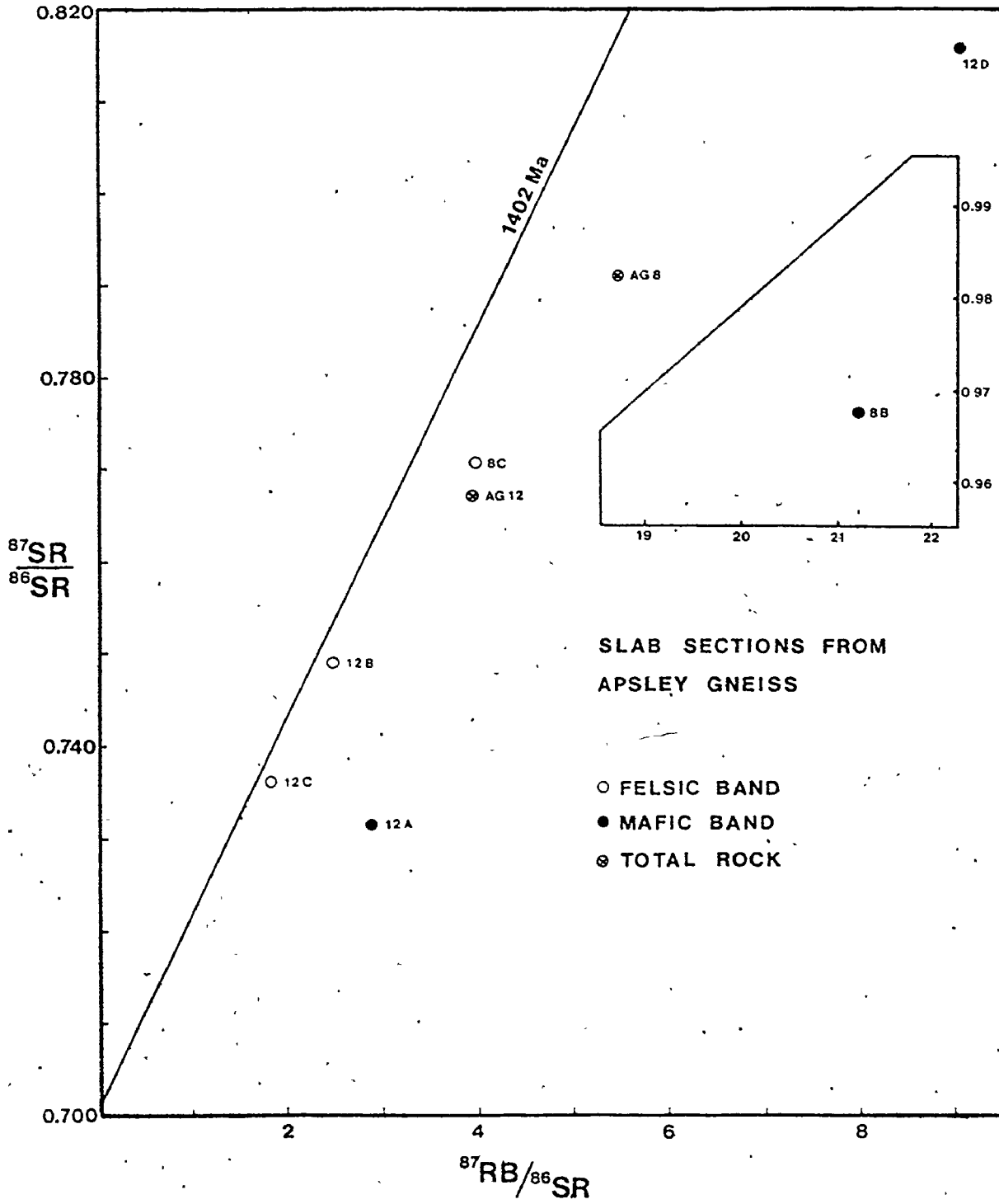


Figure 3.5 Strontium isotope results for Krogh-type slab sections from the potassic Apsley gneiss. The two felsic bands from AG12 plot close to the reference isochron and represent relatively undisturbed isotopic systems. The mafic bands (AG12D and AG8B) show the largest degree of discordance and are responsible for pulling the total rock samples below the reference isochron.

FIGURE 3.5 SR ISOTOPE RESULTS FOR SLAB SECTIONS FROM APSLEY GNEISS



equilibration of strontium isotopes in the felsic bands may have been restricted to distances less than 0.5 cm.

However, this interpretation is based only on the results from two felsic bands and more data is necessary to reinforce this hypothesis.

An important corollary from the slab study is that the mafic bands (AG 12D and AG 8B) and the mafic domain in AG 12A probably experienced some degree of isotopic re-equilibration during Grenville metamorphism. It is impossible to confirm that the errorchron age from the potassic suite (979 Ma.) represents the approximate time of re-equilibration of the mafic bands but this suggestion is inviting.

### 3.2.3 Mineral Isochrons

Support for the age and extent of final (chemical and isotopic) equilibration of individual bands might be obtained from a mineral isochron study. As demonstrated in other studies (Krogh and Davis, 1973; Grauert and Hall, 1973), mineral - whole rock pairs from individual bands often indicate younger ages reflecting the exchange of strontium between minerals during a metamorphic event.

Quartz-feldspar mineral separates from felsic and mafic bands of the Apsley gneiss plus one biotite separate (from AG 12D) were obtained using standard magnetic and hand picking techniques. Only small quantities

of pure mineral separate were collected (50 to 250 mg.) so the Rb and Sr concentrations were determined by isotope dilution (see section 2.5).

The isotopic data for a corresponding feldspar-whole rock pair (Table 3.1; Fig. 3.6) from a sample of sodic Apsley gneiss (AG 1) indicates an age of 1062 Ma. This age could represent mineral re-equilibration during a thermal event (such as emplacement of the Loon Lake pluton at 1065 Ma.) or the time when the sodic Apsley gneiss passed through the blocking temperature for Rb and Sr. The latter process is preferred considering the distance between the Loon Lake pluton and the outcrop where AG 1 was collected (ca. 7 km). Regardless of the prevailing mechanism, this data seems to indicate that strontium re-equilibration or at least partial re-equilibration may have occurred on a mineral scale within the sodic Apsley gneiss bands.

Strontium isotopic ratios for mineral-whole rock pairs from a mafic and felsic band of potassic Apsley gneiss are shown on Fig. 3.7. Both bands indicate feldspar-whole rock ages younger than the mineral isochron age for the sodic Apsley gneiss (1062 Ma.) and the errorchron age for the complete potassic suite (979 Ma.). The datum for a biotite separate from AG 12D (see inset on Fig. 3.7) was not included in the calculation of the feldspar-whole rock age (666 Ma.). Although there is a large error associated

Figure 3.6 Strontium isotopic results for a feldspar-  
whole rock pair from the sodic Apsley gneiss.

○ - whole rock

△ - quartz-feldspar separate

FIGURE 3.6

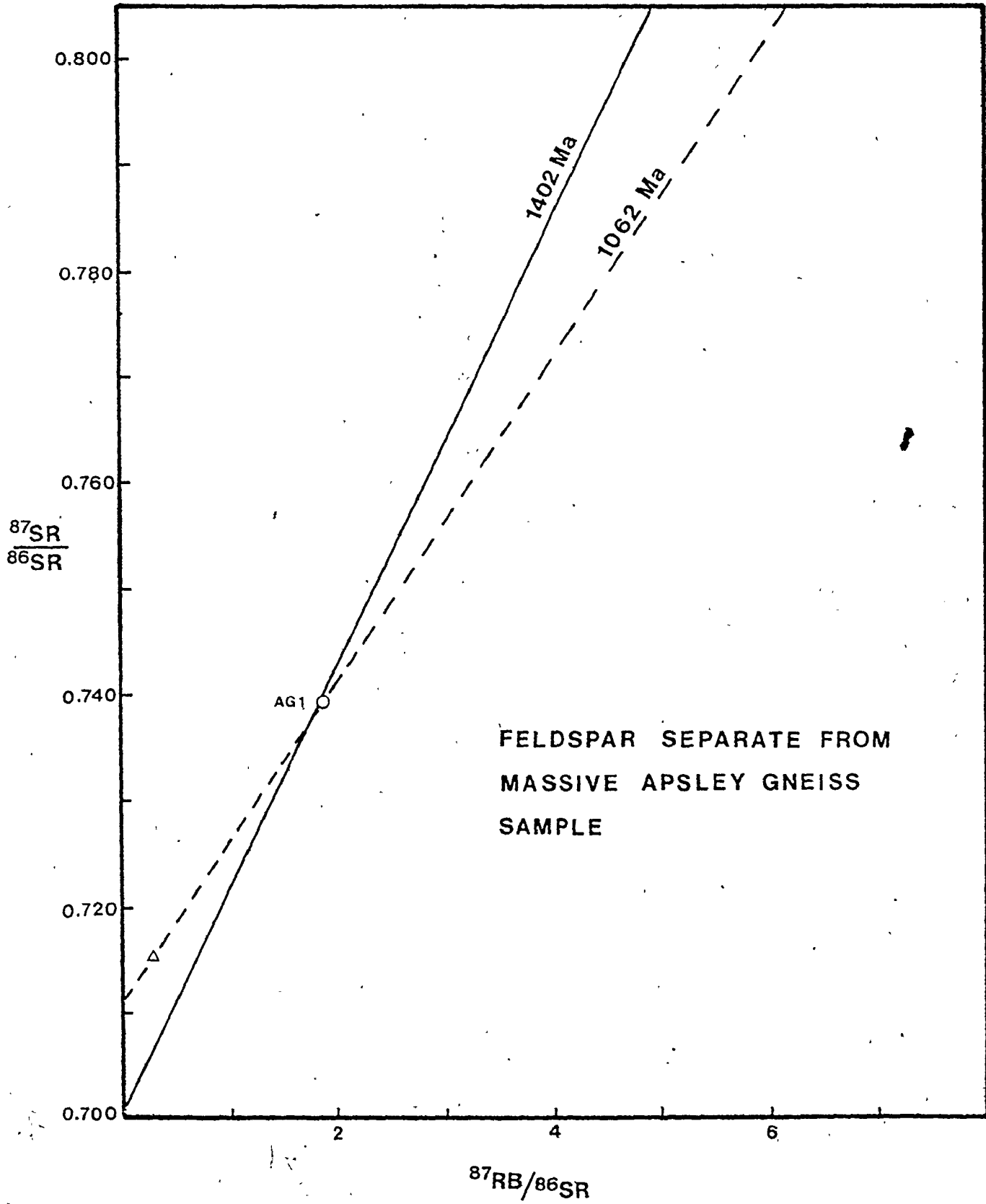


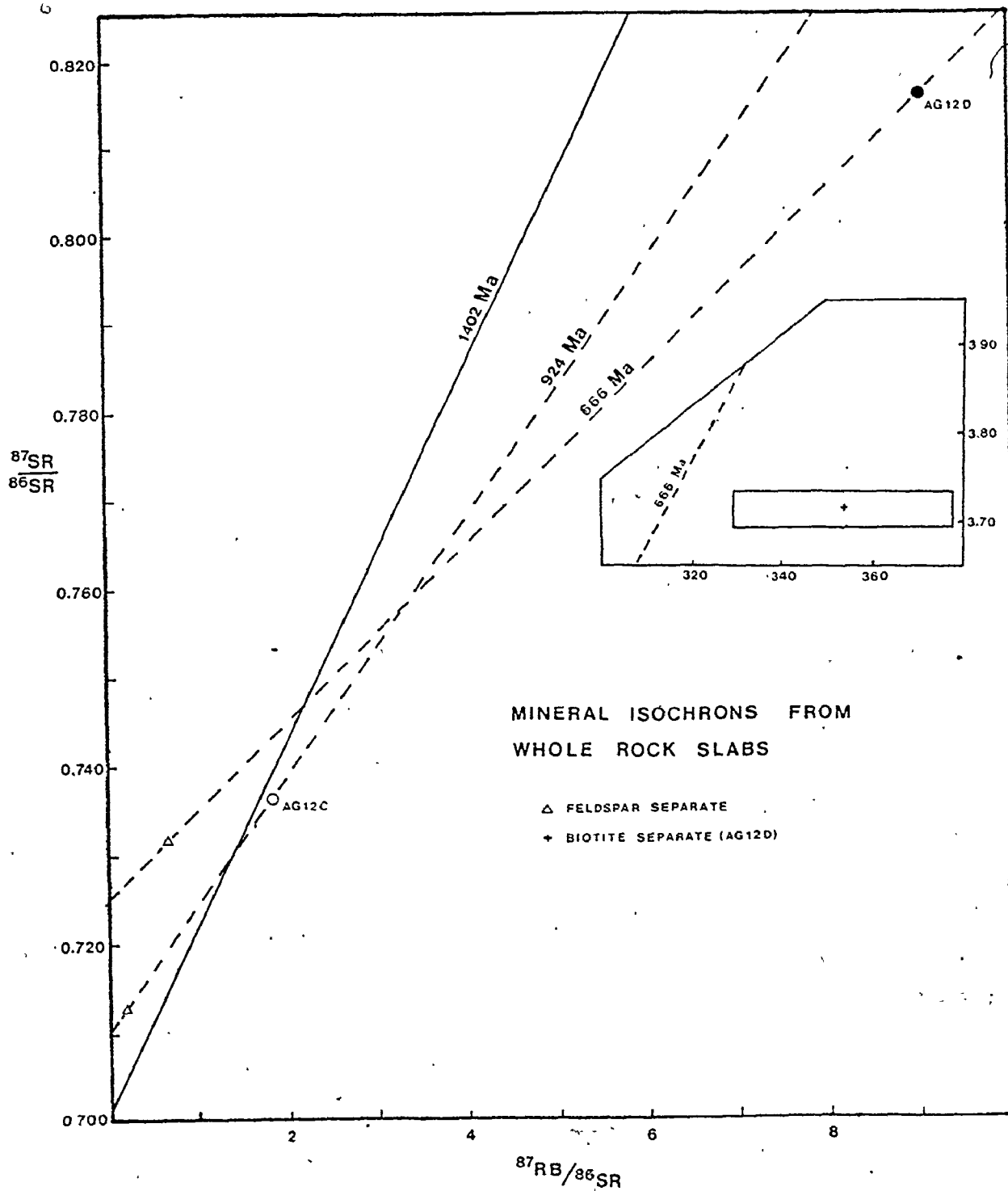


Figure 3.7 Strontium isotopic results for mineral-  
whole rock pairs from the potassic Apsley  
gneiss (sample AG12).

○ - felsic band

● - mafic band

FIGURE 3.7



with the Rb/Sr ratio of the biotite data and the strontium isotopic ratio has not been corrected for common Sr, it is interesting that similar isotopic discordancies have been reported for biotites separated from the Pointe au Baril paragneiss (Krogh and Davis, 1970). These discordancies possibly reflect the lower blocking temperature for biotite but could also indicate the necessity for blank corrections on samples with high strontium ratios. These authors also obtained a range of ages from plagioclase-whole rock pairs between 800 and 900 Ma. for the French River paragneiss (Krogh and Davis, 1970). The range of ages from feldspar-whole rock pairs in this study (666 to 1062 Ma.) indicates that a 900 Ma. thermal event, as proposed by Krogh and Davis (1970), is not well defined by the Rb/Sr systematics in the Apsley area.

One explanation for the decrease in feldspar-whole rock ages hinges on a variation in the prevalent diffusion mechanism operating within each band. For instance, if the diffusion mechanism is very sluggish (ie. volume diffusion) then a decrease in the ambient temperature conditions will severely reduce the migration of cations. Alternatively, if grain boundary diffusion, in the presence of a fluid phase, ensues then a reduction in the ambient temperature conditions has only a second order effect on cation diffusivity. To reconcile the feldspar-whole rock data with a variation in the diffusion mechanism, it is

necessary to infer a sluggish diffusion process for the felsic bands and fluid transport in the mafic bands.

Similar results could be obtained if the degree of isotopic re-equilibration was controlled by the bulk chemical composition of a band. This mechanism requires the minerals in the mafic bands to completely homogenize isotopically while the minerals in the felsic bands experience varying degrees of partial re-equilibration.

There is no simple explanation for the feldspar-whole rock data and since they are calculated using only two data points no geologic significance should be attached to them. However, it is interesting to compare the results on felsic slabs from the French River paragneiss to the north (1035 Ma.; Krogh and Davis, 1973) and the results for the two felsic bands reported here (1062 and 924 Ma.). Additional detailed study of the felsic bands from the Apsley gneiss might confirm a widespread metamorphic event ca. 1000 Ma. for this part of the Grenville.

### 3.3 Rb-Sr Whole Rock Study of the Tallan Lake Sill

The Rb-Sr data for amphibolite and syenite samples from the Tallan Lake sill are presented in Table 3.2. Most of the samples were collected around Clydesdale Lake (Map 1) but one amphibolite sample (TL 6) was collected from the main NE-SW trending portion of the sill.

Seven of the eight samples analysed indicate an

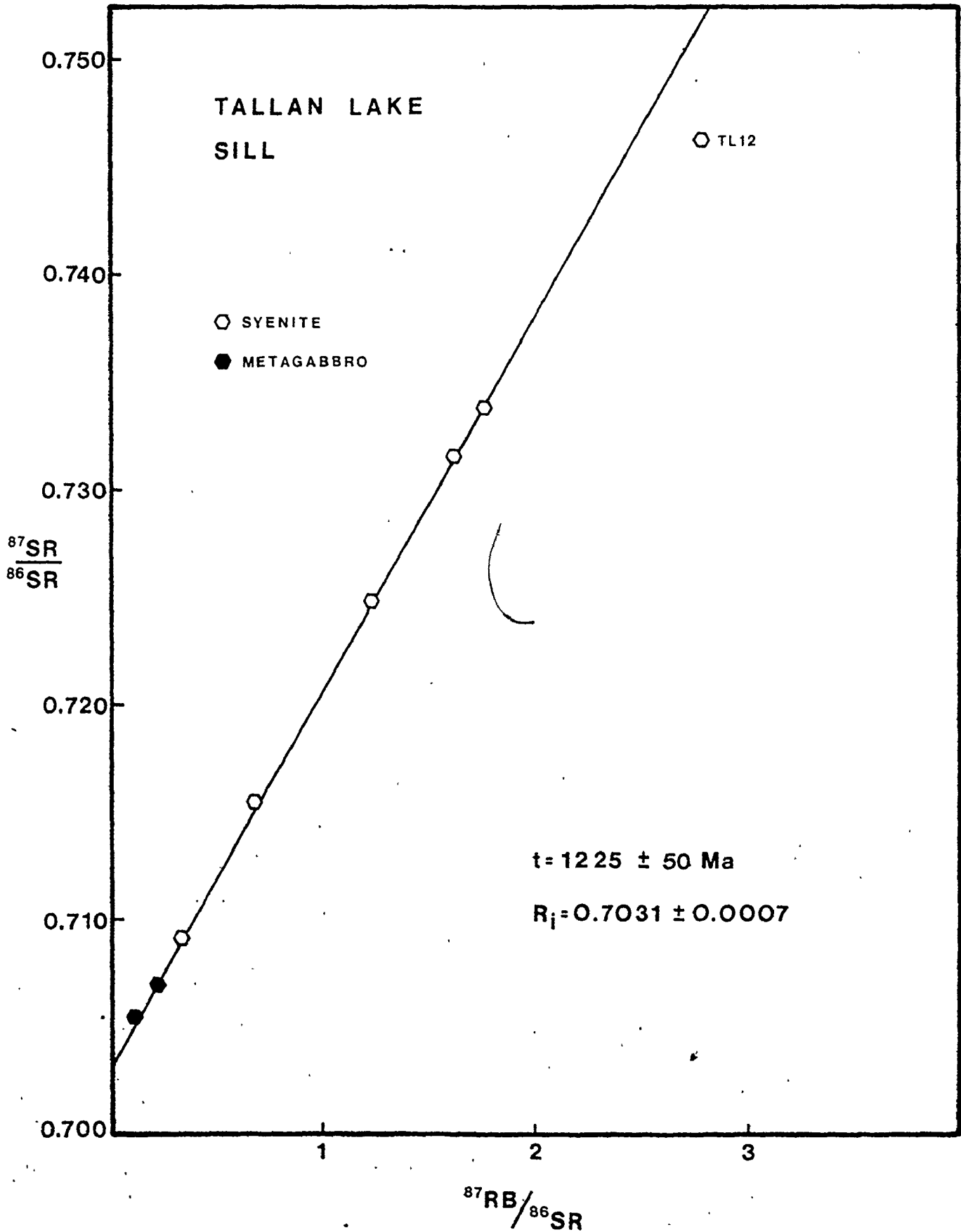
Table 3.2 Rb-Sr data for the Tallan Lake Sill

	<u>Rb</u>	<u>Sr</u>	<u>Rb/Sr</u>	$\frac{87}{86} \frac{\text{Rb}}{\text{Sr}}$	$\frac{87}{86} \frac{\text{Sr}}{\text{Sr}}^1$	$\sigma (\times 10^{-4})$
<u>Metagabbro</u>						
TL1	11.1	274	0.040	0.117	0.70552	1.4790
TL6	18.9	241	0.078	0.227	0.70707	1.4739
<u>Syenite Gneiss</u>						
TL2	16.9	143	0.119	0.344	0.70836	1.7550
TL11	29.5	127	0.232	0.673	0.71548	1.2976
TL15	35.6	83.4	0.427	1.237	0.72492	1.3481
TL8	43.8	78.1	0.560	1.626	0.73176	2.3620
TL16	45.1	74.1	0.609	1.768	0.73395	0.7911
TL12	141	150	0.938	2.725	0.74668	0.8839

<sup>1</sup>  $\frac{87}{86} \frac{\text{Sr}}{\text{Sr}}$  ratios normalized to  $\frac{86}{88} \frac{\text{Sr}}{\text{Sr}} = 0.1194$

Figure 3.8 Strontium isotopic results for the Tallan Lake sill. Seven of the samples define an errorchron age of  $1225 \pm 50$  Ma. One sample (TL12) was not included in the regression treatment because it contains a fracture with secondary calcite and epidote.

FIGURE 3.8 RB-SR ISOCHRON FOR THE TALLAN LAKE SILL



errorchron age of  $1225 \pm 50$  Ma. (Fig. 3.8) with an  $R_i$  of 0.7031 (McIntyre III geological error model). This age is similar to the results from the other regression models (Table 2.9) and considering the co-linearity of the data (Fig. 3.8) is interpreted as the approximate time of intrusion of this sill. One sample (TL 12) falls below this regression line and was not included in the regression treatment. Detailed examination of this sample revealed a micro-fracture, which may have provided a passage for fluids containing Rb and/or Sr. The late addition of strontium is attested by a 2 cm. wide saussuritized zone and the concentration of calcite near the fracture.

To test whether the amphibolite and syenite units are consanguineous, the latter unit was regressed separately (Table 2.9). The five syenite samples indicate an errorchron age of  $1239 \pm 79$  Ma. ( $R_i = 0.7029 \pm 13$ ) which overlaps with the combined data for both units. Although the Rb-Sr data is compatible with the contention of Griep (1975) that these two units are cogenetic, a more detailed study may reduce the regression errors sufficiently to allow a critical evaluation of this relationship.

### 3.4 Sr and O Isotopic Composition of the Loon Lake Pluton

#### 3.4.1 Rb-Sr Whole Rock Study

Following a comprehensive study of the petrography



and geochemistry of the Loon Lake pluton, Dostal (1973) suggested two possible origins for the monzonite core:

- (a) crystallization from a monzonitic magma, generated by partial melting of the lower crust or upper mantle
- (b) fractional crystallization of a basic magma derived from the mantle

In either case, the quartz monzonite rim was considered to form in part by fractional crystallization of a monzonitic magma and by mixing with an anatectic melt from the Apsley gneiss.

In order to evaluate this hypothesis, separate Rb-Sr whole rock isochrons were determined for the monzonite core (samples with less than 10% quartz) and the quartz monzonite rim. The results from this study are listed in Table 3.3 and plotted on separate isochron diagrams (Fig. 3.9). Considering the overlap in the initial strontium ratios and ages, the Rb/Sr data for each unit is interpreted as defining the same event. Therefore, this data was combined to produce one isochron (Fig. 3.10) which indicates an age of  $1065 \pm 13$  Ma. for the Loon Lake pluton ( $R_i = 0.7034$ ) and is interpreted as the time of intrusion (Heaman et al., 1980a,b).

Additional samples from the diorite-syeno-diorite suite were also analysed (Table 3.3) but the small variation in the Rb/Sr ratio precludes the construction of a separate isochron. This data is shown in Fig. 3.10 (inset) with the reference isochron for the Loon Lake pluton. Combining

Table 3.3 Sr and O isotopic data for the Loon Lake Pluton

	<u>Rb</u>	<u>Sr</u>	<u>Rb/Sr</u>	<u><sup>87</sup>Rb/<sup>86</sup>Sr</u>	<u><sup>87</sup>Sr/<sup>86</sup>Sr<sup>a</sup></u>	<u><math>\sigma(10^{-4})</math></u>	<u><math>\delta^{18}O^{WT}(\%)</math></u>
<u>Monzonite</u>							
LL24	41.8	682	0.061	0.177	0.70628	0.9831	9.6
LL21	54.9	208	0.264	0.765	0.71446	4.0073	9.7
LL27	73.5	186	0.396	1.148	0.72075	1.0279	9.7
LL18	62.3	124	0.501	1.453	0.72530	0.9516	9.3
LL30	60.1	102	0.592	1.718	0.72981	1.1081	9.7
LL13	71.4	63.4	1.128	3.279	0.75290	2.9366	8.8
<u>Quartz Monzonite</u>							
LL4	73.2	520	0.141	0.408	0.70959	3.1450	11.2
LL6	94.1	355	0.235	0.681	0.71429	0.7278	10.6
GN4	104	218	0.475	1.378	0.72381	1.1232	11.6
GN8	96.4	141	0.682	1.979	0.73338	1.3715	9.9
LL15	236	380	0.620	1.800	0.73096	1.5375	10.2
LL49	188	180	1.043	3.032	0.75026	1.1876	12.0
LL20	175	95.4	1.830	5.339	0.78640	1.6490	11.2
<u>Granodiorite Gneiss</u>							
GN5	50.0	444	0.113	0.326	0.70963	0.8665	9.5
LL29	51.5	222	0.232	0.672	0.71526	1.2125	9.6
LL7	61.2	173	0.354	1.026	0.72142	0.8213	8.9
LL26	100	204	0.490	1.422	0.73065	1.7481	9.7
<u>Diorite-Gabbro</u>							
LL56	8.4	1535	0.006	0.016	0.70359	0.5123	-
LL47	25.0	1903	0.013	0.038	0.70419	0.8406	-
LL25	27.1	1262	0.022	0.062	0.70455	1.4260	-
LL22	54.8	1276	0.043	0.124	0.70563	1.5140	-
LL57	48.8	809	0.060	0.175	0.70644	1.1062	-

<sup>a</sup> <sup>87</sup>Sr/<sup>86</sup>Sr ratios normalized to <sup>86</sup>Sr/<sup>88</sup>Sr = 0.1194

FIGURE 3.9 RB-SR ISOCHRONS FOR THE LOON LAKE PLUTON

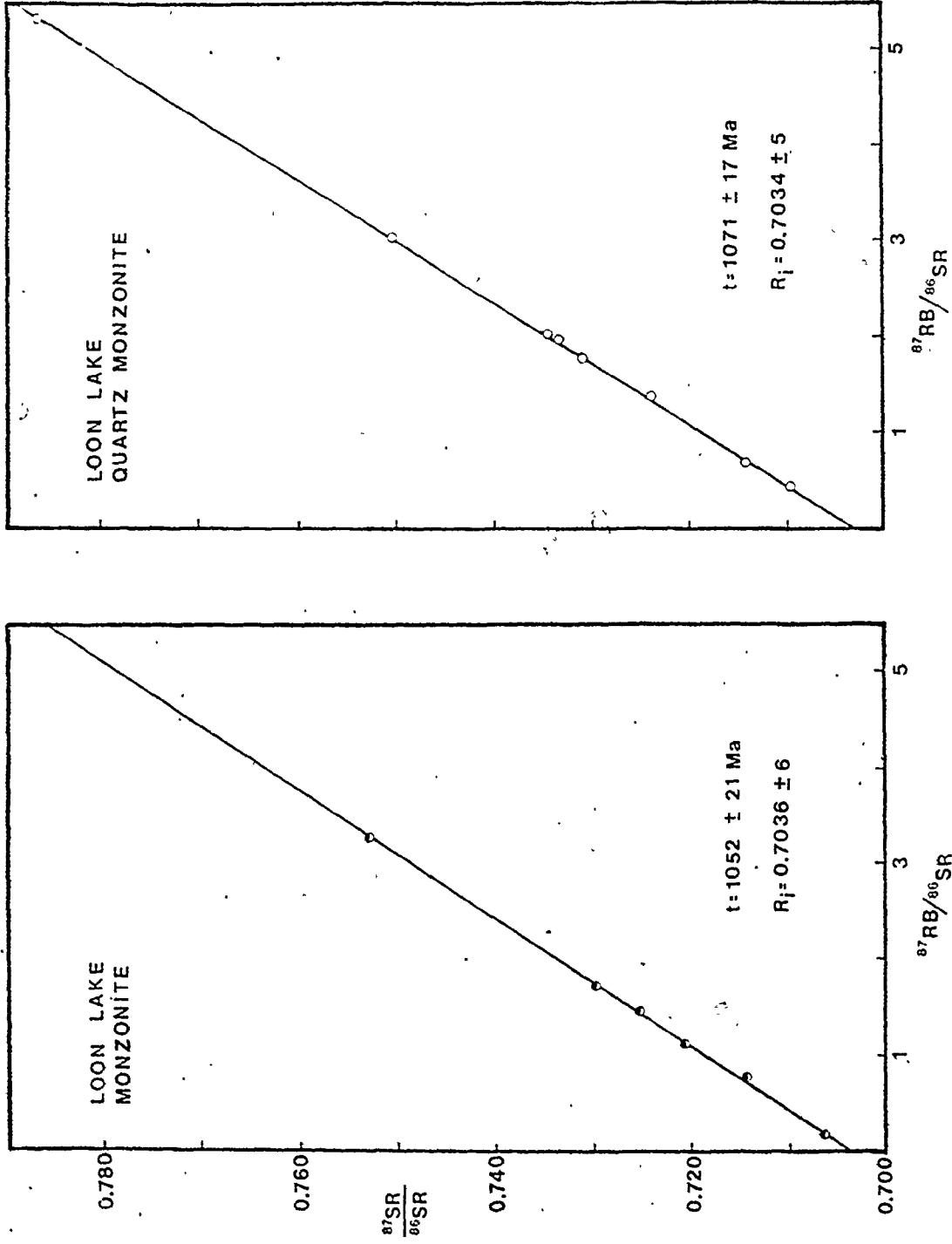
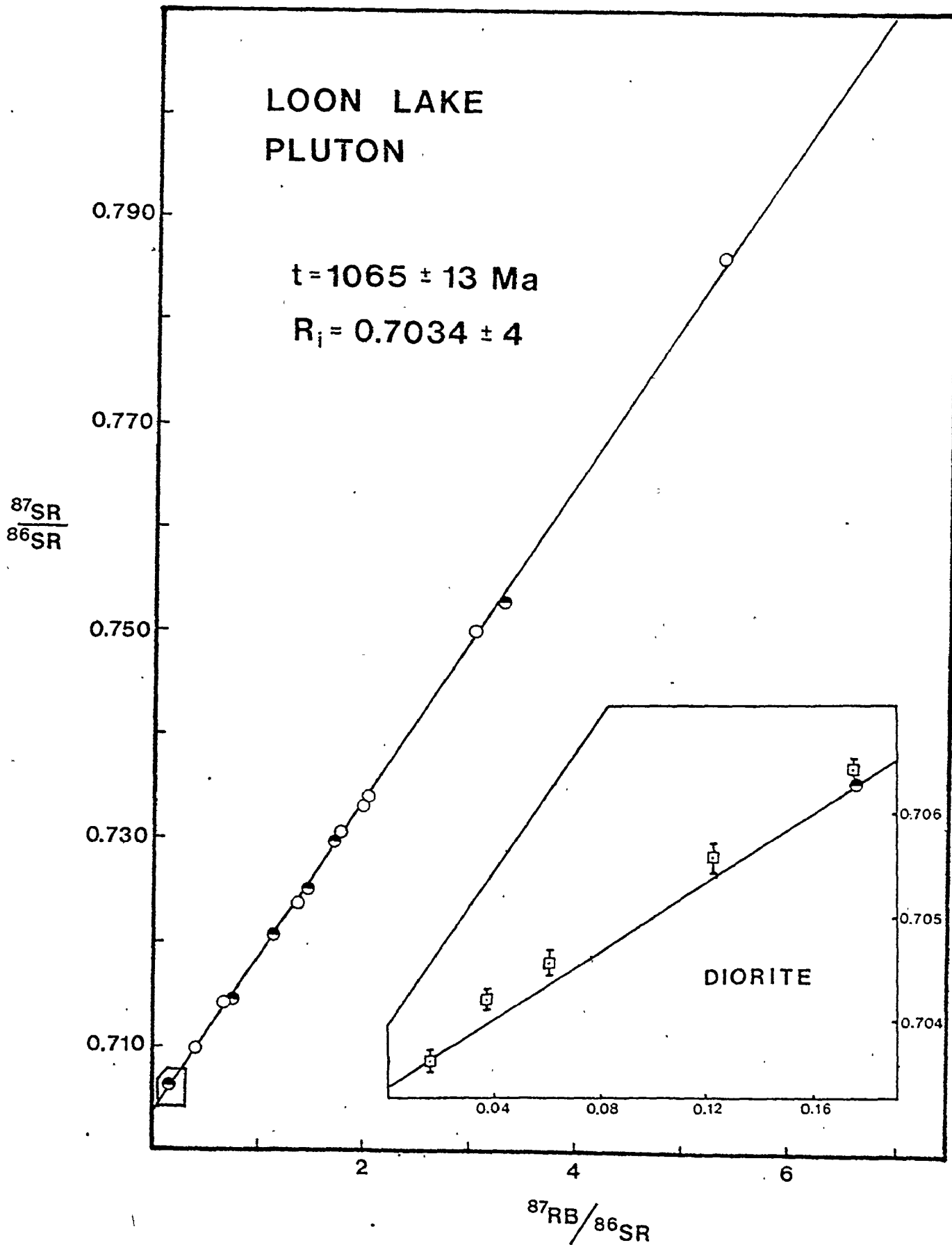


Figure 3.10 Rb-Sr whole rock composite isochron for the Loon Lake pluton. Included in the inset are the results for five diorite samples from isolated bodies within the pluton. The addition of these samples in the regression analysis does not significantly alter the age ( $t=1059$  Ma) or initial strontium ratio (0.7036).

(symbols the same as in Figure 3.9)

FIGURE 3.10 LOON LAKE COMPOSITE ISOCHRON



this data with the Loon Lake composite does not significantly alter the age or initial ratio of the pluton (ie.  $t = 1059$  Ma.;  $R_i = 0.7036$ ). The relationship of this unit to the pluton (ie. roof pendant versus cogenetic end member) cannot be resolved by the Rb-Sr method.

Strontium ratios for four granodiorite gneiss samples are shown in Fig. 3.11 together with reference isochrons for the Apsley gneiss and the Loon Lake pluton. A regression treatment of this data (Table 2.8 and 2.9) indicates a McIntyre II errorchron age of  $1286 \pm 168$  Ma. ( $R_i = 0.7036 \pm 14$ ). Since this regression is based on four samples, the data should not be interpreted as having any geological significance. A more detailed investigation of this unit may elucidate its origin (ie. mixture of Apsley gneiss and monzonite magma or an inclusion of "old" country rock).

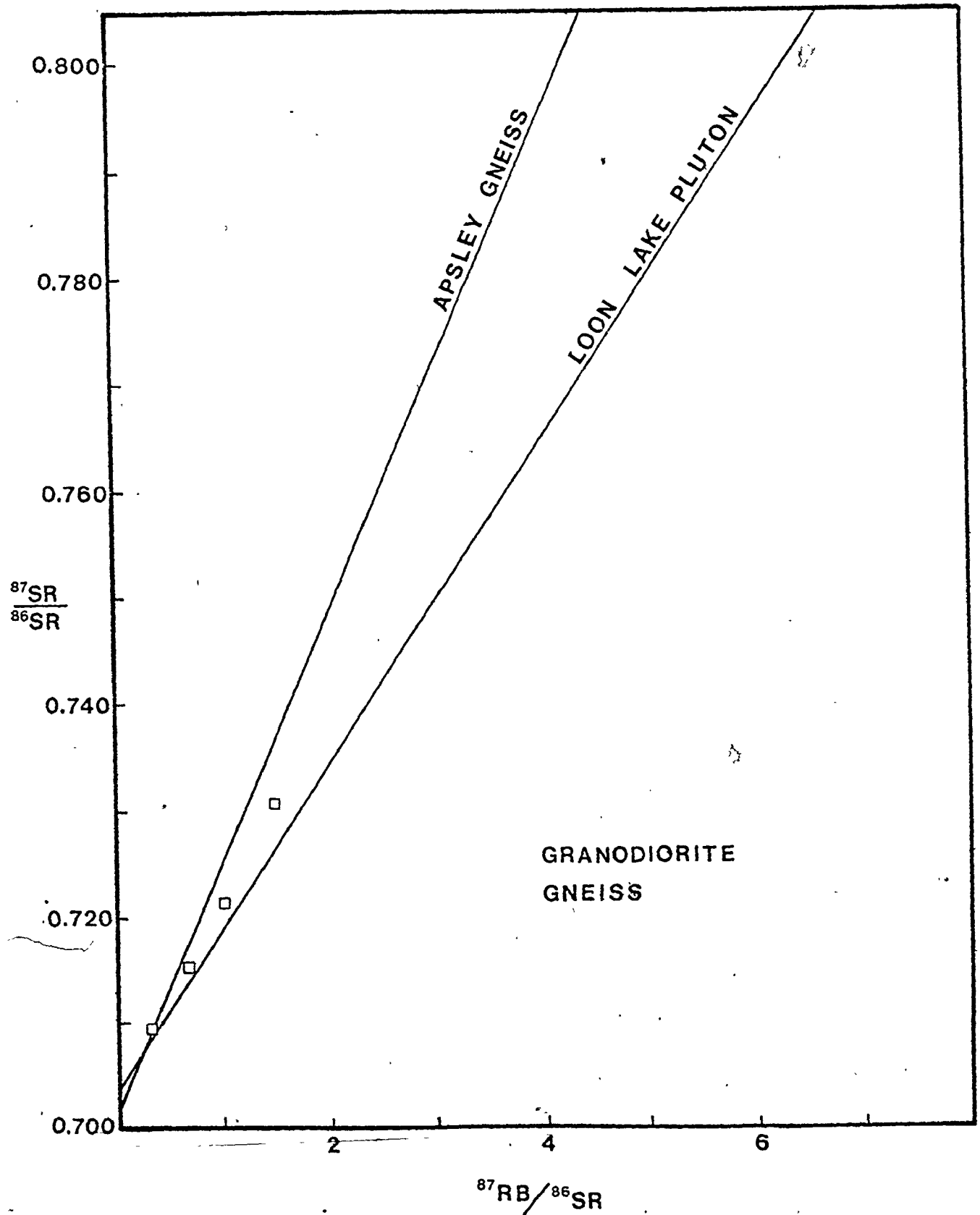
#### 3.4.2 Oxygen Isotope Data

Oxygen isotope analyses on the same whole rock samples used in the Sr isotope study were determined by Yuch-Ning Shieh at Purdue University (W.Lafayette, Indiana). These results are listed in Table 3.3 and supplement the published oxygen isotope data for mineral separates and whole rock samples from the pluton (Shieh et al., 1976).

The range of  $\delta^{18}O_{wr}$  values for the quartz monzonite and monzonite suite (8.8 to 12.0 ‰) is significantly

Figure 3.11 Strontium isotopic results for granodiorite gneiss samples from a discrete unit within the Loon Lake pluton. These samples indicate an errorchron age of  $1286 \pm 168$  Ma ( $R_1=0.7036$ ).

FIGURE 3.11 SR ISOTOPE RESULTS FOR THE GRANODIORITE GNEISS



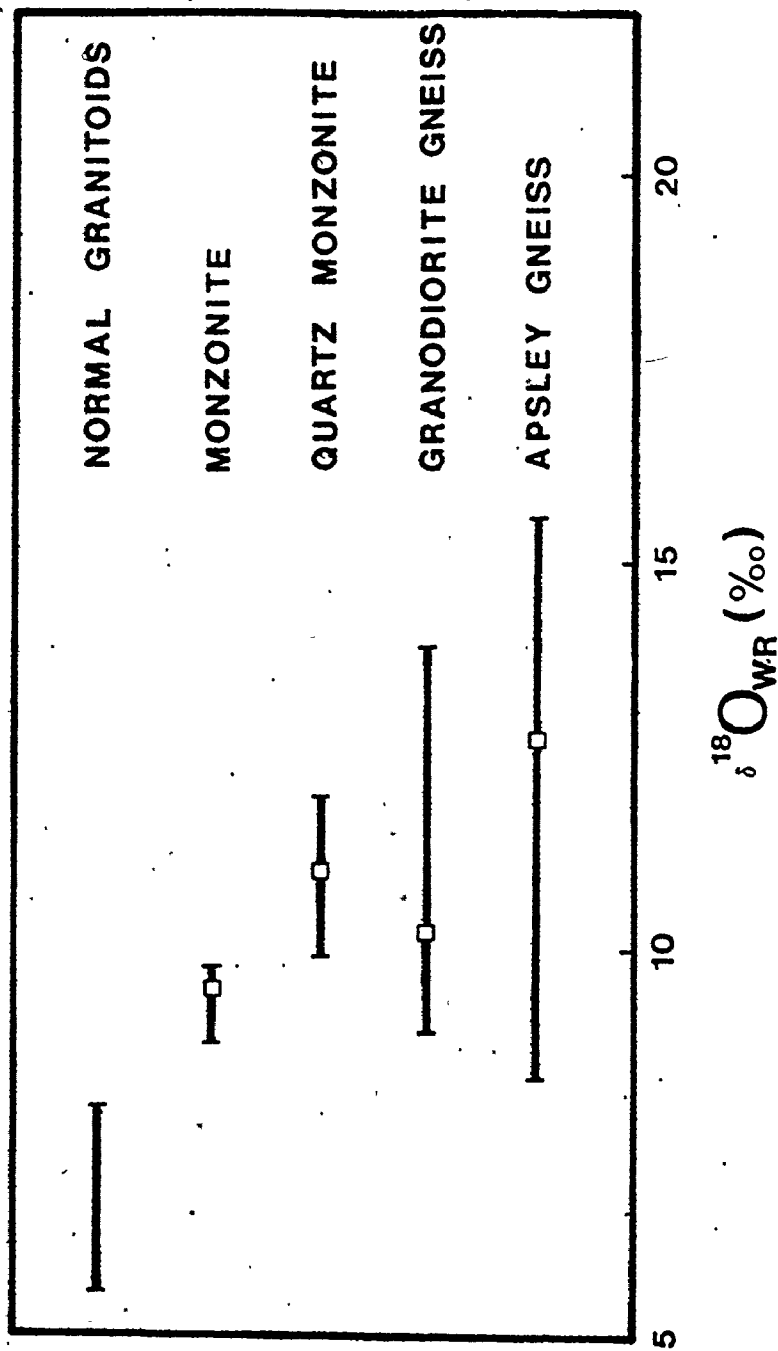


greater than values reported for the low  $\delta^{18}\text{O}$  end of normal granitoids (6.0 to 8.0 ‰) and falls partially within the group of high  $\delta^{18}\text{O}$  granitoids (Taylor, 1978). This range also overlaps with other low to intermediate  $\delta^{18}\text{O}$  plutons in this region (Shieh, 1980). Although the average  $\delta^{18}\text{O}_{\text{WR}}$  value for the quartz monzonites (11.0 ‰) is higher than the average for the monzonites (9.5 ‰), the range for each unit overlaps (Fig. 3.12).

Also included in Fig. 3.12 are the range of  $\delta^{18}\text{O}_{\text{WR}}$  values for the granodiorite gneiss unit and published data for the Apsley gneiss (Shieh et al., 1976). The range for the granodiorite gneiss unit includes the four samples listed in Table 3.3 and one sample (#88) from Shieh et al. (1976) which was incorrectly included in the quartz monzonite group. The average  $\delta^{18}\text{O}_{\text{WR}}$  value for the granodiorite gneiss (10.2 ‰) is not considered representative of the entire unit because the four samples analysed in this study were collected only from the leucocratic bands. Further investigations are necessary to understand the oxygen isotope systematics of this unit.

The monzonite - quartz monzonite data is discussed in chapter IV.

FIGURE 3.12 · OXYGEN ISOTOPE DATA



## CHAPTER IV

### DISCUSSION

#### 4.1 Introduction

In addition to the age determinations reported in the previous chapter, the strontium isotopic data can be used as a useful tracer to monitor major crustal processes. The first part of the discussion outlines the possible mechanisms for generating magmas with low initial strontium ratios. Subsequently, two major enigmas will be addressed concerning the origin and phase relationships of the Loon Lake pluton, attempting to synthesize data from several disciplines.

#### 4.2 Low Initial Strontium Ratios ( $R_i$ )

Models for the evolution of continental crust have been extensively debated over the past two decades and considerable emphasis has been placed on the isotopic systems of Sr and, more recently, Nd (Hurley et al., 1962; Moorbath, 1975a,b; 1977; 1978; DePaolo, 1980). Apart from the controversies concerning the isotopic evolution of the Archean crust (Moorbath, 1977; Fryer et al., 1979), the Proterozoic crust preserves significant variations in the initial Sr and Nd ratios and  $\delta^{18}\text{O}$  data. It is impossible to

define stringent isotopic boundaries which distinguish magmas derived from sialic or subsialic precursors but a relatively high  $R_i$  (ie.  $> 0.706$ ) and  $\delta^{18}O$  (ie.  $> 10 \text{ ‰}$ ) values almost certainly reflect a high sialic component. Since all the units studied in Chandos Twp. have a low  $R_i$  (see Fig. 4.2), four possible mechanisms for generating magmas with a low  $R_i$  will be evaluated:

- (a) Partial melting in the mantle
- (b) Fusion of sialic material with low, mantle-like, Rb/Sr ratios (e.g. granulite or mafic eclogite)
- (c) Partial melting of continental crust which experienced a short crustal residence history (Peterman et al., 1967)
- (d) Disequilibrium\* partial melting of the lower crust

#### 4.2.1 Partial Melting in the Mantle

Frequently, igneous rocks with a low  $R_i$  are assumed to be derived directly from the mantle with little or no interaction with continental crust. A low  $R_i$  should be anticipated if the source has a low, mantle-like, Rb/Sr ratio (ie. 0.02 to 0.04) but such an interpretation should be supported with data from other isotopic systems, geochemistry, and petrography. A good example of the potential danger of this approach is offered by the low  $R_i$  (0.7034) obtained for the Loon Lake pluton in this study. Although this low  $R_i$  alone would support a mantle derivation, the corresponding high  $\delta^{18}O$  values indicate a more complicated

\* refers to isotopic disequilibrium

history. It is examples like this which suggest other mechanisms must also be capable of generating magmas with a low  $R_i$ .

#### 4.2.2 Partial Melting of Low Rb/Sr Crustal Rocks

Crustal lithologies with low Rb/Sr ratios (e.g. granulite, eclogite, and anorthosite) are confined to the lower crust but exposed in Precambrian terrains where 30 to 40 kilometers of rock has been eroded away. In an attempt to characterize the strontium and oxygen isotopic composition of the lower crust, James (1980) analysed the isotopic composition of lower crustal xenoliths from Kilbourne Hole, New Mexico. His results indicated a wide variation in the isotopic composition of these xenoliths (e.g. mafic granulite -  $\delta^{18}O = 6.2$  to  $6.3$  ‰,  $R_i = 0.703$  to  $0.707$ ; garnet granulite -  $\delta^{18}O = 9.0$  to  $12.0$  ‰,  $R_i = 0.71$  to  $0.78$ ) and is one of the first studies to show that the lower crust has discrete isotopic domains. It is therefore possible to generate partial melts from these low  $R_i$  domains which would also have a low  $R_i$ .

A full spectrum of isotopic values may exist in the lower crust so it is vital to combine information from other fields with isotopic data to converge on the most probable source material (s).

#### 4.2.3 Short Crustal Residence Histories

Partial melting of average continental crust (Rb/Sr = 0.25) produces magmas with a high  $R_i$  (ie. > 0.706) because of the relatively rapid generation of radiogenic strontium (Moorbath, 1975a). However, Peterman et al. (1967) proposed a model whereby fusion of a relatively young eugeosynclinal sequence could generate magmas with a low  $R_i$ . This model requires the time lapse between formation and fusion of a protolith (ie. residence time) to be less than a few hundred Ma. Alternatively, if the sequence contains a large proportion of mantle derived volcanics with low Rb/Sr ratios then anatexis of this sequence could also generate partial melts with a low  $R_i$ .

#### 4.2.4 Disequilibrium Partial Melting

In the context of this discussion, disequilibrium refers to high grade metamorphic conditions where isotopic homogenization between individual minerals was not achieved. Equilibrium partial melting is often assumed during anatexis but rarely justified. Detailed studies on high grade metamorphic rocks indicates that Sr isotopic equilibrium may be limited to distances less than one centimeter (Krogh and Davis, 1973). Evidence from oxygen isotopes testifies to the isotopic disequilibrium between new phases which formed at some specific high grade isograd and the main reacting phases (Hoernes and Hoffer, 1979).

Other indirect evidence for isotopic disequilibrium comes from ultramafic nodules derived from the mantle. Although the role of contamination is uncertain, studies such as that of Steuber and Ikramuddin (1974) indicate that the constituent mineral phases of these nodules are not in isotopic equilibrium.

It therefore seems appropriate that disequilibrium partial melting should be evaluated as a potential mechanism for maintaining a low  $R_i$  during crustal anatexis. The following hypothetical example was selected to qualitatively evaluate the effect of disequilibrium partial melting of a high grade gneiss on the  $R_i$  of the resulting magma.

The strontium isotopic composition of partial melts derived from non-modal disequilibrium melting of a four phase system, similar to the "typical" quartz-plagioclase-K feldspar-biotite paragneiss described by Winkler (1976), is illustrated in Figure 4.1. In constructing this diagram, it was assumed that quartz contributed no strontium to the melt and the strontium isotopic composition of plagioclase, K feldspar, and biotite at the time of melting was 0.702, 0.725, and 0.770 respectively. To examine the effect of varying the strontium contribution from each phase it was necessary to maintain a constant contribution from one mineral. In this example, the K feldspar contribution (K) was assumed constant and three curves were constructed for

K values of 1, 5, and 10 respectively (Fig. 4.1).

The proportionality index (PI) is a ratio indicating the proportion of strontium contributed to the melt by plagioclase and biotite (see Table 4.1). The proportion of strontium contributed by plagioclase, for instance, is related to the strontium concentration in plagioclase and the distribution coefficient for Sr between plagioclase and melt. High PI values indicate a substantial contribution from plagioclase whereas lower PI values represent an increasing contribution from biotite.

One major constraint imposed by this example is that biotite and K feldspar must individually contribute less than 5% of the total strontium in the melt in order to retain an  $R_1$  lower than 0.706 (see Fig. 4.1). This is not unreasonable as the structure of biotite and K feldspar do not accommodate significant concentrations of strontium and field studies in migmatite terrains indicate that biotite, at least, is strongly enriched in the residual paragenesis (Mehnert, 1968; Dougan, 1979). Furthermore, experimental studies confirm the importance of quartz and plagioclase dissociation during the early stages of anatexis (Winkler, 1976). However, before a model of this nature can be advanced it is imperative to reconcile other trace and major element constraints.

Although this is only a hypothetical model, it does support the possibility of generating magmas with a low R.



72a

Figure 4.1 Theoretical calculations for the effect of disequilibrium (non-modal) partial melting on initial strontium ratios. A theoretical index (PI) is calculated which relates to the proportion of strontium contributed to the melt by plagioclase and biotite. The fraction of strontium contributed by K feldspar is kept constant and three models are calculated where K feldspar contributes 1, 5, and 10 % of strontium to the melt.

FIGURE 4.1

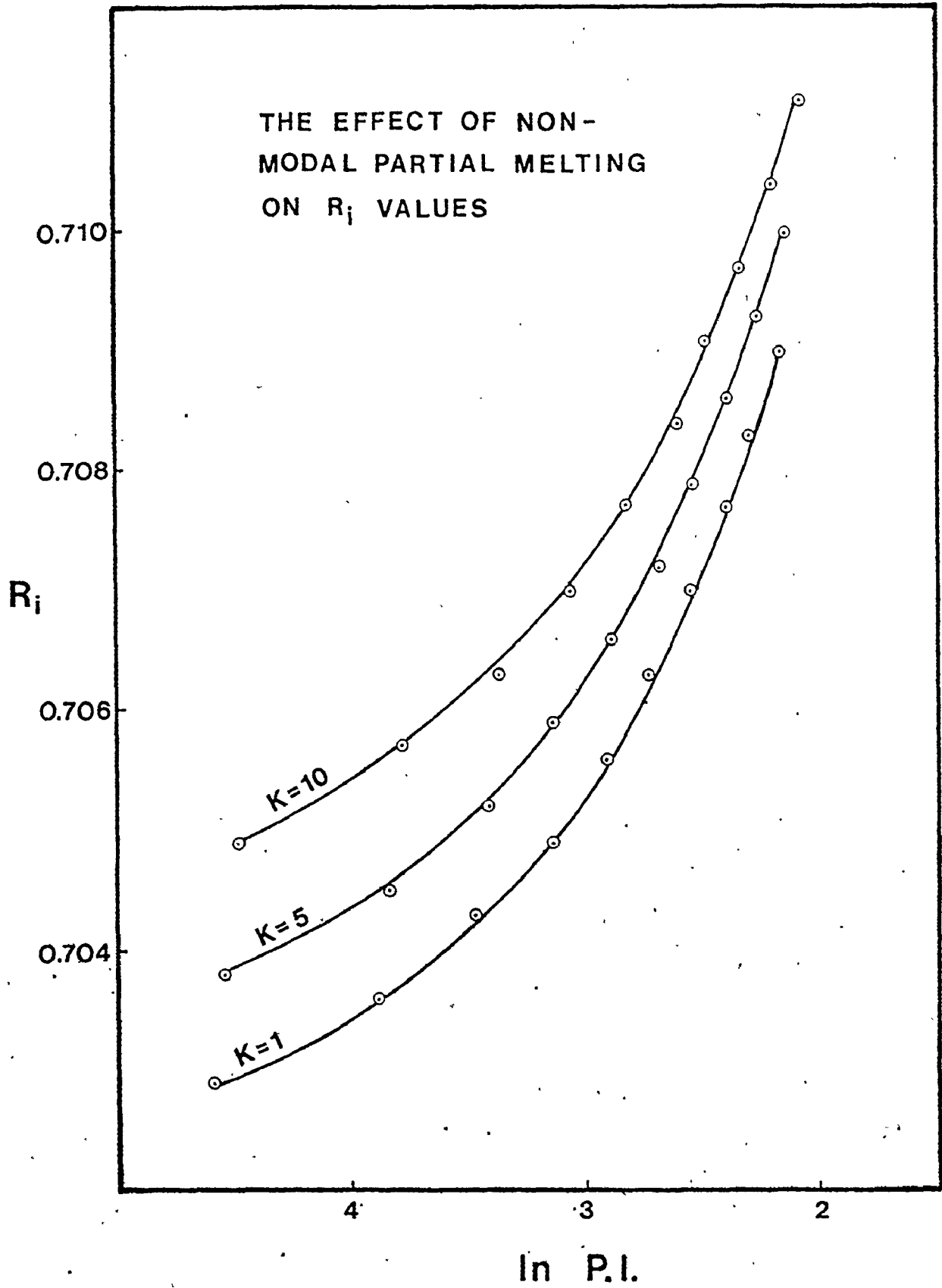


Table 4.1 Initial strontium ratio calculations for disequilibrium partial melting

K = 1 <sup>a</sup>	K = 5			K = 10					
	P:B <sup>b</sup>	PI <sup>c</sup>	$\frac{87\text{Sr}}{86\text{Sr}}$	P:B	PI	$\frac{87\text{Sr}}{86\text{Sr}}$	P:B	PI	$\frac{87\text{Sr}}{86\text{Sr}}$
	98:1	98.0	0.7029	94:1	94.0	0.7038	89:1	89.0	0.7049
	97:2	48.5	0.7036	93:2	46.5	0.7045	88:2	44.0	0.7057
	96:3	32.0	0.7043	92:3	30.6	0.7052	87:3	29.0	0.7063
	95:4	23.8	0.7049	91:4	22.8	0.7059	86:4	21.5	0.7070
	94:5	18.8	0.7056	90:5	18.0	0.7066	85:5	17.0	0.7077
	93:6	15.5	0.7063	89:6	14.8	0.7072	84:6	14.0	0.7084
	92:7	13.1	0.7070	88:7	12.6	0.7079	83:7	11.9	0.7091
	91:8	11.4	0.7077	87:8	10.9	0.7086	82:8	10.3	0.7097
	90:9	10.0	0.7083	86:9	9.6	0.7093	81:9	9.0	0.7104
	89:10	8.9	0.7090	85:10 <sup>c</sup>	8.5	0.7100	80:10	8.0	0.7111

<sup>a</sup> percent strontium contribution to the melt from k-feldspar

<sup>b</sup> percent strontium contribution to the melt from plagioclase (P):biotite (B)

<sup>c</sup> PI = (P/B)

by disequilibrium partial melting. A variation of this model which could equally be as important is the contamination of an ascending basaltic magma, which originated in the mantle, with partial melts derived by disequilibrium partial melting of continental crust.

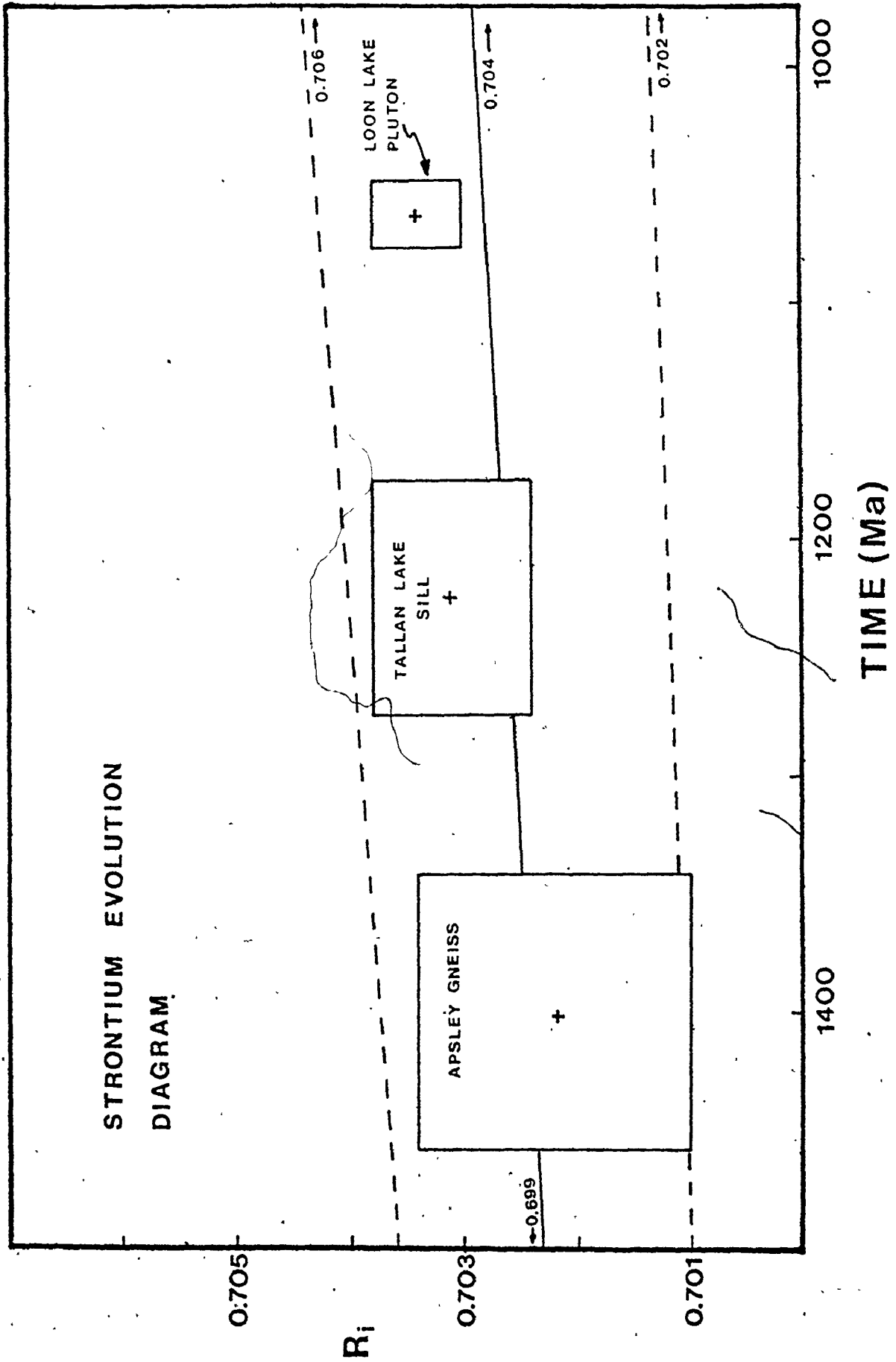
It is not the intent of this discussion to suggest ways to distinguish between each of these mechanisms but to merely clarify a common misconception that a low  $R_i$  indicates mantle derivation. With this background it is now possible to discuss the significance of each  $R_i$  determined for the rocks from Chandos Twp.

#### 4.3 Initial Strontium Ratios From Chandos Twp.

The  $R_i$  data for the sodic Apsley gneiss (0.7022), Tallan Lake sill (0.7031), and Loon Lake pluton (0.7034) are indicated on the strontium evolution diagram (Fig. 4.2) by crosses. The rectangle which surrounds each point represents the associated error. Included on this diagram is the mantle evolution line ( $^{87}\text{Rb}/^{86}\text{Sr} = 0.074$ ) which is defined at 4.6 Ga. by BABI (Basaltic Achondrite Best Initial) and at present by the average isotopic ratio for relatively unaltered oceanic basalt (0.704). There is some controversy over the present day strontium isotopic composition of the mantle so a range of values (0.702 to 0.706) are included in Fig. 4.2 to illustrate the domain of mantle evolution.

Figure 4.2 Strontium evolution diagram for units from Chandos Township. The size of the rectangle represents the error associated with each  $R_i$  and the dashed lines represent the domain for mantle evolution.

FIGURE 4.2



Preliminary examination of Figure 4.2 indicates that all the units analysed fall within the domain for mantle evolution. Considering the above discussion, there are several possible mechanisms, other than direct mantle derivation, which could explain these low  $R_1$  values so additional information must be synthesized in order to present a meaningful interpretation of this data. The interpretation of the Loon Lake data is deferred to a later section which is devoted to the origin of this pluton.

The low  $R_1$  for the Tallan Lake sill is consistent with the contention of Griep (1975) that this sill represents a product of differentiation of a basaltic magma which originated in the mantle. Although heat flow calculations for a basaltic sill predict contamination by crustal partial melts or circulating fluids (Patchett, 1980), the similarity of the Fe enrichment trend with other differentiated sequences (Griep, 1975) and the co-linearity of the strontium isotopic data (Fig. 3.8) implies that significant crustal contamination was not involved in the evolution of this sill.

It is more difficult to interpret the Apsley gneiss data. The simplest explanation for the low  $R_1$  is that the sodic Apsley gneiss (positive DF values) represents a sequence of metamorphosed silicic volcanics (see Shaw, 1972) which retained a mantle signature. However, Shieh et al. (1976) have shown that the ha

$\delta^{18}O$  values (8.3 to 13.4 ‰) and is within the range for both hydrated silicic volcanics and sandstones. This data exemplifies the difficulty in interpreting a low  $R_i$ : especially from high grade metamorphic rocks. Even after combining the available information it is still difficult to distinguish between a mantle derivation followed by selective crustal contamination  $\pm$  hydration and partial melting of a eugeosynclinal sequence which experienced a short crustal residence history.

#### 4.4 Monzonite - Quartz Monzonite Association

Numerous igneous plutons exhibit a compositional zonation from relatively mafic margins to more felsic cores (Vance, 1961; Karner, 1968; Bateman and Chappell, 1979; and Halliday et al., 1980). The most appealing hypothesis for this zonation is the preferential crystallization of the magma from the margins inward (Vance, 1961) but other models such as assimilation of mafic country rock by a felsic magma or multiple intrusion have also been advanced (Compton, 1955; Saha, 1959).

The zonal pattern in the Loon Lake pluton and other monzonitic plutons from the Grenville Province (Ermanovics, 1970) is anomalous in this regard because the more mafic end member (monzonite) occurs in the core of the pluton. This relationship is not amenable to a model which invokes early preferential crystallization at the margins so the following



alternative processes capable of enriching the margin in silica are reviewed below:

- (a) Silica Metasomatism (Shaw, 1962; Fox and Moore, 1969)
- (b) Mixing - Assimilation (Wynne-Edwards, 1957; Saha, 1959; Ermanovics, 1970)
- (c) Separate Intrusions (Saha, 1959; Dostal, 1973)
- (d) Fractional Crystallization

The zonation in the Loon Lake pluton has been previously addressed by Saha (1959), Shaw (1962), and Dostal (1973). The following discussion attempts to incorporate the isotopic and trace element data from this study with the results from their work.

#### 4.4.1 Silica Metasomatism

Silica metasomatism was initially proposed by Shaw (1962) as a viable mechanism for enriching the rim of the Loon Lake pluton in quartz. The close proximity of sillimanite-cordierite-garnet rocks was interpreted as support for this hypothesis, as they could possibly represent original country rock (biotite paragneiss) depleted in silica. Subsequently, Dostal (1973) used geochemical criteria to refute this model because both units exhibit smooth and often continuous major and trace element patterns and their normative compositions fall within the low temperature trough of the "granite" quaternary system. In addition,

the oxygen isotope data for co-existing mineral pairs (Shieh et al., 1976) indicates mineral equilibration at magmatic temperatures in both the margin and core of the pluton: thus providing further evidence against interaction of a low temperature fluid with consolidated monzonite.

A slight variation of the silica metasomatism model was advanced by Shieh et al. (1976) to reconcile the above information with the higher average  $\delta^{18}\text{O}$  data obtained for the quartz monzonites (see section 3.4.2). These authors suggested that the available data could be explained by progressive silicification at the margins of a monzonitic magma by the interaction of a high temperature fluid phase derived from the country rocks. This mechanism adequately explains the oxygen isotope data, the gradational boundary between the monzonite and quartz monzonite, and possibly the normative composition of the quartz monzonites. The position of the quartz monzonite samples in the Qz-Ab-Or ternary system (see Dostal, 1973) maybe somewhat precarious because it is possible to shift the normative composition of the monzonites from near the Ab-Or join towards the quartz apex by silica metasomatism as well as fractional crystallization.

It seems inevitable that a fluid phase derived from the country rock would be enriched in other components, besides silica, which likewise have a high affinity for the fluid phase (e.g. the alkali metals; Holloway, 1979). In fact, the quartz monzonites are strongly enriched in

rubidium (Fig. 4.3 and 4.6) beyond concentrations predicted by fractional crystallization or assimilation (see section 4.4.2 and 4.4.4). This enrichment may be further evidence for the involvement of a fluid phase in the evolution of this pluton.

There is no evidence to suggest that strontium from the Apsley gneiss was introduced into the magma as the margin and core of the pluton have similar initial strontium ratios. However, there are no strong arguments at variance with the mechanism proposed by Shieh et al. (1976).

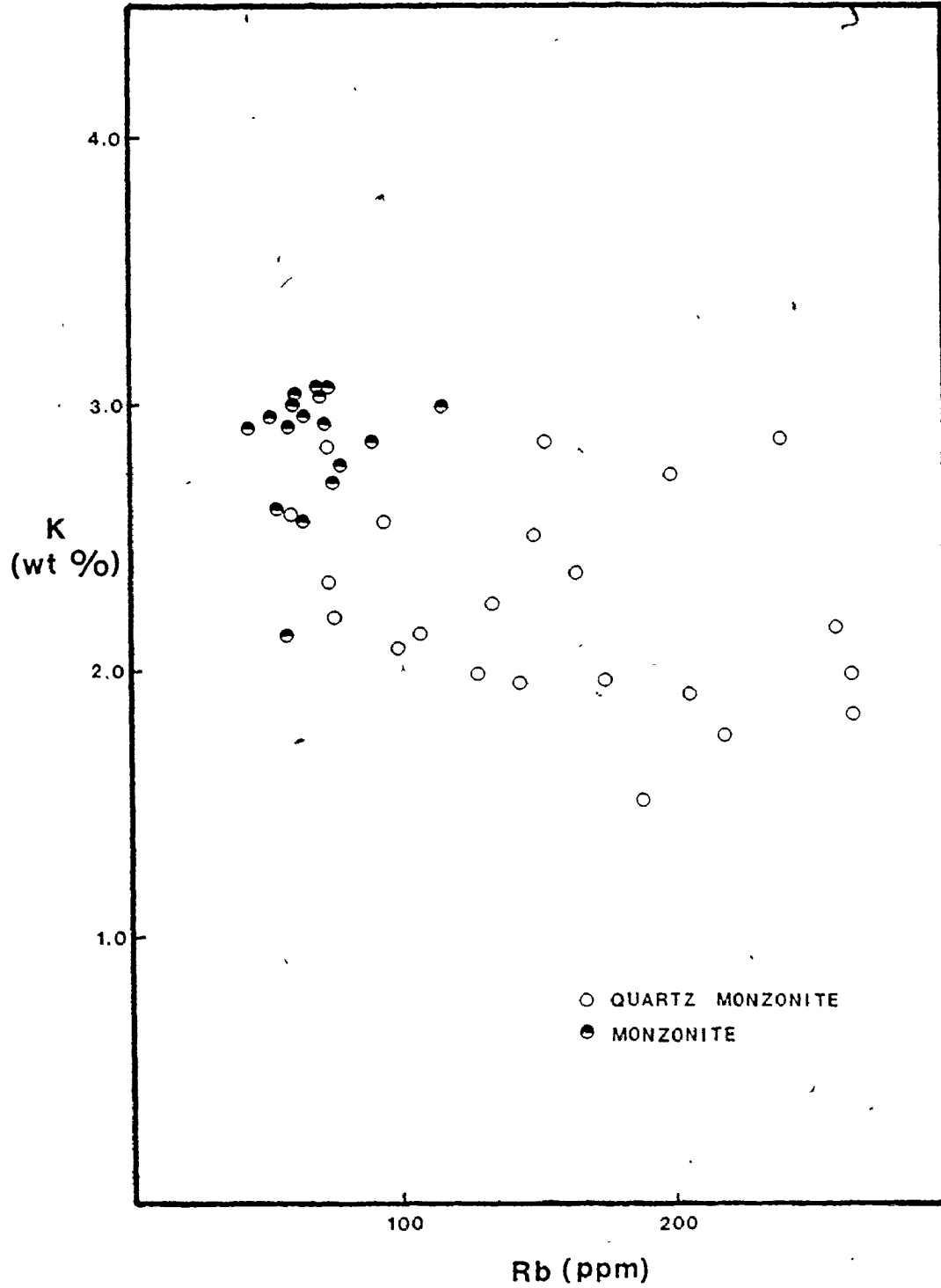
#### 4.4.2 Mixing - Assimilation

Mixing of two unique isotopic reservoirs has been suggested as an important crustal process in certain geological environments (e.g. Vollmer, 1976; Langmuir et al., 1978; Cortecchi et al., 1979; Michard-Vitrac et al., 1980; and Harmon and Halliday, 1980). These authors proposed that simple two component mixing can often be identified and are not masked by secondary processes. To evaluate the role of mixing in the evolution of the Loon Lake pluton, four potential mixing processes will be examined:

- (a) Vapor-Solid (various hydration and vein forming processes)
- (b) Vapor-Liquid (diffusion of a fluid into a magma)
- (c) Liquid-Solid (assimilation of country rock by a magma)

Figure 4.3 K-Rb variation diagram for monzonite and quartz monzonite samples from the Loon Lake pluton. This diagram shows the extreme enrichment in Rb for the quartz monzonites.

FIGURE 4.3 K - RB VARIATION DIAGRAM (LOON LAKE PLUTON)



## (d) Liquid-Liquid (mixing of two magmas)

The first two mechanisms were discussed in the previous section with regard to silica metasomatism and are not discussed further here.

An alternative mechanism for silica enrichment at the margin of this pluton is the assimilation of country rock by a monzonitic magma (Wynne-Edwards, 1957; Saha, 1959). The effect of assimilation on the evolution of a magma has been summarized by Taylor (1986):

"The heat necessary to raise the temperature and then react with and dissolve the stopped blocks of country rock is produced by the latent heat of crystallization of the minerals already crystallizing in the magma... The principle effects are simply to enhance the proportions of late differentiates and to speed up fractional crystallization with only slight perturbations in the normal liquid line-of-descent."

Consequently, the major element composition of the magma may not be significantly altered by assimilation but a contaminated magma is often reflected in isotopic and trace element patterns.

The most severe constraint on the role of assimilation in this pluton is the identical initial strontium ratios for the monzonite core and the quartz monzonite rim (see section 3.4.1). Total assimilation of Apsley gneiss would result in a higher  $R_1$  for the quartz monzonite than the primary monzonite magma.

The mixing of a monzonitic magma with an anatectic melt derived from the country rock (mechanism 4) was

proposed by Dostal (1973) to explain the origin of the quartz monzonite unit. It is possible to maintain a low  $R_i$  in an anatectic melt derived from older crustal lithologies (see sections 4.2.2; 4.2.3; and 4.2.4) but it would be somewhat coincident if this melt acquired an identical  $R_i$  as an ascending magma that probably originated in a totally different environment.

Further support against significant contamination of a monzonitic magma by locally derived melts is gained from several trace element distribution patterns. One example is the  $TiO_2$  - Zr variation diagram (Fig.4.4) in which the field for the Apsley gneiss (data from Shaw, 1972) is significantly removed from the main monzonite - quartz monzonite trend. Considering the low partition coefficients for Zr and Ti reported by Pearce and Norry (1979), melts derived from the Apsley gneiss would be too enriched in these elements to account for the quartz monzonite distribution by mixing with a monzonitic magma. Similar arguments can be developed for rubidium and strontium.

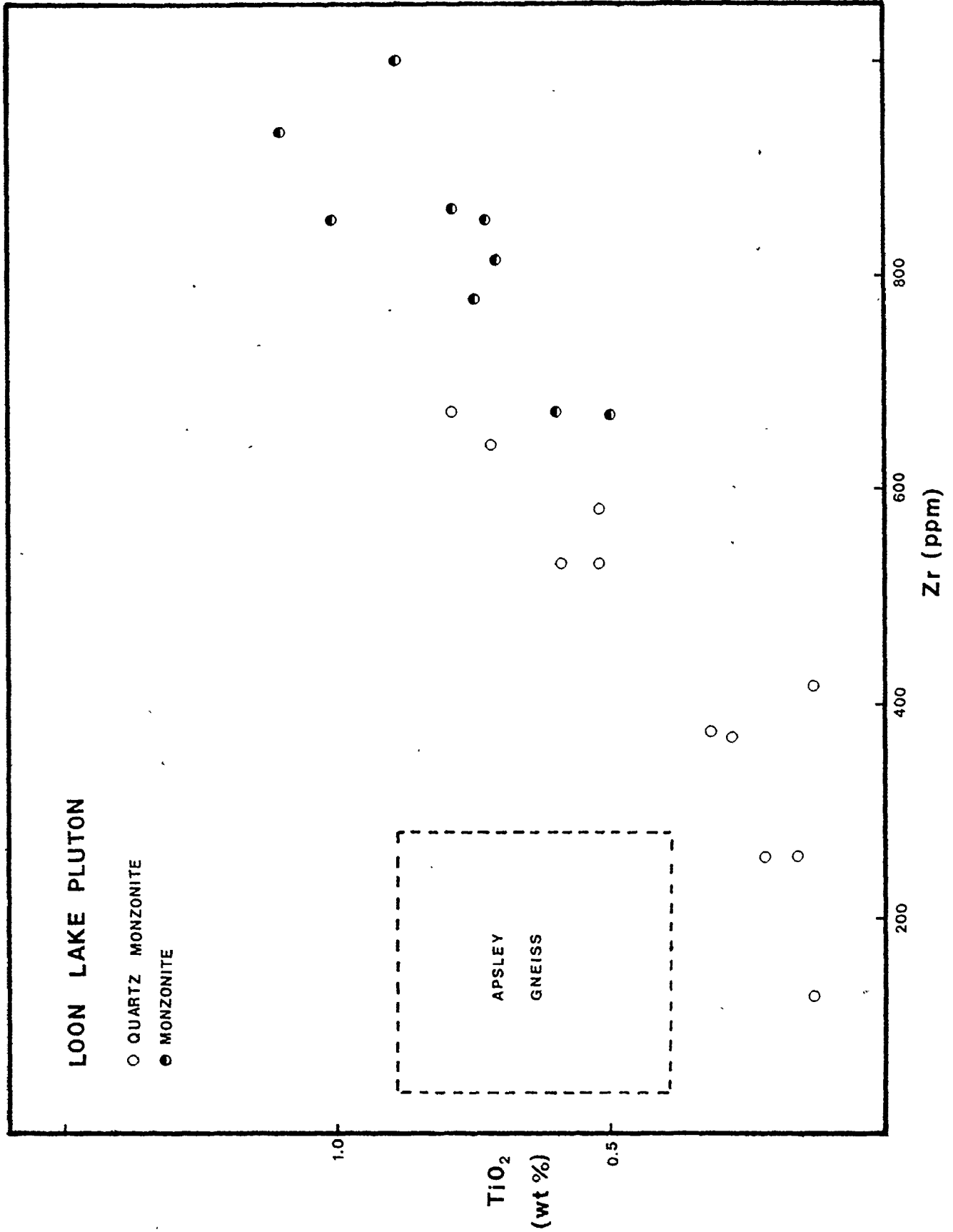
#### 4.4.3 Separate Intrusions

An alternative mechanism involves the separate intrusion of monzonitic and quartz monzonitic magma (Dostal, 1973). In order to explain the smooth geochemical variations between these units, Dostal (1973) proposed that separate melt compositions could be extracted from a

Figure 4.4  $\text{TiO}_2$  - Zr variation diagram for monzonite and quartz monzonite samples from the Loon Lake pluton. Included is the field for the Apsley gneiss (data from Shaw, 1972). The low partition coefficients for Zr indicate that partial melts from the Apsley gneiss would be too enriched in Zr to explain the trend of the quartz monzonites.



FIGURE 4.4 TiO<sub>2</sub> - Zr VARIATION DIAGRAM



chemically differentiated and stratified magma. This process was preferred over continuous fractional crystallization of a single magma because of the overlap in major and trace element chemistry and the difficulty of generating residual quartz.

The strontium isotope data (section 3.4.1), in general, is compatible with this model. If two fractions from the same magma are extracted, then the  $R_i$  of each melt should be identical provided there has been no subsequent contamination. However, there is no field evidence to indicate that these two units were emplaced separately.

In addition, fractional crystallization of a magma may cause a slight  $\delta^{18}O$  enrichment in the late stage differentiates (Harmon and Halliday, 1980) but this shift is generally less than 1.5 ‰ (Taylor, 1978). Therefore, it is questionable whether this model could generate the hiatus between average monzonite (9.5 ‰) and quartz monzonite (11.0 ‰).

#### 4.4.4 Fractional Crystallization

The smooth and often continuous geochemical trends reported for the monzonite and quartz monzonite suites (Dostal, 1973) and their similar  $R_i$  supports a cogenetic relationship between these units. To examine this contention in greater detail, the Rb and Sr data from this study were combined with the data reported by Dostal (1973) on a log

Rb versus log Sr diagram (Fig. 4.5). It is apparent from this diagram that the monzonite suite defines a smooth trend which contrasts markedly with the scatter in the quartz monzonite data. Attempts to model geochemical trends in granitoid complexes (e.g. McCarthy, 1976; Rapela and Shaw, 1979; McCarthy and Groves, 1979) indicate that primary trace element trends generated by fractional crystallization in a magma are often preserved.

In order to model the monzonite trend, the liquid line-of-descent for a monzonitic magma was traced in the granite tetrahedron (Fig. 4.6). The initial magma composition falls on the two feldspar cotectic surface near the Ab-An-Or plane. As fractional crystallization of two feldspars and mafic minerals proceed, the composition of the melt approaches the cotectic line where quartz becomes a major crystallizing phase. The minor amounts of quartz in the monzonite suite can be explained if various proportions of intercumulus melt crystallized after the melt composition reached the cotectic line.

The trace element concentrations were calculated from the Rayleigh fractionation equations:

$$C_1 = C_0 F^{(D-1)} \quad \text{and} \quad C_s = C_0 D F^{(D-1)} \quad (\text{Gast, 1968})$$

where:  $C_1$  = trace element concentration in the melt

$C_s$  = trace element concentration in the solid

$C_0$  = trace element concentration in the initial magma

F = fraction of melt remaining




Figure 4.5 Log Rb - log Sr variation diagram for monzonite and quartz monzonite samples from the Loon Lake pluton. The monzonite trend is bounded by the solidus trend (solid line) and liquidus trend (dashed line) derived from Rayleigh fractionation equations. The scatter in the quartz monzonite data cannot be attributed to a simple fractional crystallization model.

FIGURE 4.5 LOG RB - LOG SR VARIATION DIAGRAM

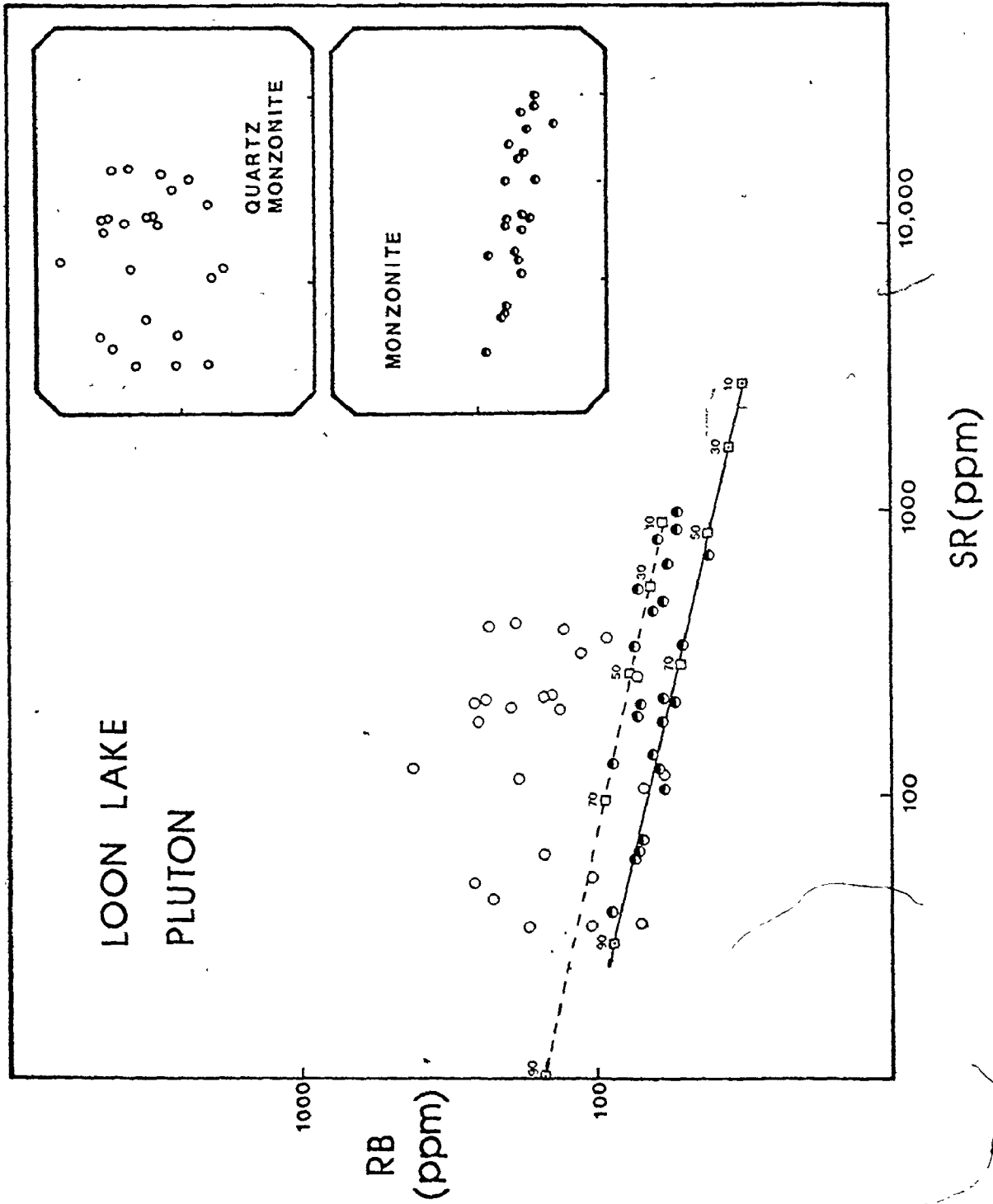
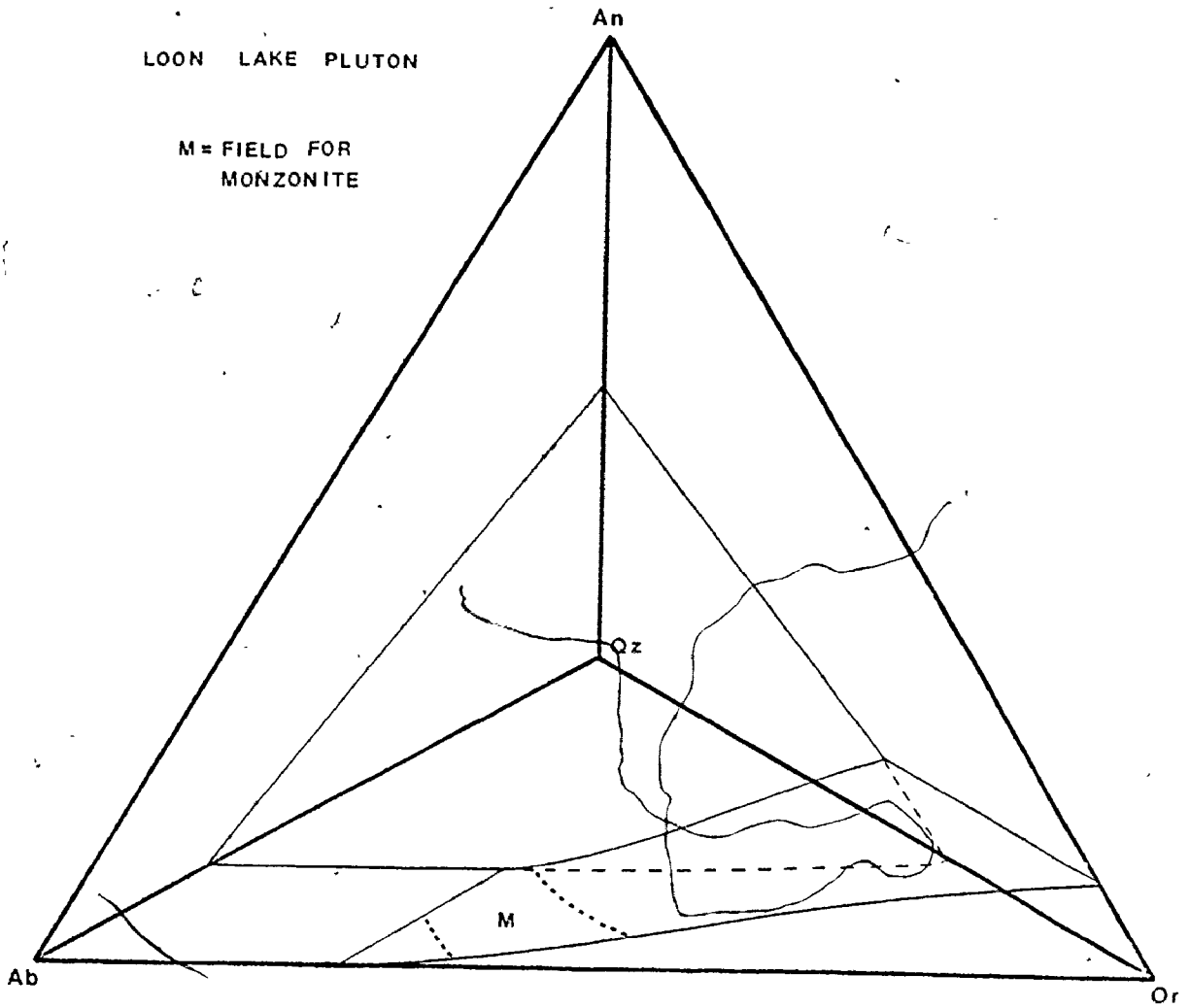


FIGURE 4.6 GRANITE QUATERNARY SYSTEM



$D$  = bulk distribution coefficient  $(\sum_i X_i K_i / 1)$

$X_i$  = modal proportion of phase  $i$  crystallizing from the magma

$K$  = solid/melt partition coefficient

Rubidium and strontium concentrations in the original monzonitic magma ( $C_0$ ) were estimated as 55 ppm and 1100 ppm respectively, while the initial proportion of phases crystallizing from this magma were considered to be equivalent to the average modal composition of the monzonite (see Table 4.2 and 4.3). The partition coefficients for Rb and Sr, used to calculate the bulk distribution coefficient ( $D$ ), are those reported by McCarthy and Groves (1979) and are reproduced in Table 4.2.

Most of the monzonite samples are confined by the liquidus (dashed line) and solidus trends (Fig. 4.5) and can be interpreted to represent various proportions of cumulate and intercumulus melt at different stages of crystallization (McCarthy, 1976).

Conversely, the scatter in the quartz monzonite data cannot be explained solely by continuous fractional crystallization of a monzonitic magma. The addition of quartz to the solidus does not alter the trace element trend sufficiently to account for this scatter. There is independent evidence that an  $H_2O-CO_2$  fluid can have a profound effect on elemental partitioning (Holloway, 1979) but there is no evidence for increased volatile activity

Table 4.2 Trace element partition coefficients used in model calculations (after McCarthy and Groves, 1979)

	<u>Plag</u>	<u>Kfeld</u>	<u>Bio</u>	<u>Hb</u>	<u>Qtz</u>
Rb	0.04	0.8	3.0	0.01	0.0001
Sr	3.35	3.6	0.4	0.06	0.0001
*	43	46	6	3	2

\* Initial Modal Proportion of Crystallizing Phases (%)

Table 4.3 Trace element concentrations (ppm) in melt ( $C_l$ ) cumulates ( $C_s$ )

<u>F<sup>a</sup></u>	<u>Sr</u>		<u>Rb</u>	
	<u>C<sub>l</sub></u>	<u>C<sub>s</sub></u>	<u>C<sub>l</sub></u>	<u>C<sub>s</sub></u>
10	8	26	155	85
30	85	267	95	52
50	253	789	75	41
70	516	1611	65	36
90	880	2746	58	32

<sup>a</sup> percent crystallization



in the rim of the pluton (ie. pegmatitic mineral development or miarolitic cavities). Unfortunately, the paucity of fluid/melt partition coefficients restrains a semi-quantitative appraisal of the effect of volatiles.

Considering all the above data, it is difficult to derive the quartz monzonites simply by fractional crystallization of a monzonitic magma. The enrichment of Rb in the margin of the pluton and the significant hiatus in average  $\delta^{18}\text{O}$  data for each unit attests to a more complicated genesis involving one or more of the processes described above. However, fractional crystallization does play an important role in the evolution of the pluton and adequately explains the systematic and often continuous variation in major and trace element compositions and the similar  $R_i$  for these units.

#### 4.5 Origin of the Loon Lake Pluton

To determine the origin of a plutonic suite, it is necessary to combine all the available geochemical and petrological information to trace the plutons evolution back to its source. In an attempt to identify the source of several Paleozoic plutons from Australia, Chappell and White (1974) differentiated between granitoids derived from sedimentary precursors (S-type) and those formed by fusion of an igneous source (I-type). The distinguishing features of each granitoid type are presented in Table 4.4 accompanied

Table 4.4 Granitoid Classification

	<u>S-type</u>	<u>I-type</u>	<u>Loon Lake Pluton</u>
Mafic minerals	musc,bio, gn, cd	bio,hb	bio,hb
Accessory minerals	mon,il , sph	sph,ap,mt	sph,ap,mt(?)
Xenoliths	metasedimentary	mafic cognates	metasediment and mafic inclusions
Variation Diagrams	irregular	smooth	smooth <sup>1</sup>
Associated mineralization	Sn	porphyry Cu	nil
$Al_2O_3/Na_2O + K_2O + CaO$	> 1.1	< 1.1	< 1.1
Normative corundum	> 1.0%	< 1.0%	< 1.0%
Compositional variation	restricted	varied-associated with mafic rocks	varied
$R_i$	> 0.708	0.704-0.706	0.7034
$\delta^{18}O_{wr}$	> 15%	5-10%	8.8-12.0%

<sup>1</sup> Dostal, 1973.

musc - muscovite; bio - biotite; gn - garnet; cd - cordierite; hb - hornblende; mon - monazite;  
 il - ilmenite; sph - sphene; ap - apatite; mt - magnetite

by the corresponding characteristics of the Loon Lake pluton.

Extreme caution should be enforced in extending this classification scheme to the Proterozoic but it is interesting that the Loon Lake pluton has many similarities to I-type granitoids. This class of granitoids was originally interpreted to be derived directly from the mantle (Chappell and White, 1974) but other sources such as subducted oceanic basalt (White, 1979) or volcanic rocks derived from the mantle (Pitcher, 1979) have also been suggested.

It seems inevitable from the data in Table 4.4 that the Loon Lake pluton was not derived directly from the mantle (too high  $\delta^{18}O$ ) and therefore has a source in the lower crust or at least reacted with the lower crust. Since the lower crust is lithologically and isotopically heterogeneous (Smithson and Brown, 1977; James, 1980; Richardson, 1980), partial melts accumulating in the lower crust are probably derived from a mixed source. The available strontium and oxygen isotopic composition of lower crustal xenoliths (e.g. James, 1980) supports the contention that the Loon Lake pluton could be derived from the lower crust. It is not possible to suggest one protolith for this pluton as Miller (1978) indicated for some Californian monzonites (ie. quartz eclogite) but detailed examination of xenoliths in the pluton may provide some

clues to the parental material(s).

## CHAPTER V

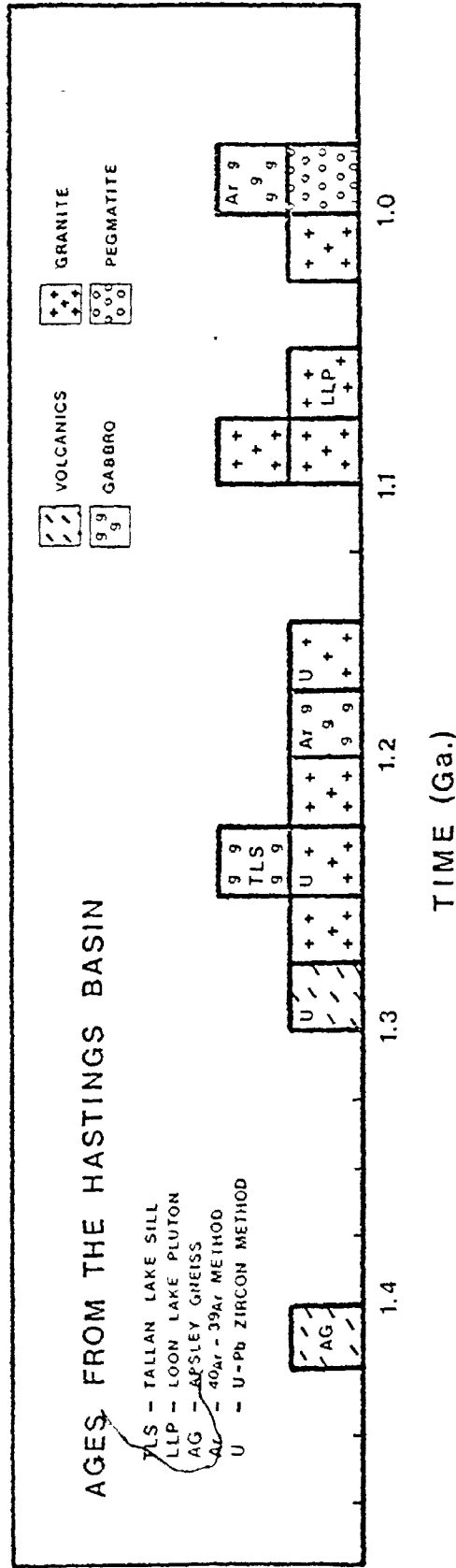
### SUMMARY

A summary of the age determinations presented in this dissertation combined with other geochronological data from the Apsley area (Table 1.2) are presented in Figure 5.1. In general, igneous activity in Chandos Twp. spans a period from 1400 to 950 Ma. The age of the Apsley gneiss (1402 Ma.) is considerably older than other units in this area but whether this is a true hiatus must await further geochronological investigations. However, there is evidence of "old" granulites east of the Elzevir batholith (ca. 1440 Ma.; J. M. Moore, personal communication) which supports the existence of relatively old crust in this segment of the Grenville Province.

An attempt to use strontium isotopes as a tracer of crustal processes has provided a better understanding of isotopic behaviour during regional metamorphism. The main conclusions from the detailed strontium isotopic study of the Apsley gneiss are:

- (a) The "sodic" Apsley gneiss bands have remained closed to whole rock strontium isotopic equilibration during amphibolite facies metamorphism. Migration of Sr between mineral phases ceased ca. 1062 Ma.

FIGURE 5.1



- (b) The "potassic" Apsley gneiss bands exhibit various degrees of whole rock strontium isotopic equilibration. The feldspar-whole rock data from these bands yield a variety of ages younger than 1062 Ma. but no geological significance is attributed to this data.
- (c) The low initial strontium ratio for the Apsley gneiss (0.7022) reflects a mantle or lower crustal protolith for the volcanic end member of this sequence.

A combined oxygen and strontium isotope study of the Loon Lake pluton ( $R_i = 0.7034$ ;  $t = 1065$  Ma.;  $\delta^{18}O_{wr} = 8.8$  to  $12.0$  ‰) indicates that this I-type granitoid was derived from a lower crustal source. The similarity of the initial strontium ratios for the monzonite and quartz monzonite indicates a cogenetic relationship between these two units but the enrichment of Rb in the quartz monzonite and higher oxygen isotopic composition suggests a more complicated history.

The Rb-Sr whole rock errorchron age of 1225 Ma. ( $R_i = 0.7031$ ) for amphibolite and syenite samples from the Tallan Lake sill is interpreted as the age of intrusion. This data supports the contention of Griep (1975) that the sill forms part of a large scale nappe structure.

## REFERENCES

- ABBEY, S. (1977) Studies in "Standard Rock Samples" for use in the general analysis of silicate rocks and minerals, Part 5: 1977 edition of "Usable Values". Geol. Surv. Can. Paper 77-34, 31p.
- ADAMS, F.D. and BARLOW, A.E. (1910) Geology of the Haliburton and Bancroft areas, Province of Ontario. Geol. Surv. Can. Memoir 6, 419 p.
- AFTALION, M. and VAN BREEMEN, O. (1980) U-Pb zircon, monazite, and Rb-Sr whole rock systematics of granite gneiss and psammitic to semi-pelitic host gneiss from Glenfinnan, N.W. Scotland. Cont. Min. Petrol., 72, pp. 87-98.
- ALDRICH, L.T., WETHERILL, G.W., DAVIS, G.L., and TILTON, G.R. (1958) Radioactive ages from micas from granitic rocks by Rb-Sr and K-Ar methods. Trans. Amer. Geophys. Union, 39, pp. 1124-1134.
- BAER, A.J. (1976) The Grenville Province in Helikian times: A possible model of evolution. Phil. Trans. Roy. Soc. London, A280, pp. 499-515.
- BAKER, J.T. (1958) Baker analysed reagent dowex ion exchange resins. Chemical Co. Product Bulletin, #103.
- BATEMAN, P.C. and WHITE, B.W. (1979) Crystallization, fractionation, and solidification of the Tuslumne Intrusive series, Yosemite National Park, California. Geol. Soc. Am. Bull., 90, pp. 465-482.
- BEAKHOUSE, G.P. and HEAMAN, L.M. (1980) The chemical separation of Rb and Sr for mass spectrometric analysis. McMaster Univ. Tech. Memo 80-6.
- BIRK, W.D. (1977) The nature and timing of granitoid plutonism in the Wabigoon volcanic-plutonic belt, NW Ontario. Geochemistry, Rb/Sr geochronology, petrography, and field investigation. Ph.D. thesis, McMaster Univ., Hamilton, Ontario, 496 p.



- BOWEN, N.L. (1956) The evolution of the igneous rocks. Dover, New York, NY. (Reprint of 1928 ed.), 332 p.
- BROOKS, C., HART, S.R., and WENDT, I. (1972) Realistic use of two-error regression treatments as applied to rubidium-strontium data. *Reviews of Geophy. and Space Phys.*, 10, no.2, pp.551-577.
- BROOKS, C. (1980) Apehbian overprinting in the Superior Province east of James Bay, Quebec. *Can. J. Earth Sci.*, 17, pp. 526-531.
- CHAPPELL, B.W., COMPSTON, W., ARRIENS, P.A., and VERNON, M.J. (1969) Rubidium and strontium determinations by X-ray fluorescence spectrometry and isotope dilution below the part per million level. *Geochim. Cosmochim. Acta*, 33, pp. 1002-1006.
- CHAPPELL, B.W. and WHITE, A.J.R. (1974) Two contrasting granite types. *Pac. Geol.*, 8, 173-174.
- CHIANG, M.C. (1965) Element partition between hornblende and biotite in rocks from the Loon Lake aureole, Chandos Twp., Ontario. Unpubl. M.Sc. thesis, McMaster Univ., Hamilton, Ontario, 328 p.
- CLOOS, E. (1934) The Loon Lake pluton, Bancroft area, Ontario, Canada. *J. Geol.*, 42, pp. 393-399.
- COMPSTON, W., CHAPPELL, B.W., ARRIENS, P.A., and VERNON, M.J. (1969) On the feasibility of NBS-70a K-feldspar as a Rb-Sr reference sample. *Geochim. Cosmochim. Acta*, 33, pp. 753-757.
- CORTECCI, G., DEL MORO, A., LEONE, G., and PARDINI, G.C. (1979) Correlation between strontium and oxygen isotopic compositions of rocks from the Adamello Massif (N. Italy). *Cont. Min. Petrol.*, 68, pp. 421-427.
- DAVIDSON, A., BRITTON, J.M., BELL, K., and BLENKINSOP, J. (1979) Regional synthesis of the Grenville Province of Ontario and Quebec. In: *Current Research, Part B, Geol. Surv. Can. Paper 79-1B*, pp. 153-172.
- DE LAETER, J.R. and ABERCROMBIE, I.D. (1970) Mass spectrometric isotope dilution analyses of rubidium and strontium in standard rocks. *Earth Plan. Sci. Lett.*, 9, pp. 327-330.

- DEPAOLO, D.J. (1980) Crustal growth and mantle evolution: Inferences from models of element transport and Nd and Sr isotopes. *Geochim. Cosmochim. Acta*, 44, pp. 1185-1197.
- DOERING, W.P. (1968) A rapid method for measuring the Rb/Sr ratio in silicate rocks. U.S. Geol. Surv. Prof. Paper 600-C, pp. 164-168.
- DOSTAL, J. (1973) Geochemistry and petrology of the Loon Lake pluton, Ontario. Unpubl. Ph.D. thesis, McMaster Univ., Hamilton, Ontario. 328 p.
- DOSTAL, J. (1975) Geochemistry and petrology of the Loon Lake pluton, Ontario. *Can. J. Earth Sci.*, 12, pp. 1331-1345.
- DOUGAN, T.W. (1979) Compositional and modal relationships and melting reactions in some migmatitic metapelites from New Hampshire and Maine. *Am. J. Sci.*, 279, pp. 897-935.
- ERMANOVICS, I.F. (1970) Zonal structure of the Perth Road monzonite, Grenville Province, Ontario. *Can. J. Earth Sci.*, 7, pp. 414-434.
- FAIRBAIRN, H.W. and HURLEY, P.M. (1971) Evaluation of X-ray fluorescence and mass spectrometric analyses of Rb and Sr in some silicate standards. *Geochim. Cosmochim. Acta*, 35, pp. 149-156.
- FAURE, G. and POWELL, J.L. (1972) *Strontium Isotope Geology*. Springer-Verlag, New York. 188 p.
- FAURE, G. (1977) *Principles of Isotope Geology*. John Wiley and Sons, New York. 464 p.
- FOWLER, A.D. and DOIG, R. (1979) Origin of uraniferous granitoids, Grenville Province, Quebec and Ontario. *Geol. Ass. Can. Abstr.*, Quebec City.
- FOWLER, A.D. (1980) The age, origin, and Rare-Earth element distributions of Grenville Province uraniferous granites and pegmatites. Unpubl. Ph.D. Thesis, McGill Un., Montreal, Quebec.
- FOX, P.E. and MOORE, J.M. Jr. (1969) Feldspars from the Adamant pluton, British Columbia. *Can. J. Earth Sci.*, 6, pp. 1199-1209.
- FRYER, B.J., FYFE, W.S., and KERRICH, R. (1979) Archaean volcanogenic oceans. *Chem Geol.*, 24, pp. 25-33.

- GAST, P.W. (1960) Limitations on the composition of the upper mantle. *J. Geophys. Res.*, 65, pp. 1287-1297.
- GIBBINS, W. (1972) Experimental procedures for Rb-Sr age determinations. McMaster Univ. Tech. Memo 72-4, 5 p.
- GIBBINS, W. (1973) Rubidium-strontium mineral and rock ages at Sudbury, Ontario. Unpubl. Ph.D. thesis, McMaster Univ., Hamilton, Ontario. 230 p.
- GITTINS, J., HAYATSU, A., and YORK, D. (1969) A strontium isotope study of metamorphosed limestones. *Lithos*, 3, pp. 51-58.
- GRAUERT, B. and HALL, L.M. (1973) Rb-Sr isotopic study on small whole-rock slabs and their minerals from the Manhattan Schist, Manhattan Prong, N.Y. *Carn. Inst. Yearbook* 73, pp. 1007-1010.
- GRAY, C.M. and COMPSTON, W. (1978) A rubidium-strontium chronology of the metamorphism and prehistory of central Australian granulites. *Geochim. Cosmochim. Acta*, 42, pp. 1735-1747.
- GRIEP, J.I. (1975) Petrochemistry and metamorphism of the Tallan Lake sill, Bancroft area, Ontario. Unpubl. M.Sc. thesis, McMaster Univ., Hamilton, Ontario 166 p.
- HALLIDAY, A.N., STEPHENS, W.E., and HARMON, R.S. (1980) Rb-Sr and O isotopic relationships in three zoned Caledonian granitic plutons, Southern Uplands, Scotland: Evidence for varied sources and hybridization of magmas. *J. Geol. Soc. London*, 137, pp. 329-348.
- HARMON, R.S. and HALLIDAY, A.N. (1980) Oxygen and strontium isotope relationships in the British late Caledonian granites. *Nature*, 283, pp. 21-25.
- HARPER, C.T. (1967) On the interpretation of potassium-argon ages from Precambrian shields and Phanerozoic orogens. *Earth Plan. Sci. Lett.*, 3, pp. 128-132.
- HEAMAN, L.M., McNUTT, R.H., and SHAW, D.M. (1980a) Rb-Sr whole rock ages from the Hastings Basin, Grenville Province, Ontario. *Geol. Assoc. Can. (Abstr.)*, Halifax, Nova Scotia.
- HEAMAN, L.M., SHIEH, Y.N., McNUTT, R.H., and SHAW, D.M. (1980b) Interpretation of strontium and oxygen isotope data from the Loon Lake pluton and the Apsley gneiss, Grenville Province, Ontario. *Trans. Am. Geophys. Union (EOS)*, v. 61, p. 387.

- HEWITT, D.F. (1956) The Grenville region of Ontario. In: The Grenville Problem, ed. J.E. Thomson. Roy. Soc. Can. Spec. Publ. 1, pp. 22-41.
- HEWITT, D.F. (1957) The Grenville Province. In: The Proterozoic in Canada, ed. J.E. Gill. Roy. Soc. Can. Spec. Publ. 2.
- HEWITT, D.F. (1961) Nepheline syenite deposits of S. Ontario. Ont. Dept. Mines, 69, 194 p.
- HOERNES, S. and HOFFER, E. (1979) Equilibrium relations in prograde metamorphic mineral assemblages. A stable isotope study of rocks of the Damara orogen, from Namibia. Cont. Min. Petrol., 68, pp. 377-389.
- HOFMANN, A.W. (1975) Diffusion of Ca and Sr in a basalt melt. Carn. Inst. Washington Yearbook 75, pp. 183.
- HOFMANN, A.W. (1977) Rb-Sr dating of thin slabs: an imperfect method to determine the age of metamorphism. In: Lectures in Isotope Geology, ed. E. Jager and J.C. Hunziker. Springer-Verlag, N.Y., 329 p.
- HOLLOWAY, J.R. (1979) Volatiles and the evolution of granitic magmas. Geol. Soc. Am. Abstr., San Diego, California, pp. 445.
- HURLEY, P.M., HUGHES, H., PINSON, W.H., and FAIRBAIRN, H.W. (1962) Radiogenic argon and strontium diffusion parameters in biotite at low temperatures obtained from the Alpine fault uplift in New Zealand. Geochim. Cosmochim. Acta, 26, pp. 67-80.
- HURLEY, P.M., HUGHES, H., FAURE, G., FAIRBAIRN, H.W., and PINSON, W.H. (1962) Radiogenic strontium-87 model of continental formation. J. Geophys. Res., 67, pp. 5315-5334.
- JACOBSEN, S.B. and HEIER, K.S. (1978) Rb-Sr isotope systematics in metamorphic rocks, Kongsberg sector, S. Norway. Lithos, 11, pp. 257-276.
- JAMES, D.E. (1980) O-isotopic composition of lower crustal xenoliths, Kilbourn Hole, New Mexico. Am. Geophys. Union Abstr., Toronto, Ontario. EOS, 61, p. 388.

- JENNINGS, D.S. (1970) Origin and metamorphism of part of the Hermon Group near Bancroft, Ontario. Unpubl. Ph.D. thesis, McMaster Univ., Hamilton, Ontario. 225 p.
- KARNER, F.R. (1968) Compositional variation in the Tunk Lake granite pluton, SE Maine. Geol. Soc. Am. Bull., 79, pp. 193-222.
- KROGH, T.E. and HURLEY, P.M. (1968) Strontium isotope variation and whole-rock isochron studies, Grenville Province of Ontario. J. Geophys. Res., 73, pp. 7107-7125.
- KROGH, T.E. and DAVIS, G.L. (1969) Old isotopic ages in the NW Grenville Province, Ontario. In: Age relations in high grade metamorphic terrains, ed. H.R. Wynne-Edwards, Geol. Ass. Can. Spec. Paper, 5, pp. 189-192.
- KROGH, T.E. and DAVIS, G.L. (1970) Metamorphism 1700 ± 100 m.y. and 900 ± 100 m.y. ago in the northwest part of the Grenville Province in Ontario. Carn. Inst. Washington Yearbook, 69, pp. 308-309.
- KROGH, T.E. and DAVIS, G.L. (1973) The effect of regional metamorphism on U-Pb systems in zircons and a comparison with Rb-Sr systems in the same whole rock and its constituent minerals. Carn. Inst. Washington Yearbook, 72, pp. 601-610.
- LAASKO, R.K. (1968) Geology of Lake Township, Hastings County, Ontario. Ont. Dept. Mines Geol. Rept. 54.
- LANGMUIR, C.H., VOCKE, R.D., HANSON, G.N., and HART, S.R. (1978) A general mixing equation with applications to Icelandic basalts. Earth Plan. Sci. Lett., 37, pp. 380-392.
- LONG, L.E. (1966) Isotope dilution analysis of common and radiogenic strontium using  $^{84}\text{Sr}$  enriched spike. Earth Plan. Sci. Lett., 41, pp. 289-292.
- LOWDON, J.A. (1960) Age determinations by the Geological Survey of Canada. Rept. 2 - Isotopic Ages. Geol. Surv. Can. Paper 61-17.
- LUMBERS, S.B. (1967) Stratigraphy, plutonism, and metamorphism in the Ottawa River remnant in the Bancroft-Madoc area of the Grenville Province of SE Ontario. Unpubl. Ph.D. thesis, Princeton Univ., Princeton, New Jersey.

- MACINTYRE, R.M., YORK, D., and MOORHOUSE, W.W. (1967) Potassium-argon age determinations in the Madoc-Bancroft area in the Grenville Province of the Canadian shield. *Can. J. Earth Sci.*, 4, pp. 815-828.
- MARCHAND, M. (1973) Determination of Rb, Sr, and Rb/Sr by XRF. *McMaster Univ. Tech. Memo*, 73-2, 16 p.
- MATTINSON, J.M. (1972) Preparation of HF, HCl, and HNO<sub>3</sub> at ultralow lead levels. *Anal. Chem.*, 44, pp. 1715-1716.
- McCAMMON, B.W. (1968) A geochemical study of some igneous rocks from the Loon Lake complex using spectrographic methods. Unpubl. B.Sc. thesis, McMaster Univ., Hamilton, Ontario. 34 p.
- McCARTHY, T.S. (1976) Trace element distribution patterns and their relationship to the crystallization of granitic melts. *Geochim. Cosmochim. Acta*, 40, pp. 1351-1358.
- McCARTHY, T.S. and GROVES, D.I. (1979) The Blue Tier Batholith, NE Tasmania. A cumulate-like product of fractional crystallization. *Cont. Min. Petrol.*, 71, pp. 193-209.
- McINTYRE, G.A., BROOKS, C., COMPSTON, W., and TUREK, A. (1966) The statistical assessment of Rb-Sr isochrons. *J. Geophys. Res.*, 71, pp. 5456-5469.
- MEHNERT, K.R. (1968) Migmatites and the origin of granitic rocks. Elsevier, Amsterdam. p. 405.
- MENZIES, M. and MURTHY, V.R. (1978) Strontium isotope geochemistry of Alpine tectonite lherzolites: Data compatible with a mantle origin. *Earth Plan. Sci. Lett.*, 38, pp. 346-354.
- MICHARD-VITRAC, A., ALBAREDE, F., DUPUIS, C., and TAYLOR, Jr. H.P. (1980) The genesis of Variscan (Hercynian) plutonic rocks: Inferences from Sr, Pb, and O studies on the Maladeta igneous complex, Central Pyrenees (Spain). *Cont. Min. Petrol.*, 72, pp. 57-72.
- MILLER, C.F. (1978) Monzonitic plutons, California, and a model for generation of alkali-rich, near silica saturated magmas. *Cont. Min. Petrol.*, 67, pp. 349-355.

- MONTGOMERY, C.W. and HURLEY, P.M. (1978) Total rock U-Pb and Rb-Sr systematics in the Inataca series, Guayana Shield, Venezuela. *Earth Plan. Sci. Lett.*, 39, pp. 281-290.
- MOORBATH, S. (1975a) The geological significance of early Precambrian rocks. *Proc. Geol. Assoc.*, 86, pp. 259-279.
- MOORBATH, S. (1975b) Evolution of Precambrian crust from strontium isotopic evidence. *Nature*, 254, pp. 395-397.
- MOORBATH, S. (1977) Age, isotopes, and the evolution of continental crust. *Chem. Geol.*, 20, pp. 151-187.
- MOORBATH, S. (1978) Age and isotope evidence for the evolution of continental crust. *Phil. Trans. Roy. Soc. London, Series A*, 288, pp. 401-413.
- MOORE, J.M. (1980) An old age for granulites east of the Elzevir batholith. Personal communication.
- PANKHURST, R.J. and O'NIONS, R.K. (1973) Determination of Rb/Sr and  $^{87}\text{Sr}/^{86}\text{Sr}$  ratios of some standard rocks and evaluation of X-ray fluorescence spectrometry in Rb-Sr geochemistry. *Chem. Geol.*, 12, pp. 127-136.
- PATCHETT, P.J. (1980) Thermal effects of basalt on continental crust and crustal contamination of magmas. *Nature*, 283, pp. 559-561.
- PEARCE, J.A. and NORRY, M.J. (1979) Petrogenetic implications of Ti, Zr, Y, and Nb variations in volcanic rocks. *Cont. Min. Petrol.*, 69, pp. 33-47.
- PETERMAN, Z.E., DOE, B.R., and BARTEL, A.J. (1967) Data on the rock GSP-1 (Granodiorite) and the isotope dilution method of analysis for Rb and Sr. U.S. Geol. Surv. Prof. Paper 575-B, pp. B181-186.
- PETERMAN, Z.E., HEDGE, C.E., COLEMAN, R.G., and SNAVELY, Jr., P.D. (1967)  $^{87}\text{Sr}/^{86}\text{Sr}$  ratios in some eugeosynclinal sedimentary rocks and their bearing on the origin of granitic magma in orogenic belts. *Earth Plan. Sci. Lett.*, 2, pp. 433-439.

- PITCHER, W.S. (1979) The nature, ascent, and emplacement of granitic magmas: *J. Geol. Soc. London*, 136, pp. 627-662.
- RAPELA, C.W. and SHAW, D.M. (1979) Trace and major element models of granitoid genesis in the Pampean Ranges, Argentina. *Geochim. Cosmochim. Acta*, 43, pp. 1117-1129.
- REYNOLDS, R.C. (1963) Matrix corrections in trace element analysis by X-ray fluorescence. Estimation of the mass absorption coefficient by compton scattering. *Am. Mineral.*, 48, pp. 1133-1143.
- REYNOLDS, R.C. (1967) Estimation of mass absorption coefficients by compton scattering. Improvements and extensions of the method. *Am. Mineral.*, 52, pp. 1493-1502.
- RICHARDSON, S.R. (1980) The gneiss syndrome: Nd and Sr isotopic relationships in lower crustal granulite xenoliths, Kilbourne Hole, New Mexico. *Am. Geophys. Union Abstr.*, Toronto, Ontario. *EOS*, 61, p. 388.
- RODDICK, J.C. and COMPSTON, W. (1977) Strontium isotopic equilibration: a solution to a paradox. *Earth Plan. Sci. Lett.*, 34, pp. 238-246.
- SAHA, A.K. (1957) Mode of emplacement some granitic plutons in SE Ontario. Unpubl. Ph.D. thesis, Univ. of Toronto, Toronto.
- SAHA, A.K. (1959) Emplacement of three granitic plutons in SE Ontario, Canada. *Geol. Soc. Am. Bull.*, 70, pp. 1293-1326.
- SHAW, D.M. (1962) Geology of Chandos Township, Peterborough County, Ontario. *Ont. Dept. Mines Geol. Rept.* 11, pp. 1-28.
- SHAW, D.M. and KUDO, A.M. (1965) A test of the discriminant function in the amphibolite problem. *Mineral. Mag.*, 34, pp. 423-435.
- SHAW, D.M. (1972) The origin of the Apsley gneiss, Ontario. *Can. J. Earth Sci.*, 5, pp. 561-583.



- SHEPPARD, S.M.F. (1966) Carbon and oxygen isotope studies in marbles. Unpubl. Ph.D. thesis, McMaster Univ., Hamilton, Ontario. 185 p.
- SHEPPARD, S.M.F. and SCHWARCZ, H.P. (1970) Fractionation of carbon and oxygen isotopes and magnesium between coexisting metamorphic calcite and dolomite. *Cont. Min. Petrol.*, 26, pp. 161-198.
- SHIEH, Y.N. and SCHWARCZ, H.P. (1974) Oxygen isotope studies of granite and migmatite, Grenville Province of Ontario, Canada. *Geochim. Cosmochim. Acta*, 38, pp. 21-45.
- SHIEH, Y.N., SCHWARCZ, H.P., and SHAW, D.M. (1976) An oxygen isotope study of the Loon Lake pluton and the Apsley gneiss, Ontario. *Cont. Min. Petrol.*, 54, pp. 1-16.
- SHIEH, Y.N. (1980) Oxygen isotopic compositions of granitic and syenitic plutons in the Central Metasedimentary Belt, Grenville Province of Ontario. *Am. Geophys. Union Abstr.*, Toronto, Ontario. EOS, 61, p. 410.
- SIMONY, P.S. (1960) Origin of the Apsley paragneiss. Unpubl. M.Sc. thesis, McMaster Univ., Hamilton, Ontario. 79 p.
- SILVER, L.T. and LUMBERS, S.B. (1965) Geochronological studies in the Bancroft-Madoc area of the Grenville Province, Ontario, Canada. (Abstr.) *Geol. Soc. Am. Spec. Publ.* 87, p. 156.
- SMITHSON, S.B. and BROWN, S.K. (1977) A model for lower continental crust. *Earth Plan. Sci. Lett.*, 35, pp. 134-144.
- STACEY, J., WILSON, E., PETERMAN, Z., and TERRAZAS, R. (1971) Digital recording of mass spectra in geologic studies. *Can. J. Earth Sci.*, 8, pp. 371-377.
- STUEBER, A.M. and IKRAMUDDIN, M. (1974) Rubidium, strontium, and the isotopic composition of strontium in ultramafic nodule minerals and host basalts. *Geochim. Cosmochim. Acta*, 38, pp. 207-216.
- STEIGER, R.H., HARNIK-SOPTRAJANOVA, G., ZIMMERMANN, E., and HENRIKSEN, N. (1976) Isotopic age and metamorphic history of the banded gneiss at Danmarkshaun, East Greenland. *Cont. Min. Petrol.*, 57, pp. 1-24.

- STEIGER, R.H. and JAGER, E. (1977) Subcommittee on geochronology: Convention on the use of decay constants in geology and cosmochronology. *Earth Plan. Sci. Lett.*, 36, pp. 359-362.
- SYMONS, D.T.A. (1973) Paleomagnetism of the 1180 Ma Grenvillian Umfraville gabbro, Ontario. *Can. J. Earth Sci.*, v. 15, pp. 956-962.
- TAYLOR, H.P. Jr. (1978) Oxygen and hydrogen isotope studies of plutonic granitic rocks. *Earth Plan. Sci. Lett.*, 38, pp. 177-210.
- TAYLOR, H.P. Jr. (1980) The effects of assimilation of country rocks by magmas on  $^{18}\text{O}/^{16}\text{O}$  and  $^{87}\text{Sr}/^{86}\text{Sr}$  systematics in igneous rocks. *Earth Plan. Sci. Lett.*, 47, pp. 243-254.
- TUREK, A., RIDDLE, C., and SMITH, T.E. (1977) Determination of Rb and Sr by X-ray fluorescence in the measurement of radiometric ages. *Can. J. Spectroscopy*, 22, no. 1, pp. 20-24.
- VAN SCHMUS, W. (1966) Data reduction for  $^{84}\text{Sr}$  spiked samples. In: Variations in isotopic abundances of strontium, calcium, and argon and related topics. MIT Ann. Progress Rept., 14, pp. 179-185.
- VANCE, J.A. (1961) Zoned granitic intrusions - an alternative hypothesis of origin. *Geol. Soc. Am. Bull.*, 72, pp. 1723-1728.
- VEIZER, J. and COMPSTON, W. (1976a)  $^{87}\text{Sr}/^{86}\text{Sr}$  in Precambrian carbonates as an index of crustal evolution. *Geochim. Cosmochim. Acta*, 40, pp. 905-914.
- VERPAELST, P., BROOKS, E., and FRANCONI, A. (1980) The 2.5 Ga. Duxbury massif, Quebec: a remobilized piece of pre - 3.0 Ga. sialic basement(?). *Can. J. Earth Sci.*, 17, pp. 1-18.
- VOGEL, D.E. and GARLICK, G.D. (1970) Oxygen isotope ratios in metamorphic eclogites. *Cont. Min. Petrol.*, 28, pp. 183-191.
- VOLLMER, R. (1976) Rb-Sr and U-Th-Pb systematics of alkaline rocks: the alkaline rocks from Italy. *Geochim. Cosmochim. Acta*, 40, pp. 283-295.

- WANLESS, R.K. and LOVERIDGE, W.D. (1972) Rb-Sr isochron age studies, Report 1. Geol. Surv. Can. Paper 72-23, 77 p.
- WENDT, I. (1969) Derivation of the formula for a regression line based on a least squares analysis. Internal Report, Bundesanstalt für Bodenforschung, Hanover, W. Germany.
- WHITE, A.J.R. (1979) Source of granitic magmas. Geol. Soc. Am. Abstr., San Diego, California, p. 539.
- WINKLER, A.J.F. (1976) Petrogenesis of metamorphic rocks. (4th ed.). Springer-Verlag, New York, 334 p.
- WOLFF, J.M. (1977a) An operation guide and technical discussion of mass spectrometer SS-2, McMaster Geochronology Lab. McMaster Univ. Tech. Memo 77-1, 7 p.
- WOLFF, J.M. (1977b) The geochemical nature of an Archean plutonic-volcanic suite as exemplified by the Kakagi-Stephen Lakes area, NW Ontario. Unpubl. M.Sc. thesis, McMaster Univ., Hamilton, Ontario. p. 137.
- WOODEN, J.L. and GOODWIN, A.M. (1980) A Rb-Sr isotopic study of Archean rocks of the eastern Lac Seul region, English River sub-province, NW Ontario. Can. J. Earth Sci., 17, pp. 569-576.
- WYNNE-EDWARDS, H.R. (1957) Structure of the Westport concordant pluton in the Grenville, Ontario. J. Geol., 65, pp. 639-649.
- WYNNE-EDWARDS, H.R. (1972) The Grenville Province. In: Variations in tectonic styles in Canada. Ed. R.A. Price and R. Douglas. Geol. Assoc. Can. Spec. Paper, 11, pp. 263-334.
- YORK, D. (1966) Least squares fitting of a straight line. Can. J. Phys., 44, pp. 1079-1086.
- YORK, D. (1967) The best isochron. Earth Plan. Sci. Lett., 2, pp. 479-482.
- YORK, D. (1969) Least squares fitting of a straight line with correlated errors. Earth Plan. Sci. Lett., 5, pp. 320-324.
- YORK, D. (1979) Thermal history of shield areas from  $^{40}\text{Ar}/^{39}\text{Ar}$  studies. Geol. Assoc. Can. Abstr., Quebec City, Quebec.

/

APPENDIX A

3

0

### A.1 Sample Dissolution

4

A detailed outline of the chemical procedure used in this laboratory is reported by Beakhouse and Heaman (1980). The reagents used for sample dissolution include HCl, HNO<sub>3</sub>, HF (Analar), and distilled H<sub>2</sub>O. The HNO<sub>3</sub> and HF were distilled following the sub-boiling technique outlined by Mattinson (1972). The collector and feed bottles were F.E.P. containers and these were connected by a teflon elbow. Large quantities of distilled HCl were required for the preparation of 2.5 N and 6.0 N acid therefore reagent grade HCl (ca. 12 N) was continuously distilled (sub-boiling) in a quartz still. Distilled tap water was further purified using a Corning "Mega Pure" vycor still and subsequently passed through a Barnstead ultrapure deionizer.

The teflon bombs, used for sample dissolution, and other pyrex apparatus repeatedly used in the chemical procedure were stored in a concentrated HNO<sub>3</sub> bath until needed. This cleaning acid was replaced regularly to eliminate the possibility of contamination. Prior to use, the teflon bombs were removed from the acid bath and rinsed repeatedly with 2.5 N HCl followed by double distilled H<sub>2</sub>O.

For normal isotopic analyses, 250 mg. of sample powder was weighed into the clean teflon bombs and 5 ml. of HF and 0.5 ml. of HNO<sub>3</sub> were added. The bomb assembly was placed in its metal retaining jacket and heated in a muffle furnace at 135 °C for a minimum of 12 hours. After removal

5

from the furnace, the bombs were allowed to cool for 2 hours before the covers were removed. The solution was evaporated in a controlled, filtered air flow chamber. All subsequent evaporations were also done in this chamber. The residue was re-dissolved in 1 ml. of  $\text{HNO}_3$  to ensure the complete dissociation of sulfides, evaporated to dryness, and taken up in 5 ml. of 6 N HCl. The bomb assembly was then returned to the furnace ( $135^\circ\text{C}$ ) for another 4 to 6 hours of digestion. Following this, the solution was evaporated to dryness and re-dissolved in 2 ml. of 2.5 N HCl.

This solution was transferred to a clean pyrex test tube using a disposable pipette and centrifuged for 3 to 5 minutes. Significant quantities of residue occasionally formed in the bottom of the test tube, especially from mafic samples. Modifications of the above procedure, such as increasing the volume of acids used for sample digestion and the digestion period, allowed complete dissolution of such samples.

The chemical procedure for spiked samples is identical to that described above except that measured quantities of  $^{87}\text{Rb}$  and  $^{84}\text{Sr}$  spike solution were added to the sample powder. The optimum quantity of spike solution required was calculated such that the concentration ratio of spike to sample was approximately one.

## A.2 Cation Exchange Column Chemistry

The cation exchange columns consist of 30 cm. x 15 cm. pyrex tubes, tapered at the lower end, supporting a 100 ml. reservoir at the top. The columns are fitted with a medium pore size fritted disk which supports 20 cm. of Dowex Bio-Rad AG 50W-X8, 200-400 mesh resin (Hydrogen form). Before loading the resin into the columns, the fines were removed by repeatedly decanting the 2.5 N solution. During this study, the quantity of resin in each column was increased from 15 cm. to 20 cm. to improve the separation of  $\text{Ca}^{+2}$  from  $\text{Sr}^{+2}$ .

The columns were prepared for Sr extraction by rinsing the resin with 50 ml. of 6.0 N HCl, backwashing with double distilled  $\text{H}_2\text{O}$  to eliminate channels or imperfections, and re-equilibrating the resin with 50-75 ml. of 2.5 N HCl. Any irregularities on the resin surface were levelled with a circular glass rod.

The supernatant solution from each test tube was loaded into a separate column using a disposable pipette, attempting not to disturb the resin surface. Elution was achieved by passing a total of 104 ml. of 2.5 N HCl as follows: 2 ml., 2 ml., 10 ml., 40 ml., and 50 ml. Each aliquot was allowed to pass through before the addition of subsequent aliquots. Rubidium was collected as a 5 ml. aliquot after 45 ml. of HCl was collected. Strontium was collected in a 15 ml. aliquot after 70 ml. of HCl was

collected. The relative selectivity of common monovalent and divalent cations for this resin was reported in the J.T. Baker Chemical Co. product bulletin #103 (1958).

Calibration of the exchange columns was determined using a Perkin-Elmer (model 603) Atomic Absorbtion Spectrometer (AAS). Small aliquots of discharge (5 ml.) were collected in 30 ml. disposable polypropylene beakers and the relative concentration of Sr in each aliquot was determined by AAS.

The first aliquot which contained Sr was discarded and the following three aliquots (ie. 15 ml.) were combined into one beaker. This solution was evaporated until the volume remaining was 4 ml. At this stage, the solution was transfered to a clean pyrex vial, evaporated to dryness, and stored for mass spectrometer analysis.



APPENDIX B

## B.1 Major and trace element data for the Loon Lake pluton

	<u>Rb</u>	<u>Sr</u>	<u>Y</u>	<u>Zr</u>	<u>Nb</u>	TiO <sub>2</sub> <sup>a</sup>	K <sub>2</sub> O <sup>a</sup>
<u>Monzonite</u>							
LL10	60	179	34	670	10	0.50	7.66
LL13	71	63	89	816	29	0.71	7.38
LL18	62	124	43	778	20	0.75	7.51
LL21	55	208	63	1000	21	0.89	7.21
LL24	42	682	31	934	13	1.10	7.07
LL27	74	186	81	674	25	0.60	6.92
LL30	60	106	182	923	33	0.80	7.18
LL40	65	430	54	1056	13	*	*
LL42	90	38	75	1282	15	*	*
LL45	53	973	39	613	10	*	*
<u>Quartz Monzonite</u>							
LL2	243	211	120	674	40	0.79	4.32
LL3	430	121	97	532	32	0.52	6.13
LL4	73	520	35	835	20	1.01	5.36
LL5	134	198	47	375	26	0.32	5.59
LL6	94	355	34	583	23	0.59	6.44
LL8	153	218	67	320	25	0.28	5.93
LL11	230	42	152	417	70	0.13	4.63
LL14	200	441	48	851	23	0.73	6.81
LL15	236	380	57	875	25	0.79	7.11
LL19	265	206	123	643	43	0.72	5.07
LL20	175	95	26	260	13	0.16	3.82
LL28	115	66	106	265	17	0.22	4.98
LL31	153	60	72	422	21	0.30	7.17
LL49	188	180	137	517	16	*	*
LL50	131	371	75	391	15	*	*
GN4	218	104	20	328	4	*	*
GN8	96	141	65	365	4	*	*
<u>Granodiorite Gneiss</u>							
LL7	61	173	59	243	17	*	*
LL26	100	204	53	270	18	*	*
LL29	52	222	33	228	3	*	*
GN1	76	250	45	189	4	*	*
GN2	82	208	54	203	-	*	*
GN3	89	180	60	225	-	*	*
GN5	50	444	35	199	2	*	*
GN6	82	220	44	164	2	*	*
GN7	90	213	52	209	2	*	*

## B.1 (continued)

	<u>Rb</u>	<u>Sr</u>	<u>Y</u>	<u>Zr</u>	<u>Nb</u>	TiO <sub>2</sub>	K <sub>2</sub> O
GN9	82	361	41	439	5	*	*
GN10	58	315	46	332	2	*	*
GN11	98	265	30	344	14	*	*
<u>Diorite-</u>							
<u>Gabbro</u>							
LL17	39	1435	26	46	14	*	*
LL22	55	1276	21	370	12	*	*
LL23	31	1156	80	148	19	*	*
LL25	27	1262	46	117	13	*	*
LL46	31	2209	21	135	3	*	*
LL47	25	1903	51	183	3	*	*
LL48	29	1272	40	235	3	*	*
LL56	8	1535	31	96	-	*	*
LL57	49	809	32	546	4	*	*

<sup>a</sup> data reported in weight percent

\* no data available

APPENDIX C

### C.1 TRS-80 Microprocessor Programs

During this dissertation, a TRS-80 microprocessor (Radio Shack Inc.) was interfaced with the mass spectrometer to facilitate on-line data acquisition and calculations. Four separate programs were written in Level II Basic to allow for normal strontium isotope analyses (Program "Q"), isotope dilution analyses for strontium (Programs "S" and "Z"), and isotope dilution for rubidium. The fortran program reported by Stacey et al. (1971), with modifications similar to those incorporated by Birk (1977), was used as a guide in designing the structure of program "Q".

For normal strontium isotopic analyses, the peak data is collected in blocks of 10 scans with provision to collect a maximum of 30 scans without focusing or adjusting the beam. The peak data is collected in the following sequence: mass 88, 87, 86, 88 ... etc. and each peak value is compared to a previous value in order to eliminate spurious data (see subroutine 900).

Background data is collected at four positions: 40 volts down mass from each peak plus at mass 85. A set of background data (5 scans) is collected before each set of peak scans. The average background data is tested for co-linearity and then regressed to determine a baseline. The background values corresponding to each peak position are then interpolated along this baseline. After two sets of backgrounds have been collected and the corresponding

backgrounds for each peak calculated, the two sets of corrected background data are used to calculate the change in the background as a function of time. Therefore, if the baseline drifts significantly during a run then an appropriate background value can be assigned to each peak measurement.

If there is a strong "88 tail" then the background data collected between mass 88 and 87 is not used in the baseline calculation. An "88 tail" correction is then applied to the 87 peak (subroutine 1115). This correction is at best an approximation because the tail is assumed to be linear. Similarly, if there is a Rb85 peak then this background is also not used in the baseline calculation. In the case of a Rb85 peak, a correction is made to the peak at mass 87 to account for a Rb87 component.

After a set of peak and background data have been collected, the program computes the  $^{87}\text{Sr}/^{86}\text{Sr}$  and  $^{88}\text{Sr}/^{86}\text{Sr}$  ratios and then normalizes all the  $^{87}\text{Sr}/^{86}\text{Sr}$  ratios to an  $^{88}\text{Sr}/^{86}\text{Sr}$  ratio of 0.1194. For one set of 10 peak scans, 24 ratios are calculated plus the mean and standard deviation. Additional provision is made to calculate a cumulative mean and standard deviation at the end of each run.

Program "S" and program "Z" are modified versions of program "Q" which allows the collection of one more peak position (mass 84) for strontium isotope dilution. Data collection (Program S) was not combined with the calculations

because the large amount of time required for the calculations wasted valuable data collection time. The order of peak data collection was changed to the following: mass 88, 87, 86, 85, 84, 88 ... etc. and all the backgrounds were collected 40 volts down mass from these peaks. Otherwise, the structure of the calculations is essentially the same.

The data collected using program "S" was simultaneously stored on cassette tapes then recalled when the run was finished. Program "Z" re-loads the data from the tape and makes the calculations with no need for outside input. These two programs are not very efficient and do not allow the operator to monitor the behaviour of the sample throughout the run.

For rubidium isotope dilution the accelerating voltage is set for mass 89. The magnetic field offsets are then reserved for mass 87, 85, and 83 respectively. Four background positions are measured: 40 volts down mass from each position described above. Only two peak positions are measured (mass 87 and 85) but these are analysed at successively higher ionization temperatures to check for severe fractionation. The background calculations are essentially identical to those described for program "Q".

PROGRAM "Q" - STRONTIUM DATA COLLECTION AND  
REDUCTION FOR 3 PEAK POSITIONS

```

4 'STATEMENT 5 DIMENSIONS MEMORY FOR PFAK MATRICES (X,Y);Z(X,Y)),BACKGROUND COR
RCTIONS(NV(33,3)),RB PFAK CORRECTION(VR(33)),TIME CORRECTED PFAKS(PK(30,2,2)),E
10.
5 DIM N(9,2),PK(30,2,2),Z(9,2),RR(25),RA(25),NV(33,3),VR(33),UV(33),MFANX(30),N
U(26),NP(26)
10 I=0:Q=0
15 FORR=0:Q20:MFANX(R)=0:NFXIR
20 RS=INP(0)
23 'BACKGROUND CODES ARE: 87.4=OUT10.0; 86.4=OUT10.1; 85.4=OUT10.2; 85=OUT10.3
25 OUT10.0
30 FORP=0:Q1500:NFXIP
35 L=INP(9)AND15:IFL=0:IFL=35
40 CLS:PRINT "4 BKGS - 5 SCANS EACH"
43 'LINE 45 COLLECTS THE BACKGROUND DATA - 5 SCANS OF 4 BACKGROUND POSITIONS
45 FORN=0:Q04:FORM=0:Q03:OUT10.M:PRINT350,M+1:GOSUB610:GOSUB650:PRINT3(192+64*N+16*M)
,X(N,M):GOSUB935:NFXIM,M
50 FORN=0:Q03:SN(R)=0:NFXIR
55 FORN=0:Q03:FORS=1:Q05:SM(R)=SM(R)+X(S-1,R):BG(R)=SM(R)/5:NFXTS,R
58 'LINES 55-60 AVERAGES BACKGROUND VALUES FOR EACH SCAN POSITION AND ROUNDS TH
E VALUE TO THE NEAREST WHOLE NUMBER
60 FORN=0:Q03:PRINT3(576+16*R),CINT(BG(R)):PC*(R)=CDBL(BG(R)):NFXTR
65 LPRINT CHR$(10):LPRINT "BACKGROUNDS":LPRINT "87.4","86.4","85.4","85":FORN=0
:Q04:LPRINT X(N,0),X(N,1),X(N,2),X(N,3):NEXIN
70 POKE 14312,13:LPRINT CINT(BG(0)),CINT(BG(1)),CINT(BG(2)),CINT(BG(3))
75 UU=0
80 GOSUB250
83 'PEAK CODES ARE: 88=OUT10.8; 87=OUT10.9; 86=OUT10.10
85 OUT10.8:STOP:OUT10.9:STOP:OUT10.10:STOP:J=0
90 INPUT "NUMBER OF PEAK SCANS DESIRED? 1=10 2=20":J
95 IF J>=2:IFN GOSUB100
100 RT=INP(0):OUT10.8
105 FORP=0:Q1500:NEXIP
110 L=INP(9)AND15:IFL=0:IFL=110
115 CLS:PRINT "3 PEAKS - 10 SCANS EACH"
118 'LINE 120 COLLECTS PFAK DATA AND DISCARDS ANOMALOUS READINGS
120 FORU=0:Q09:FORV=0:Q02:OUT10.(V+8):PRINT350,(U+1):GOSUB610:GOSUB600:PRINT3(192+64*U
+16*V),Y(U,V):GOSUB900:NFXIV,U
124 'ALL LPRINT STATEMENTS CONTROL DATA PRINTED ON THE IFLIYFF
125 POKE 14312,13:LPRINT TAB(1)"RUN":TAB(4)Q+J:TAB(7)"PEAKS":FORU=0:Q09:LPRINT
Y(U,0),Y(U,1),Y(U,2):NFXIU
130 INPUT "DO YOU WANT ANOTHER 10 PEAK SCANS? 1=YES 2=NO":K
135 I=I+1
140 FORR=0:Q03:UG*(R)=PC*(R):NEXTR
145 IF K<=2:IFN=20
150 IF K=1:IFN=20
155 IF K=1:IFN=20
160 R1=INP(0)
165 OUT10.8

```



```

170 FOPP=0101500:VEXTP
175 L=INP(9)AND 15:IFL=01HEN175
180 CLS:PRINT "3 PEAKS - 10 SCANS EACH"
183 'LINE 185 COLLECTS THE SECOND SET OF PFAK SCANS
185 FORU=0T09:FORV=0T02:OUT10,(V+8):PRINT350,(U+1):GOSUB610:GOSUB600:PRINT3(192+64*
U+1C*V),Y(U,V):GOSUB900:NEXTV,U
190 LPRINT CHR$(10):LPRINT TAB(1)"RUN":TAB(4)Q+1:TAB(7)"(PEAKS)":LPRINT TAB(3)"88":T
AB(19)"87":TAB(35)"86"
195 FORU=0109:LPRINT Y(U,0),Y(U,1),Y(U,2):NEXIU
198 'LINES 200 AND 210 STORE PEAK DATA FOR MORE THAN ONE RUN IN SEPARATE MATRIC
ES
200 FORG=0109:FORH=0102:W(G,H)=Y(G,H):NFX1H,G
205 RETURN
210 FORP=0109:FORO=0102:Z(P,O)=Y(P,O):NEX1O,P
215 RU=INP(10):OUT10.8
220 FOPP=0101500:NEXIP
225 L=INP(9)AND15:IF L=0 THEN225
230 CLS:PRINT "3 PEAKS - 10 SCANS EACH"
233 'LINE 235 COLLECTS PEAK DATA FOR THE THIRD RUN OF 30 SCANS
235 FORU=0T09:FORV=0T02:OUT10,(V+8):PRINT350,(U+1):GOSUB610:GOSUB600:PRINT3(192+64*U
+1C*V),Y(U,V):GOSUB900:NEXTV,U
240 POKE 14312,13:LPRINT TAB(1)"RUN":TAB(4)Q+J+1:TAB(7)"(PEAKS)":FORU=0T09:LPRINT Y
U,0),Y(U,1),Y(U,2):NEXIU
245 RETURN
248 'SUBROUTINE 250 CONTROLS THE ISOTOPIC DATA REDUCTION
250 IFT=0THEN RETURN
255 Q=Q+1:P#(0)=87.4#:P#(1)=86.4#:P#(2)=85.4#:P#(3)=85#:FUNX#=0#:SUMY#=0#:SVY#=0#:FV
X#=0#:SIMX#=0#:TIMX#=0#:UIMX#=0#
260 FORR=11031:VR(R)=0:UV(R)=0:NFX1R
265 IF J=1 THEN GOSUB810
267 'LINES 265-330 FILTER OUT BACKGROUNDS WHICH MAY BE AFFECTED BY AN 88 TAIL O
R 88 PEAK IN ORDER TO CALCULATE A BASELINE
270 IF J=1 THEN 280
275 IF J=2 THEN GOSUB855
278 'G,YC, AND KC ARE THE VALUES OF THE SLOPE BETWEEN VARIOUS BAGS
280 #G=#G(0)-#G(1):YC=#G(1)-#G(2):KC=(#G(2)-#G(3))/0.4
285 IF #G>(0.85*YC)THEN315
290 IF KC<-15 THEN305
295 FORR=0103:N#=4#:GOSUB1075:NEXTR
300 IF SIMX#>0 THEN335
305 FORR=0T02:N#=3#:GOSUB1075:NFX1R
310 IF SIMX#>0 THEN335
315 IF KC<-15 THEN330
320 FORR=1103:N#=3#:GOSUB1075:NEXTR
325 IF SIMX#>0 THEN335
330 FORR=1T02:N#=2#:GOSUB1075:NEXTR
335 GOSUB1090
338 'LINES 340-350 CALCULATE TIME,88 TAIL,88 PFAK, AND BASELINECORRECTED SR PEA
KS. FOR CONVENIENCE THESE VALUES ARE STORED IN A 9X3X3 MATRIX
340 FORE=0T08:FORF=1T025 STEP 3:PK(E,0,0)=Y(E,0)-NV(F,0):PK(F,1,0)=Y(E,1)-NV(F+1,1)-
W(F+1)-UV(F+1):PK(E,2,0)=Y(E,2)-NV(F+2,2):NEXTF,E

```

```

345 FORR=0108:FORI=21026 STEP 3:PK(E,0,1)=(Y(E+1,0)-Y(E,0))/3+Y(E,0)-NV(F,0):PK(E,1,
1)=(Y(F+1,1)-Y(E,1))/3+Y(E,1)-NV(F+1,1)-VR(F+1)-UV(F+1):PK(E,2,1)=(Y(E+1,2)-Y(E,
2))/3+Y(E,2)-NV(F+2,2):NEX1F,E
350 FORR=0108:FORI=31027 STEP 3:PK(E,0,2)=((Y(E+1,0)-Y(F,0))*2)/3+Y(F,0)-NV(F,0):PK(
E,1,2)=((Y(E+1,1)-Y(E,1))*2)/3+Y(E,1)-NV(F+1,1)-VR(F+1)-UV(F+1):PK(E,2,2)=((Y(E+
1,2)-Y(E,2))*2)/3+Y(E,2)-NV(F+2,2):NEX1F,E
353 'LINE 355 CALCULATES THE 86/88 RATIO
355 FORR=1108:QN(R)=PK(R-1,2,1)/PK(R,0,0):QM(R)=PK(R-1,2,2)/PK(R,0,1):QO(R)=PK(R,2,0
)/PK(R,0,2):NEXTR
358 'LINE 360 CALCULATES THE 87/86 RATIO. LINE 365 CALCULATES THE NORMALIZED 87
/86 RATIO TO AN 86/88 VALUE OF 0.1194
360 FORR=1108:RN(R)=PK(R-1,1,2)/PK(R-1,2,1):RM(R)=PK(R,1,0)/PK(R-1,2,2):RO(R)=PK(R,1
,1)/PK(R,2,0):NEXTR
365 FORR=1108:NN(R)=(2*RN(R)*QN(R))/(QN(R)+.1194):NM(R)=(2*RM(R)*QM(R))/(QM(R)+.1194
):NO(R)=(2*QO(R)*RO(R))/(QO(R)+.1194):NEXTR
370 CLS:PRINT3(2),"86/88":PRINT3(12),"87/88":PRINT3(24),"86/88":PRINT3(34),"8
7/88":PRINT3(46),"86/88":PRINT3(56),"87/88"
375 FORR=1108:PRINT3(64*R),QN(R):PRINT3(64*R+11),NN(R):PRINT3(64*R+22),QM(R):PRINT3(
64*R+33),NM(R):PRINT3(64*R+44),QO(R):PRINT3(64*R+55),NO(R):NEXTR
380 @PRINT CHR(10):LPRINT TAB(2)"(86/88)":TAB(12)"(87/88)":TAB(23)"(86/88)"
:TAB(32)"(87/88)":TAB(43)"(86/88)":TAB(52)"(87/88)"
385 FORR=1108:LPRINT TAB(1)QN(R):TAB(12)NN(R):TAB(22)QM(R):TAB(32)NM(R):TAB(42)
QO(R):TAB(52)NO(R):NEXTR
388 'MEANX(Q) AND JEANX ARE THE AVERAGE NORMALIZED 87/86 RATIOS AND 86/88 RATIO
S FOR A SINGLE RUN. PP IS THE STANDARD DEVIATION FOR THE RUN
390 FORR=1108:IA(R)=IA(R-1)+NO(R)+NM(R)+NN(R):BA(R)=BA(R-1)+QN(R)+QO(R)+QM(R):NEXTR
395 MEANX(Q)=IA(8)/24:JFANX=BA(8)/24
400 FORR=1108:PH(R)=(NN(R)-MEANX(Q))/(2:PM(R)=(NM(R)-MEANX(Q))/(2:PO(R)=(NO(R)-MEANX(Q
))/(2:PL(R)=PH(R)+PO(R)+PM(R)+PL(R-1):NEXTR
405 PP=(PL(8)/23)(0.5
410 IFQ=21HEN440
413 'IF THE STANDARD DEVIATION IS GREATER THAN 0.0015 THEN THE MFAN 87/86 RATIO
FOR THE RUN IS RECALCULATED IN SUBROUTINE 675 EXCLUDING SPURIOUS DATA
415 IF PP<0.0015 THEN XI=24
420 IFPP>0.0015THEN COSUBC75
425 PRINT3(653),"START":PRINT3(660),"END":PRINT3(675),"MFAN(87/86)N="MFANX(Q):PRINT3
(698),XI:PRINT3(709),"88 TAIL="CINT(UV(1))"TO"CINT(UV(30)):PRINT3(739),"STD DEV="
"PP:PRINT3(773),"RB CORR="CINT(VR(1))"TO"CINT(VR(31)):PRINT3(803),"MFAN 86/88="J
FANX
430 LPRINT CHR(10):LPRINT TAB(1)"MEAN(87/86)N=":TAB(1)MFANX(Q):TAB(31)"START":TAB(3
9)"END":LPRINT TAB(1)"STD DEV=":TAB(1)PP:TAB(24)"88 TAIL=":TAB(32)CINT(UV(1)):TA
B(35)"10":TAB(38)CINT(UV(30))
435 LPRINT TAB(1)"MEAN(86/88)N=":TAB(1)JEANX:TAB(24)"RB CORR=":TAB(32)CINT(VR(1)):TAB
(35)"TO":TAB(38)CINT(VR(31)):LPRINT TAB(1)"NUMBER OF RATIOS USED IN MEAN CALCULA
TION=":TAB(1)XI
438 'SFANX IS THE CUMULATIVE MEAN (87/86)N RATIO FOR ALL RUNS
440 RB(Q)=RB(Q-1)+MFANX(Q)
445 SFANX=RB(Q)/Q
450 RA(Q)=(MEANX(Q)-SFANX)/2
455 RC=PC+RA(Q)
460 IFQ=21HEN505

```

```

463 MI IS THE CUMULATIVE STANDARD DEVIATION FOR ALL THE RUNS
465 M1=RC/(Q-1)**0.5
470 IF PP<0.0015 THEN XX=24
475 IF PP>0.0015 THEN GOSUB675
480 PRINT(628);"START":PRINT(635);"END":PRINT(640);"TOTAL STATS(  )":PRINT(652)
  2*10:PRINT(656);" )":PRINT(661);"10 SCANS ONLY":PRINT(677);"X":PRINT(683);"88
  1AIL="CINT(UV(1))"TO"CINT(UV(31)):PRINT(704);"MEAN87/86N="SFANX
485 PRINT(725);"MEAN87/86N="MEANX(10):PRINT(747);"RB CORR="CINT(VR(1))"TO"CINT
  (VR(31)):PRINT(768);"STD DEV="M1:PRINT(789);"STD DEV="PP:PRINT(811);"MFAN86/8
  6="JEANX
490 LPRINT CHR$(10):LPRINT TAB(1)"TOTAL STATS("TAB(13)Q*10:TAB(17)"SCANS":TAB(22)"
  "TAB(25)"10 SCANS ONLY":TAB(56)"START":TAB(63)"END"
495 LPRINT TAB(1)"MEAN(87/86)N="TAB(14)SFANX:TAB(25)"MEAN(87/86)N="TAB(38)MEANX(1)
  TAB(49)"88 1AIL="TAB(57)CINT(UV(1)):TAB(60)"TO":TAB(64)CINT(UV(30))
500 LPRINT TAB(1)"STD DEV="TAB(9)M1:TAB(25)"STD DEV="TAB(33)PP:TAB(49)"RB CORR="TAB
  (57)CINT(VR(1)):TAB(60)"10":TAB(64)CINT(VR(31)):LPRINT TAB(1)"MEAN(86/88)="TAB
  (13)JEANX:LPRINT TAB(1)"NUMBER OF RATIOS USED IN MEAN CALCULATION="TAB(1)XX
505 IF K=21 THEN 525
510 FORP=0 TO 9:FORO=0 TO 2:Y(P,O)=Z(P,O):NEXT O,P
515 K=2:STOP
520 IF K=21 THEN 250
525 IF J=1 THEN 540
530 FORG=0 TO 9:FORH=0 TO 2:Y(G,H)=X(G,H):NEXT H,G:J=1:STOP
535 IF J=1 THEN 250
540 IF T=1 THEN 605
545 INPUT "DO YOU WISH TO RE-CALCULATE TOTAL STATISTICS EXCLUDING RUNS OUTSIDE
  A 99% CONFIDENCE INTERVAL? 1=YES 2=NO":P
550 IF P=2 THEN 605
555 AE=0:W=0:RE=0:LE=0:X=1:O=0:SP=0
565 CLS:PRINT(10);"MEANS WITHIN A 99% CONFIDENCE INTERVAL":PRINT(76);"RUN#":P
  RINT(92);"RUN#":PRINT(108);"RUN#"
570 LPRINT CHR$(10):LPRINT TAB(1)"MEANS WITHIN A 99% CONFIDENCE INTERVAL"
575 FORR=1 TO Q
578 'LINE 580 TESTS MEAN (87/86)N VALUES FOR EACH RUN WITH THE GRAND MEAN FOR A
  LL THE RUNS (SEANX). IF THE INDIVIDUAL MEANS ARE WITHIN THE APPROXIMATE 99% CONFI
  DENCE INTERVAL THEY PASS INTO SUBRO=0
580 IF MEANX(R)>=(SEANX-0.002)AND MEANX(R)<=(SEANX+0.002) THEN GOSUB970:
585 NEXT R
590 IF R=1 THEN GOSUB1035
595 PRINT(644);"MFAN(87/86)N="LEANX:PRINT(680);"STD DEV="P1
600 LPRINT CHR$(10):LPRINT TAB(1)"MEAN(87/86)N="TAB(14)ZE:TAB(25)"STD DEV="TAB
  (33)PT
605 RETURN
608 'LINES 610-660 CONVERT THE BINARY VALUES FOR PFAA AND BKQ DATA TO DIGITAL F
  ORM

```

✓

```

610 L= INP(9) AND 15: IF L=0 THEN 610
615 A= INP(10) AND 15
620 B= INP(1) AND 15
625 C= INP(2) AND 15: IF C=15 THEN C=0
630 D= INP(3) AND 15: IF D=15 THEN D=0
635 E= INP(4) AND 15: IF E=15 THEN E=0
640 F= INP(5) AND 15: IF F=15 THEN F=0
645 RETURN
650 X(N,M)=A+10*B+10(2*C+10(3*D+10(4*E+10(5*F
655 RETURN
660 70  N=N+1
675  UV(N)=R
680  NP(N)=MFANX(R)
685  O=O+1
690  IF O=4 THEN GOSUB 1060
695  ORR=O*103: NG(N)=UG(N): MG(N)=PG(N): NEXTR
696  RETURN
697  IF K=1 THEN 890
698  IF UU=1 THEN 880
699  FORR=O*103: MG(N)=NG(N): NG(N)=((PG(N)-UG(N))/3)+UG(N): NEXTR
700  UU=1
701  IF UU=1 THEN 895
702  FORR=O*103: MG(N)=NG(N): NG(N)=UG(N): NEXTR
703  IF UU=1 THEN 895
704  FORR=O*103: MG(N)=PG(N): NG(N)=(((PG(N)-UG(N))*2)/3)+UG(N): NEXTR
705  RETURN
706  *LINES 900-930 CHECKS FOR SPURIOUS PEAK DATA AND REPEATS A SCAN IF NECESSARY
707  IF U<1 THEN RETURN
708  IF Y(U-1,V)<(Y(U,V)-0.15*Y(U,V)) THEN 920
709  IF Y(U-1,V)>(Y(U,V)+0.15*Y(U,V)) THEN 920
710  RETURN
711  U=U-1
712  V=V-1
713  RETURN
714  *LINES 935-965 CHECKS FOR SPURIOUS BKG DATA AND REPEATS A SCAN IF NECESSARY
715  IF N<1 THEN RETURN
716  IF X(N-1,M)<(X(N,M)-0.15*X(N,M)) THEN 955
717  IF X(N-1,M)>(X(N,M)+0.15*X(N,M)) THEN 955
718  RETURN
719  N=N-1
720  RETURN
721  *SUBROUTINE 970 ACTS AS A COUNTER FOR THE 99% CONFIDENCE INTERVAL CALCULATION
722  AND CONTROLS THE PRINTING OF THE ACCEPTED DATA
723  N=N+1
724  UV(N)=R

```

```

980 NP(I)=MEANX(I)
985 O=O+1
990 IF O=4 THEN GOSUB1060
995 PRINT$(X*64+(O*16-4)+64),R:PRINT$(X*64+O*16+64),MEANX(I)
1000 ISP<4THEN1010
1005 POKE 14312,13:SP=0
1010 LPRINT R " MEANX(I):
1015 SP=SP+1
1020 IE=XE+NP(I)
1025 ZE=XE/I
1030 RETURN
1035 FORR=1TOI:RE=RE+(NP(I)-ZE)*(2):NEXTR
1040 IF I*(I-2)<1 THEN1055
1045 PT=(RE/(I*(I-1)))(0.5
1050 SEANX=ZE
1055 RETURN
1060 O=1
1065 I=X+1
1070 RETURN
1073 *STATEMENT 1075 CALCULATES VARIOUS VALUFS USED IN THE BASELINE CALCULATION.
SLPX AND TTX ARE THE SLOPES OF THE BASELINE BEFORE AND AFTER THE RUN. LPX AND
TTX ARE THE INITIAL BASFLINE VALUES AT MASS 88
1075 SUMY#=SUMY#+MG#(R):FUMX#=FUMX#+(NG#(R)*P#(R)):SVY#=SVY#+NG#(R):FVX#=FVX#+(NG#(R)
*P#(R)):SIMX#=SIMX#+P#(R):TIMX#=TIMX#+(P#(R)*2):UIMX#=SIMX#(2
1080 SLPX=(FUMX#-(SIMX#*SUMY#)/N#)/(TIMX#-(UIMX#/N#)):VLPX=(FVX#-(SIMX#*SVY#)/N#)
/ (TIMX#-(UIMX#/N#)):TNTX=((SIMX#*FUMX#)-(SUMY#*TIMX#)/(UIMX#-(N#*TIMX#)):TVTX=
(SIMX#*FVX#)-(SVY#*TIMX#)/(UIMX#-(N#*TIMX#))
1085 RETURN
1089 *B(R) AND MV(R) ARE THE CALCULATED BASELINE VALUFS AT MASSES 88,87,86,AND
86
1090 FORR=0103:B(R)=SLPX*(88-R)+TNTX:MV(R)=VLPX*(88-R)+TVTX:VA(R)=(B(R)-MV(R))/32:NEX
TR
1093 *NV(R,S) IS THE INTERPOLATED BASELINE VALUES TO CORRESPOND WITH THE TIME C
CORRECTED PEAKS
1095 FORR=01031:FOR S=0103:NV(R,S)=VA(S)*R+MV(S):NEXTR,S,R
1100 IF *G>(0.85*YG) THEN1115
1105 IF KC<-15 THEN1135
1110 RETURN
1113 *UV(R) IS THE 88 TAIL CORRECTION. VR(R) IS THE 86 PEAK CORRECTION
1115 UV(0)=(NG#(0)-NG#(1))*0.6+NG#(1)-MV(1):UV(31)=(MG#(0)-MG#(1))*0.6+MG#(1)-B(1)
1120 IF UV(0)<=0 THENUV(0)=0:IF UV(31)<=0 THENUV(31)=0
1125 FORR=1TO31:UV(R)=(UV(31)-UV(0))/32)*R+UV(0):NEXTR
1130 IF KC>-15 THEN1150
1135 VI=(NG#(3)-MV(3))*0.3856:VS=(MG#(3)-B(3))*0.3856:VT=(VS-VI)/32
1140 FORR=1TO31:VR(R)=VI*R+VI:NEXTR
1145 IF VR(0)<=0 THEN VR(0)=0:IF VR(31)<=0 THEN VR(31)=0
1150 RETURN

```

## PROGRAM "S"

## SR84 SPIKE DATA COLLECTION

```

5 DIM X(9,4),FK(30,3,3),Z(9,4),N(43,4),UV(41),VR(41),PFANA(30),NU(26),NP(26),RB
(25),FA(25)
6 I=0:J=0:AZ=0:AY=0
7 FORR=0:Q20:PFANA(R)=0:NFAIR
10 NS=INP(0)
11 OUT10,0
12 AZ=AZ+1
15 FORP=0:1000:N=XTP
20 L=INP(9)AND15:IFL=0 THEN 20
25 CLS:PRINT "4 SACS - 5 SCANS EACH"
27 PRINT(128),"87.4":PRINT(138),"86.4":PRINT(148),"85.4":PRINT(158),"84.4":
PRINT(168),"83.4"
160 FORR=0:104:FORR=0:104:OUT10,M:PRINT(50,4+1):GOSUB1000:GOSUB1070:PRINT(192+64*N+10*
M),X(N,R):GOSUB2055:NFAIR=N
165 FORR=0:104:SAIF=0:NFAIR
170 FORR=0:104:FORR=1:105:SM(N)=SM(N)+X(S-1,N):BG(R)=SM(N)/5:NEXTR,R
172 FORR=0:104:PRINT(576+10*R),CINT(BG(N)):PG#(R)=CDEL(BG(R)):NEXTR
175 LPRINT CHR(10):LPRINT "BACKGROUND":LPRINT TAB(1)"87.4":TAB(7)"86.4":TAB(13)"85
.4":TAB(19)"84.4":TAB(25)"83.4":FORR=0:104:PRINT TAB(1)X(N,0):TAB(7)X(N,1):TAB(1
3)X(N,2):TAB(19)X(N,3):TAB(25)X(N,4):NEXTR
174 FORR=143:12,13:LPRINT TAB(1)CINT(BG(0)):TAB(7)CINT(BG(1)):TAB(13)CINT(BG(2)):TAB
(19)CINT(BG(3)):TAB(25)CINT(BG(4)):SU=0
175 PRINT(7-1-AZ),CINT(BG(0)),CINT(BG(1)),CINT(BG(2)),CINT(BG(3)),CINT(BG(4))
162 OUT10,8:STOP:OUT10,9:STOP:OUT10,10:STOP:OUT10,11:STOP:OUT10,12:STOP:J=0
185 INPUT "NUMBER OF PEAK SCANS DESIRED? 1=10 2=20":J
164 J=J
185 GOSUB400
191 INPUT "DO YOU WISH ANOTHER 10 PEAK SCANS? 1=YES 2=NO":K
192 I=I+1
193 FORR=0:103:UG#(R)=PG#(R):NFAIR
194 IFK=2 THEN 10
196 FORR=0:109:FORR=0:104:Z(IP,0)=Y(IP,0):NEXTR,P:JK=1
198 GOSUB400
200 IFK=1 THEN 10
400 AT=INP(0):OUT10,8
405 FORP=0:1000:N=XTP
410 L=INP(9)AND15:IFL=0 THEN 410
412 AY=AY+1

```

```

420 CLS:PRINT"ISOTOPE DILUTION RUN "3" - 5 PEAKS - 10 SCANS EACH"
421 PRINTB(129),"SR88":PRINTB(141),"SR87":PRINTB(153),"SR86":PRINTB(165),"RB85"
:PRINTB(177),"SR84"
430 FORU=0TO9:FORV=0TO4:OUT10:(V+8):PRINT#50,U+1:GOSUB1000:GOSUB1075:PRINT#(192+64*U
+12*V),Y(U,V):GOSUB2040:NEXTV,U
440 POKE 14312,13:LPRINT TAB(1)"RUN":TAB(4)Q:TAB(7)"(PEAKS)":LPRINT TAB(2)"SR88":TAB
(12)"SR87":TAB(22)"SR86":TAB(32)"RB85":TAB(42)"SR84":FORU=0TO9:LPRINT TAB(1)Y(U,
0):TAB(11)Y(U,1):TAB(21)Y(U,2):TAB(31)Y(U,3):TAB(41)Y(U,4):NEXTU
441 FORU=0TO9:PRINT#-1,AY,Y(U,0),Y(U,1),Y(U,2),Y(U,3),Y(U,4):NEXTU
450 IFJK=1 THEN490
455 IFJK=2THENGOSUB620 ELSE470
460 IFJ=2THEN400
490 RETURN
620 FORC=0TO9:FORH=0TO4:W(C,H)=Y(C,H):NEXTH,C:JK=1
625 RETURN
1000 L=INP(9) AND15:IF L=0 THEN1000
1010 A=INP(10) AND 15
1020 B=INP(1) AND 15
1030 C=INP(2) AND 15:IF C=15 THEN C=0
1040 D=INP(3) AND 15:IF D=15 THEN D=0
1050 E=INP(4) AND 15:IF E=15 THEN E=0
1060 F=INP(5) AND 15:IF F=15 THEN F=0
1065 RETURN
1070 X(N,0)=A+10*B+10(2*C+10(3*D+10(4*E+10(5*F
1072 RETURN
1075 Y(U,V)=A+10*B+10(2*C+10(3*D+10(4*E+10(5*F
1080 RETURN
1089 STOP
2040 IF U<1 THEN RETURN
2050 IF Y(U-1,V)<(Y(U,V)-0.15*Y(U,V)) THEN 2080
2060 IF Y(U-1,V)>(Y(U,V)+0.15*Y(U,V)) THEN 2080
2070 RETURN
2080 U=U-1
2085 V=V-1
2090 RETURN
2095 IF V<1 THEN RETURN
2100 IF X(U-1,M)<(X(U,M)-0.15*X(U,M)) THEN 2130
2110 IF X(U-1,M)>(X(U,M)+0.15*X(U,M)) THEN2130
2120 RETURN
2130 M=M-1
2140 M=-1
2150 RETURN

```

## PROGRAM "Z"

SR84 SPIKE - SAMPLE DATA REDUCTION WITH TEST DATA

```

5 INOH
7 THE PFAF AND BACKGROUND DATA ARE OBTAINED FROM CASSETTES USING INPUT=-1 SIAI
  EASYS
10 INPUT "CONCENTRATION OF SR84 SPIKE USED(PPM) =" :CS
15 INPUT "ENTER THE WEIGHT OF SR84 SPIKE USED (GRAMS) =" :LS
20 INPUT "WEIGHT OF SAMPLE DIGESTED(GRAMS) =" :AI
21 INPUT "DO YOU WISH TO RUN A TEST PROGRAM? 1=YES 2=NO" :VV:IFVV=1 THEN 25
22 LPRINT CHR$(10):LPRINT "CONCENTRATION OF SR84 SPIKE USED(PPM) ="CS:LPRINT "
  WEIGHT OF SR84 SPIKE SOLUTION USED(GRAMS) ="AS:LPRINT "WEIGHT OF SAMPLE DIGESTED(
  GRAMS) ="AI
25 DIM A(9:4),P(100:3:4),Z(9:4),I(9:4),S(43:1),U(41),M(41),PEANX(30),
  M(33),NP(33),K(25),M(25)
30 I=0:Q=0
35 FORR=01020:MEANX(I)=0:MEANR
37 I=I+2:IF I=90
38 FORR=0104:READ BC(I):IFATE
39 IFVV=1:IF I=45
40 INPUT "1-AZ,BC(1),BC(2),BC(3),BC(4)
45 JA=0
50 UU=1:ZI=0
55 FORR=0104:FOR I=1 TO 4:READ M(I):MEANR
60 Q)=SU=110
65 IF I=0 THEN J=2 ELSE J=1
70 CLS
71 IFVV=2 THEN 74
72 FORU=0109:FORV=0104:READ Y(U,V):NEXTV,U
73 IFVV=1 THEN 80
74 ON ERROR GOTO1200
75 FORU=0109:INPUT "1-AZ, Y(U,0),Y(U,1),Y(U,2),Y(U,3),Y(U,4):PRINT"(64*U), Y(U,0):PRINT
  M(64*U+10),Y(U,1):PRINT"(64*U+20), Y(U,2):PRINT"(64*U+30), Y(U,3):PRINT"(64*U+40
  ),Y(U,4):GOTO
60 IF J=1 THEN 95
85 FORP=0109:FORQ=0104:Z(P,Q)=Y(P,Q):NEXTQ,P
86 I=I+2:IF I=90
87 FORU=0109:FORV=0104:READ Y(U,V):NEXTV,U
88 IFVV=1 THEN 95
89 ZI=1

```



```

90 CLS:FORU=0TO9:INPUT#-1,41,Y(U,0),Y(U,1),Y(U,2),Y(U,3),Y(U,4):PRINT#(64*U),Y(U,0)
:PRINT#(64*U+10),Y(U,1):PRINT#(64*U+20),Y(U,2):PRINT#(64*U+30),Y(U,3):PRINT#(64*
U+40),Y(U,4):NEXTU
95 I=1#1
100 FORN=0TO4:UG#(N)=PG#(N):NEXTN
105 IF J>0:IF=N55
110 IFI=0:INEM N EICRM
115 J=J+1:P#(0)=87.4#:P#(1)=86.4#:P#(2)=85.4#:P#(3)=84.4#:P#(4)=83.4#:FUMX#=#:SUM1#
=#:SUM2#=#:SUM3#=#:SUM4#=#:SUM5#=#:SUM6#=#:SUM7#=#:SUM8#=#:SUM9#=#:SUM10#=#
120 FORK=1TO4:UY(F)=0:Y(R)=0:NELRN
125 IF J=1:IF=N 135
130 IF J=2:IF=N 140
135 IF J=3:IF=N 145
140 M0=M0+(0)-M0*(1):M0=(M0(1)-M0*(2)):K0=K0*(3)-K0*(4)
145 IF M0>10.60*10:IF=N 150
150 IF K0<-15:IF=N 155
155 FORN=0TO4:N#=#:JOSUB855:NELRN
160 IF SIMA#>0:IF=N 165
165 FORN=0TO3:N#=#:JOSUB855:NELRN
170 IF SIMA#>0:IF=N 175
175 IF K0<-15:IF=N 180
180 FORN=1TO4:N#=#:JOSUB855:NELRN
185 IF SIMA#>0:IF=N 190
190 FORN=1TO3:N#=#:JOSUB855:NELRN
195 JOSUB855
200 FOR E=0TO8:FOR F=1TO34:SI#P 4:P(K(E,0))=I(F,0)-M(Y(F,0)):P(K(F,1))=Y(F,1)-M(Y(F,1)+
U(Y(F,1)+1)-I(F,1)):P(K(F,2))=I(E,2)-M(Y(F,2)+2):P(K(F,3))=Y(F,4)-M(Y(F,4)+3):NEXT F,F
205 FOR F=0TO8:FOR E=7TO35:SI#P 4:P(K(F,0))=I(F,0)-I(E,0)/4+I(F,0)-M(Y(F,0)):P(K(E,1)
)=I(Y(F,1)+1)-I(F,1)/4+I(E,1)-M(Y(F,1)+1):P(K(F,2))=I(E,2)-I(F,2)
210 M0#F=0:FOR N=5TO36:SI#P 4:P(K(E,0,2))=I(F,0)-I(E,0)/2+I(F,0)-M(Y(F,0)):P(K(E,1)
)=I(F,1)-I(E,1)/2+I(F,1)-M(Y(F,1)+1):P(K(F,2,2))=I(F,2)-I(E,2)
215 FOR E=0TO8:FOR F=5TO37:SI#P 4:P(K(F,0,3))=I(E,0)-I(F,0)/3+I(F,0)-M(Y(F,0)):P(K(F
,1,3))=I(F,1)-I(E,1)/3+I(F,1)-M(Y(F,1)+1):P(K(F,2,3))=I(F,2)-I(E,2)
220 P(K(F,3,3))=I(Y(F,4)-I(F,4))/3+I(F,4)-M(Y(F,4)+3):NEXT F,F
225 FOR E=1TO8:FOR N=1TO3:SI#P 4:P(K(N,1,2))=P(K(N,1,0,3)):L4(N)=P(K(N,1,2,2))/P(K(N,0,0)):L0(N)=P(K(N-1
,2,3))/P(K(N,0,1)):L2(N)=P(K(N,2,0))/P(K(N,0,2)):L1(N)=P(K(N-1,1,2))/P(K(N-1,2,1)):L(N)=P(K
(N-1,1,3))/P(K(N-1,2,2)):I0(N)=P(K(N,1,0))/P(K(N-1,2,2))
230 I2(N)=P(K(N,1,1))/P(K(N,2,0)):L3(N)=P(K(N-1,2,1))/P(K(N-1,3,0)):M(N)=P(K(N-1,2,2))/P(K(N-1
,3,1)):K(N)=P(K(N-1,3,3))/P(K(N-1,0,2)):L(N)=P(K(N,2,0))/P(K(N-1,3,3)):J(N)=P(K(N-1,0,4)
)/P(K(N-1,3,0)):J(N)=P(K(N,0,0))/P(K(N-1,3,1))
235 J(N)=P(K(N,0,1))/P(K(N-1,3,2)):J(N)=P(K(N,0,2))/P(K(N-1,3,3)):J(N)=P(K(N-1,1,2))/P(K(N-1
,3,0)):J(N)=P(K(N-1,1,3))/P(K(N-1,3,1)):J(N)=P(K(N,1,0))/P(K(N-1,3,2)):J(N)=P(K(N,1,1)/
P(K(N-1,3,3))
240 M E L R N
245 FOR E=1TO8:FOR N=1TO3:SI#P 4:P(K(N,1,2))=P(K(N,1,0,3)):L4(N)=P(K(N,1,2,2))/P(K(N,0,0)):L0(N)=P(K(N-1
,2,3))/P(K(N,0,1)):L2(N)=P(K(N,2,0))/P(K(N,0,2)):L1(N)=P(K(N-1,1,2))/P(K(N-1,2,1)):L(N)=P(K
(N-1,1,3))/P(K(N-1,2,2)):I0(N)=P(K(N,1,0))/P(K(N-1,2,2))
250 I2(N)=P(K(N,1,1))/P(K(N,2,0)):L3(N)=P(K(N-1,2,1))/P(K(N-1,3,0)):M(N)=P(K(N-1,2,2))/P(K(N-1
,3,1)):K(N)=P(K(N-1,3,3))/P(K(N-1,0,2)):L(N)=P(K(N,2,0))/P(K(N-1,3,3)):J(N)=P(K(N-1,0,4)
)/P(K(N-1,3,0)):J(N)=P(K(N,0,0))/P(K(N-1,3,1))
255 J(N)=P(K(N,0,1))/P(K(N-1,3,2)):J(N)=P(K(N,0,2))/P(K(N-1,3,3)):J(N)=P(K(N-1,1,2))/P(K(N-1
,3,0)):J(N)=P(K(N-1,1,3))/P(K(N-1,3,1)):J(N)=P(K(N,1,0))/P(K(N-1,3,2)):J(N)=P(K(N,1,1)/
P(K(N-1,3,3))

```



```

370 GOSUB 695
375 RB(Q)=R*(Q-1)+EANX(Q)
380 SFANX=RB(Q)/Q
385 RA(Q)=(MEANX(Q)-SEANX)/2
390 RC=RC+RA(Q)
395 IF Q<2 THEN 445
400 M1=(RC/(Q-1))*10.5
405 IF PP<0.0015 THEN AX=32
410 IF PP>0.0015 THEN GOSUB 540
415 PRINT(628); "START":PRINT(635); "END":PRINT(640); "TOTAL STATS ( )":PRINT(652)
; Q*10:PRINT(656); "":PRINT(661); "10 SCANS ONLY":PRINT(677); XX:PRINT(683); "88
; IAIL="CINT(UV(1))"10"CINT(UV(31)):PRINT(704); "MEAN 87/86N="SFANX
420 PRINT(725); "MEAN 87/86N="MEANX(J):PRINT(747); "RB CORR="CINT(VR(1))"10"CINT
(VR(31)):PRINT(768); "SID DEV="MI:PRINT(789); "SID DEV="PP:PRINT(611); "MEAN 86/8
6="JEANX
425 LPRINT CHR$(10):LPRINT TAB(1)"TOTAL STATS":TAB(13)Q*10:TAB(17)"SCANS":TAB(22)"
":TAB(25)"10 SCANS ONLY":TAB(56)"START":TAB(63)"END"
430 LPRINT TAB(1)"MEAN 87/86N=":TAB(14)JEANX:TAB(25)"MEAN 87/86N=":TAB(38)MEANX(Q)
; TAB(49)"88 IAIL=":TAB(57)CINT(UV(1)):TAB(60)"10":TAB(64)CINT(UV(31))
435 LPRINT TAB(1)"SID DEV=":TAB(9)MI:TAB(25)"SID DEV=":TAB(33)PP:TAB(49)"RB CORR=":
TAB(57)CINT(VR(1)):TAB(60)"10":TAB(64)CINT(VR(31)):LPRINT TAB(1)"MEAN(86/88)=":
TAB(13)JEANX:LPRINT TAB(1)"NUMBER OF RATIOS USED IN MEAN CALCULATION=":TAB(1)AX
440 GOSUB 695
445 IF J=1 THEN 465
450 IF JK=1 THEN 465
455 FOR P=0 TO 9:FOR Q=0 TO 3:Y(P,Q)=Z(P,Q):DEFIN P:JK=1
460 IF J=2 THEN 410
465 IF I=1 THEN 520
470 Y=0:P=0:Q=0:Z=0:Z=1:Q=0:SP=0
475 FOR K=1 TO 26:Y(P,Q)=0:NEXT K
480 CLS:PRINT(10); "MEANS WITHIN A 99% CONFIDENCE INTERVAL":PRINT(76); "ROW#":P
; MI(92); "ROW#":PRINT(108); "ROW#"
485 LPRINT CHR$(10):LPRINT TAB(1)"MEANS WITHIN A 99% CONFIDENCE INTERVAL"
490 FOR I=1 TO 5
495 IF MEANX(I)>=(SEANX-0.002)AND MEANX(I)<=(SEANX+0.002) THEN GOSUB 730:
500 NEXT I
505 IF I>1 THEN GOSUB 795
510 PRINT(644); "MEAN(87/86)N=" ZEANX:PRINT(680); "SID DEV="PI
515 LPRINT CHR$(10):LPRINT TAB(1)"MEAN(87/86)N=":TAB(14)ZEANX:TAB(25)"SID DEV=":
TAB(33)PI
520 RETURN
525 I(O,I)=A+10^I+10(2^C+10(3^D+10(4^E+10(5^F
530 RETURN
535 STOP
540 FD 88/80 RATIO ="NA:PRINT(640); "AVERAGE MEASURED 87/84 RATIO ="PI
715 LPRINT CHR$(10):LPRINT "SIPHONUM CONCENTRATION CALCULATION":PRINT 14712.13:
LPRINT "SIPHONUM CONCENTRATION USING 86/84 RATIO ="MX"PPM":LPRINT "SIPHONUM CON
CENTRATION USING 88/84 RATIO ="NA
720 LPRINT "AVERAGE MEASURED 86/84 RATIO ="MI:LPRINT "AVERAGE MEASURED 88/84 RA
TIO ="NA
725 RETURN

```

```

730 A=A+1
735 UY(A)=R
740 NP(A)=MEANX(R)
745 O=O+1
750 IF O=4 THEN GOSUB820
755 O
630 IF A=2 THEN645
635 IF O=1 THEN640
640 MAA=A(R)=MR
645 RETURN
650 FORN=0104:NG*(R)=UG*(R):NC*(R)=PG*(R):NEXTR
655 RETURN
660 IF UU=2 THEN680
665 UU=2
670 FORR=0104:NG*(R)=PG*(R):NC*(R)=((PG*(R)-UG*(R))/2)+UG*(R):NEXTR
675 RETURN
680 FORR=0104:MG*(R)=NC*(R):NG*(R)=UG*(R):NEXTR
685 RETURN
690 RETURN
695 CLS:PRINT(200),"STRONTIUM CONCENTRATION CALCULATION"
700 PRINT(304),"STRONTIUM CONCENTRATION USING 86/84 RATIO =" ;NX;"PPM"
705 PRINT(448),"STRONTIUM CONCENTRATION USING 88/84 RATIO =" ;NA;"PPM"
710 PRINT(512),"AVERAGE MEASURED 86/84 RATIO =" ;HT:PRINT(576),"AVERAGE
MEAS 88/84 RATIO =" ;HA:PRINT(640),"AVERAGE MEASURED 87/84 RATIO =" ;PI
715 LPRINT CHR$(10):LPRINT "STRONTIUM CONCENTRATION CALCULATION":POKE 14312,13:
LPRINT "STRONTIUM CONCENTRATION USING 86/84 RATIO =" ;NX;"PPM":LPRINT "STRONTIUM CON
CENTRATION USING 88/84 RATIO =" ;NA
720 LPRINT "AVERAGE MEASURED 86/84 RATIO =" ;HT:LPRINT "AVERAGE MEASURED 88/84 RA
TIO =" ;HA
725 RETURN
730 A=A+1
735 UY(A)=R
740 NP(A)=MEANX(R)
745 O=O+1
750 IF O=4 THEN GOSUB820
755 PRINT(X*64+(O*16-4)+64),R:PRINT(X*64+O*16+64),MEANX(R)
760 IF SP<4 THEN770
765 POKE 14312,13:SP=0
770 LPRINT R" "MEANX(R);
775 SP=SP+1
780 XE=XE+NP(A)
785 ZE=XE/A
790 RETURN
795 FORN=1104:KE=KE+((NP(R)-ZE)*(2):NEXTR
800 IF A*(A-2)<1 THEN815
805 PI=(KE/(A*(A-1)))*0.5
810 SPAN=ZE
815 RETURN
820 O=1
825 X=X+1
830 RETURN

```

```

835 SUNY#=#SUNY#+NG*(R):FUMX#=#FUMX#+(NG*(R)*P*(R)):SVY#=#SVY#+NG*(R):FVX#=#FVX#+(NG*(R)
  *P*(R)):SIX#=#SIX#+P*(R):TIMX#=#TIMX#+(P*(R)*2):UIX#=#SIX*(2
840 SLPX#=(FUMX#-(SIX#*SUNY#)/N#)/(TIMX#-(UIX#*P#)):VLPX#=(FVX#-(SIX#*SVY#)/N#)
  / (TIMX#-(UIX#*P#)):TAX#=(SIX#*FUMX#)-(SUMX#*TIMX#)/(UIX#-(N#*TIMX#)):TVX#=(
  (SIX#*FVX#)-(SVY#*TIMX#)/(UIX#-(N#*TIMX#))
845 RETURN
850 FORR=#0104:B(R)=SLPX*(88-R)+TNTX:VY(R)=VLPX*(88-R)+VTX:VA(R)=(B(R)-VY(R))/41:NFX
  TR
855 FORR=#01041:FORS=#0104:NY(R,S)=VA(S)*R+VY(S):NEXIS,R
860 IF (0,3)>(B(3)+10)THEN875
865 IF R<#(0.85*16) THEN895
870 RETURN
875 FORR=#0306 STEP4:VX(R)=(Y(R/5,3)-Y((R-5)/5,3))/4+Y((R-5)/5,3):VX(R+1)=(Y(R/5,
  3)-Y((R-5)/5,3))/2+Y((R-5)/5,3):VX(R+2)=(Y(R/5,3)-Y((R-5)/5,3))^2/4+Y((R-5)
  /5,3):VX(R+3)=(Y(R/5,3)-Y((R-5)/5,3))^3/4+Y((R-5)/5,3):NEXTR
880 FORR=#01041:VR(R)=(VX(R)-VY(R,3))^0.3856:NEXTR
885 FORR=#0104:VB(R)=VR(R+5):NEXTR
890 FORR=#37041:VR(R)=VR(R-5):NEXTR
895 UV(0)=(NG*(0)-NG*(1))*0.6+NG*(1)-PV(1):UV(31)=(RC#(0)-NG*(1))*0.6+NG*(1)-B(1)
900 5,18007,1907,41552,147170,14450,18620,1005,41807,147978,14524,18730,1010,41803,1
  48017,14544,18743,1006,41746
1335 DATA 147771,14524,18614,1012,41297,144424,14369,18463,1004,41119,146340,14
  379,18467,1010,41275,146144,14375,18540,1007,41367,146129,14371,18516,1008,41420

1340 DATA 982,995,988,995,1003

1305 DATA 137900,13660,17569,1009,39174,138243,13662,17619,1014,39247,139081,13
  755,17711,1012,39564,139494,13710,17608,1009,39425,139721,13743,17670,1008,39355

1310 DATA 139666,13801,17726,1015,39674,140624,13678,17811,1011,39528,139595,13
  767,17727,1010,39322,139027,13796,17778,1010,39633,140312,13671,17870,1007,39974

1315 DATA 982,994,995,995,1006
1320 DATA 143085,14119,18171,1012,40721,144014,14193,18271,1009,40908,144791,14
  232,18260,1012,40853,144785,14294,18166,1007,40734,144059,14185,18286,1010,40903

1325 DATA 144586,14243,18346,1006,40989,145074,14240,18323,1010,40873,144731,14
  251,18259,1008,40873,144897,14261,18301,1005,41055,145384,14269,18364,1011,4110
  8
1330 DATA 146261,14379,18520,1010,41429,146
  5,18007,1907,41552,147170,14450,18628,1005,41807,147978,14524,18730,1010,4180
  3,148017,14544,18743,1006,41746
1335 DATA 147771,14524,18614,1012,41297,144424,14369,18463,1004,41119,146340,14
  379,18467,1010,41275,146144,14375,18540,1007,41367,146129,14371,18516,1008,41420

1340 DATA 982,995,988,995,1003

```

## RUBIDIUM ISOTOPE DILUTION PROGRAM

```

1 TROFF
2 INPUT "CONCENTRATION OF RB87 SPIKE SOLUTION (PPM) =" ; CS
3 INPUT "WEIGHT OF RB87 SPIKE SOLUTION ADDED (GRAMS) =" ; WR
4 INPUT "WEIGHT OF SAMPLE USED (GRAMS) =" ; WT
5 DIM PK(10),W(9,3),Z(9,3),HY(20),MEANX(30),NU(26),NP(26),RB(25),RA(25)
6 T=0:Q=0
7 FORR=0 TO 20:MEANX(R)=0:NEXTR
8 PRINT "FOR RB ISOTOPE DILUTION RUNS SET THE ACCELERATING VOLTAGE FOR MASS 89.
  THE FIRST FIELD OFFSET IS RESERVED FOR RB87 AND THE SECOND FIELD OFFSET IS FOR
  RB85. THE THIRD OFFSET IS SET FOR MASS 83."
9 STOP
10 RS=INP(0)
11 OUT10,0
15 FORP=0 TO 1500:NEXTP
20 L=INP(9)AND15:IFL=0 THEN 20
25 CLS:PRINT "4 BGCS - 5 SCANS EACH"
30 UU=0
160 FORN=0 TO 4:FORM=0 TO 3:OUT10,M:PRINT#50,M+1:GOSUB1000:GOSUB1070:PRINT#(192+64*M+16*
  M),X(N,M):GOSUB2095:NEXTM,N
165 "FOUR BACKGROUND POSITIONS ARE COLLECTED AT MASS 88.4, 86.4, 84.4, AND 82.4

169 FORR=0 TO 3:SM(R)=0:NEXTR
170 FORR=0 TO 3:FORS=1 TO 5:SM(R)=SM(R)+X(S-1,R):BG(R)=SM(R)/5:NEXTS,R
172 FORR=0 TO 3:PRINT#(576+16*R),CINT(BG(R)):PG*(R)=CDBL(BG(R)):NEXTR
173 LPRINT CHR$(10):LPRINT "BACKGROUNDS":LPRINT TAB(1)"88.4":TAB(8)"86.4":TAB(1
  5)"84.4":TAB(22)"82.4"
174 FORN=0 TO 3:LPRINT TAB(1)X(N,0):TAB(8)X(N,1):TAB(15)X(N,2):TAB(22)X(N,3):NEXTN:POK
  E 14312,13:LPRINT TAB(1)CINT(BG(0)):TAB(8)CINT(BG(1)):TAB(15)CINT(BG(2)):TAB(22)
  CINT(BG(3)):UU=0:GOSUB700
180 PRINT#-1,CINT(BG(0)),CINT(BG(1)),CINT(BG(2)),CINT(BG(3))
182 OUT10,9:STOP:OUT10,10:STOP:J=0
183 INPUT "NUMBER OF PEAK SCANS DESIRED? 1=10 2=20":J
184 JK=J:GOSUB400
191 INPUT "DO YOU WISH ANOTHER 10 PEAK SCANS? 1=YES 2=NO":K
192 T=T+1
193 FORR=0 TO 3:UG*(R)=PG*(R):NEXTR
194 IFK=2 THEN 10
198 GOSUB400
200 IFK=1 THEN 10
400 RT=INP(0):OUT10,9
405 FORP=0 TO 1500:NEXTP
410 L=INP(9)AND15:IFL=0 THEN 410
420 CLS:PRINT "RB ISOTOPE DILUTION RUN - 2 PEAKS - 10 SCANS EACH"
425 PRINT#(145),"RB87":PRINT#(161),"RB85"
430 FORU=0 TO 9:FORV=1 TO 2:OUT10,V+8:PRINT#(50),U+1:GOSUB1000:GOSUB1075:PRINT#(192+64*U
  +16*V),Y(U,V):GOSUB2040:NEXTV,U
433 "DATA FOR TWO RB PEAKS ARE COLLECTED AT MASS 87(OUT10,9) AND 85(OUT10,10)
440 POKE 14312,13:LPRINT TAB(1)"RUN":TAB(4)Q+1:TAB(7)"(PEAKS)":LPRINT "RB87","RB85":
  FORU=0 TO 9:LPRINT Y(U,1),Y(U,2):NEXTU
445 FORU=0 TO 9:PRINT#-1,Y(U,1),Y(U,2):NEXTU
450 IFJK=1 THEN 490

```

```

455 IFJK=2THENGOSUB620 ELSE470
460 IFJ=2THEN400
470 IFJK=1THENGOSUB600
490 RETURN
600 FORP=0TO9:FORO=1TO2:Z(P,O)=Y(P,O):NEXTO,P
605 RETURN
620 FORG=0TO9:FORH=1TO2:W(C,H)=Y(C,H):NEXTH,G:JK=1
625 RETURN
700 IFT=0THEN RETURN
710 Q=Q+1:P#(0)=88.4#:P#(1)=86.4#:P#(2)=84.4#:P#(3)=82.4#:FUMX#=0#:SUMY#=0#:SVY#=0#:
  FVX#=0#:SINX#=0#:TIMX#=0#:UINX#=0#
711 IF J=1 THEN GOSUB1680
712 IFUU=1 THEN GOSUB1560
714 IF J=2 THEN GOSUB1500
720 'SUBROUTINES 1500,1560, AND 1680 CALCULATE BASELINE DATA FOR 10 OR 20 SCANS

735 FORR=0TO3:N#=4#:GOSUB4000:NEXTR
760 GOSUB4030
790 'LINE 800 INTERPOLATES BETWEEN PEAK DATA AND MAKES BACKGROUND CORRECTIONS T
  O ALL REAL AND INTERPOLATED PEAK DATA
791 'LWF 803 CALCULATES THE RB87/RB85 RATIO
800 FORR=0TO8:PK(R)=((Y(R+1,1)-Y(R,1))/2)+Y(R,1)-NV(R):PA(R)=Y(R+1,1)-NT(R):PV(R)=
  Y(R,2)-NS(R):PB(R)=((Y(R+1,2)-Y(R,2))/2)+Y(R,2)-NR(R):NEXTR
803 FORR=0TO8:LM(R)=PK(R)/PY(R):LN(R)=PA(R)/PB(R):NEXTR
804 FORR=1TO9:LO(R)=LO(R-1)+LM(R-1)+LN(R-1):NEXTR
808 LQ=LO(9)/18
810 'LINE 815 CALCULATES THE RB CONCENTRATION(NN) FROM THE AVERAGE 87/85 RATIO(
  LQ)
815 NN=((CS*W*85.4677)/86.8971)*((10.994-(LQ*0.006))/((LQ*0.7217)-0.2783))/WT
835 CLS:PRINT(2),"87/85 RB":PRINT(13),"87/85 RB":FORR=1TO9:PRINT(64*R),LN(R-1):PR
  INT(64*R+14),LM(R-1):NEXTR
838 LPRINT CHR$(10):LPRINT TAB(2)"RB(87/85)":TAB(15)"RB(87/85)":FORR=0TO8:LPRINT TAB
  (1)LN(R):TAB(15)LM(R):NEXTR
843 MEANX(Q)=LQ
844 'NUMBER OF RATIOS USED ="XX
932 Z:PN(R)=(LM(R)-MEANX(Q))/2:NEXTR
945 FORR=1TO9:PL(R)=PL(R-1)+PN(R-1)+PM(R-1):NEXTR
946 PP=(PL(9)/17)(0.5
947 IFO>=2THEN900
948 IF PP<0.0015 THEN XX=18
949 IFPP>0.0015THEN GOSUB1200
950 PRINT(641),"MEAN RB(87/85) RATIO ="LQ:PRINT(675),STD DEV ="PP:PRINT(7
  05),"RB CONCENTRATION ="NN:PRINT(769),"NUMBER OF RATIOS USED IN MEAN CALCULATI
  ON ="XX
952 LPRINT CHR$(10):LPRINT TAB(1)"MEAN RB(87/85) RATIO ="LQ:TAB(32)"STD DEV ="
  PP:LPRINT TAB(1)"RB CONCENTRATION ="NN:LPRINT TAB(1)"NUMBER OF RATIOS USED IN
  MEAN CALCULATION ="XX
900 RB(Q)=RB(Q-1)+MEANX(Q)
905 SEANX=RB(Q)/Q
910 RA(Q)=(MEANX(Q)-SEANX)(2
915 RC=HC+RA(Q)
924 IFO<2THEN936
925 MT=(RC/(Q-1))(0.5
926 IF PP<0.0015 THEN XX=18
927 IF PP>0.0015 THEN GOSUB1200
930 PRINT(640),"TOTAL STATS( )":PRINT(652),Q*10:PRINT(656),")":PRINT(671)
  "10 SCANS ONLY":PRINT(704),"AVERAGE RB(87/85) ="SEANX:PRINT(735),"MEAN RB(87/8
  5 ) ="LQ:PRINT(768),"STD DEV ="MT:PRINT(799),"STD DEV ="PP
931 PRINT(832),"RUBIDIUM CONCENTRATION ="NN:PRINT(833),"NUMBER OF RATIOS USED
  ="XX

```

```

932 LPRINT CHR$(10):LPRINT TAB(1)"TOTAL STATS("TAB(13)Q*10:TAB(17)"SCANS":TAB(22)"
":TAB(25)"10 SCANS ONLY":LPRINT TAB(1)"MEAN RB(87/85)="+SEANX:TAB(25)"MEAN RB(87/
85)="+LQ:LPRINT TAB(1)"STD DEV "+MT:TAB(25)"STD DEV "+PP:LPRINT TAB(1)"NUMBER OF
RATIOS USED="+XX
933 LPRINT TAB(1)"RUBIDIUM CONCENTRATION "+NW
936 IF K=2 THEN 941
937 FOR P=0 TO 9:FOR O=1 TO 2:Y(P,O)=Z(P,O):NEXT O,P
938 K=2:STOP
939 IF K=2 THEN 700
941 IF J=1 THEN 949
942 FOR G=0 TO 9:FOR H=1 TO 2:Y(G,H)=B(G,H):NEXT H,G:J=1+J:STOP
943 IF J=1 THEN 700
949 IF I=1 THEN 990
950 INPUT "DO YOU WISH TO RE-CALCULATE TOTAL STATISTICS EXCLUDING RUNS OUTSIDE
A 99% CONFIDENCE INTERVAL? 1=YES 2=NO":P
951 IF P=2 THEN 990
952 XE=0:W=0:RE=0:ZE=0:X=1:O=0:SP=0
953 FOR R=1 TO 26:NP(R)=0:NEXTR
955 CLS:PRINT(10)."MEANS WITHIN A 99% CONFIDENCE INTERVAL":PRINT(76)."RUN#":P
R INT(92)."RUN#":PRINT(108)."RUN#"
956 LPRINT CHR$(10):LPRINT TAB(1)"MEANS WITHIN A 99% CONFIDENCE INTERVAL"
960 FOR R=1 TO Q
965 IF MEANX(R)>=(SEANX-0.002)AND MEANX(R)<=(SEANX+0.002) THEN GOSUB 3000:
970 NEXTR
975 IF R>1 THEN GOSUB 3030
980 PRINT(644)."MEAN(87/86)="+ZEANX:PRINT(680)."STD DEV="+PT
982 LPRINT CHR$(10):LPRINT TAB(1)"MEAN(87/86)="+ZE:TAB(14)ZE:TAB(25)"STD DEV="+TA
B(33)PT
990 RETURN
998 'SUBROUTINES 1000,1070,1075 CONVERT THE BINARY SIGNAL TO DIGITAL FORM
1000 L=INP(9) AND 15:IF L=0 THEN 1000
1010 A=INP(0) AND 15
1020 B=INP(1) AND 15
1030 C=INP(2) AND 15:IF C=15 THEN C=0
1040 D=INP(3) AND 15:IF D=15 THEN D=0
1050 E=INP(4) AND 15:IF E=15 THEN E=0
1060 F=INP(5) AND 15:IF F=15 THEN F=0
1065 RETURN
1070 X(U,M)=A+10*B+10(2*C+10(3*D+10(4*E+10(5*F
1072 RETURN
1075 Y(U,V)=A+10*B+10(2*C+10(3*D+10(4*E+10(5*F
1080 RETURN
1099 STOP
1200 FOR F=1 TO 8:NU(F)=LN(F-1):NU(F+8)=LN(F-1):NEXT F
1205 TT=1
1206 FOR F=1 TO 25:NP(F)=0:NEXTF
1209 XX=0:VC=0:DR=0:MR=0
1210 FOR F=1 TO 25
1212 IF NU(F)<=(MEANX(TT)+0.002)AND NU(F)>=(MEANX(TT)-0.002) THEN GOSUB 1300:
1214 NEXTF
1220 IF I>1 THEN 1320
1300 XI=XI+1
1305 NP(XI)=NU(F)
1310 DR=DR+NP(XI)
1312 MR=DR/XI
1315 RETURN
1320 FOR R=1 TO XX:VC=VC+(NP(R)-MR)(2):NEXTR
1321 IF XX>15 THEN 1332
1322 IF Q=1 THEN 1350
1323 TT=(Q-1):XX=XX+1
1324 IF A=1 THEN 1206
1327 IF Q=1 THEN 1332
1332 MEANX(R)=MR
1350 RETURN

```



```

1500 UU=1
1530 FORR=OTO3:MG#(R)=PG#(R):NG#(R)=((PG#(R)-UG#(R))/2)+UG#(R):NEXT R
1560 FORR=OTO3:MG#(R)=NG#(R):NG#(R)=UG#(R):NEXT R
1570 RETURN
1690 FORR=OTO3:MG#(R)=UG#(R):MG#(R)=PG#(R):NEXT R
1690 RETURN
1700 IF K=1 THEN 1850
1710 IF UU=1 THEN 1750
1720 FORR=OTO3:MG#(R)=NG#(R):NG#(R)=((PG#(R)-UG#(R))/3)+UG#(R):NEXT R
1730 UU=1
1740 IF UU=1 THEN 1860
1750 FORR=OTO3:MG#(R)=MG#(R):NG#(R)=UG#(R):NEXT R
1760 IF UU=1 THEN 1860
1850 FORR=OTO3:MG#(R)=PG#(R):NG#(R)=((PG#(R)-UG#(R))*2)/3+UG#(R):NEXT R
1860 RETURN
2038 *SUBROUTINES 2040,2100,2130, AND 2080 TEST FOR ANOMALOUS PEAK AND BACKGROU
ND DATA AND RE-COLLECTS DATA IF NECESSARY
2040 IF U<1 THEN RETURN
2050 IF Y(U-1,V)<(Y(U,V)-0.15*Y(U,V)) THEN 2080
2060 IF Y(U-1,V)>(Y(U,V)-0.15*Y(U,V)) THEN 2080
2070 RETURN
2080 U=U-1
2085 V=0
2090 RETURN
2095 IF N<1 THEN RETURN
2100 IF X(N-1,M)<(X(N,M)-0.15*X(N,M)) THEN 2130
2110 IF X(N-1,M)>(X(N,M)+0.15*X(N,M)) THEN 2130
2120 RETURN
2130 N=N-1
2140 M=-1
2150 RETURN
3000 h=h+1
3009 UT(h)=R
3010 MP(h)=MEANX(R)
3012 O=O+1
3013 IF O=4 THEN GOSUB 3060
3014 PRINT3(X*64+(O*16-4)+64),R:PRINT3(X*64+O*16+64),MEANX(R)
3015 IF SP<4 THEN 3018
3016 POKE 14312,13:SP=0
3018 LPRINT R" "MEANX(R),:
3019 SP=SP+1
3020 IE=XE+MP(h)
3025 ZE=XE/h
3026 RETURN
3030 FORR=110h:RE=XE+((MP(h)-ZE)(2)):NEXT R
3035 IF h*(h-2)<1 THEN 3050
3040 PT=(RE/(h*(h-1)))(0.5
3045 SEANX=ZE
3050 RETURN
3060 O=1
3070 X=X+1
3080 RETURN
4000 SUMY#=SUMY#+MG#(R):FUMX#=FUMX#+(MG#(R)*P#(R)):SVY#=SVY#+MG#(R):FVX#=FVX#+(MG#(R)
*P#(R)):SIMX#=SIMX#+P#(R):TIMX#=TIMX#+(P#(R)(2):UIMX#=SIMX#(2
4010 *SUBROUTINE 4000 CALCULATES BACKGROUND VALUES UNDER 87 AND 85 PEAKS BY REG
RESSING THE FOUR BACKGROUND DATA POINTS AND APPLYING THE APPROPRIATE INTERPOLATI
ON

```

```
4020 SLPX=(FUMX#-(SIX#*SOMY#/N#))/(TIMX#-(UIMX#/N#));VLPX=(FVX#-(SIX#*SVY#/N#))
/ (TIMX#-(UIMX#/N#));TNTX=((SIX#*FUMX#)-(SUMY#*TIMX#))/(UIMX#-(N#*TIMX#));TVTX=(
(SIX#*FVX#)-(SVY#*TIMX#))/(UIMX#-(N#*TIMX#))
4025 RETURN
4030 FORR=1 TO 3 STEP 2: B(R)=SLPX*(88-R)+TNTX:KV(R)=VLPX*(88-R)+TVTX:VA(R)=(B(R)-KV(R))/
18:NEXTR
4040 FORR=0 TO 8:NV(R)=VA(1)*(R*2+1)+NV(1):NT(R)=VA(1)*(R*2+2)+NV(1):NR(R)=VA(3)*(R*2+1
)+NV(3):NS(R)=VA(3)*(R*2+2)+NV(3):NEXTR
4050 RETURN
```

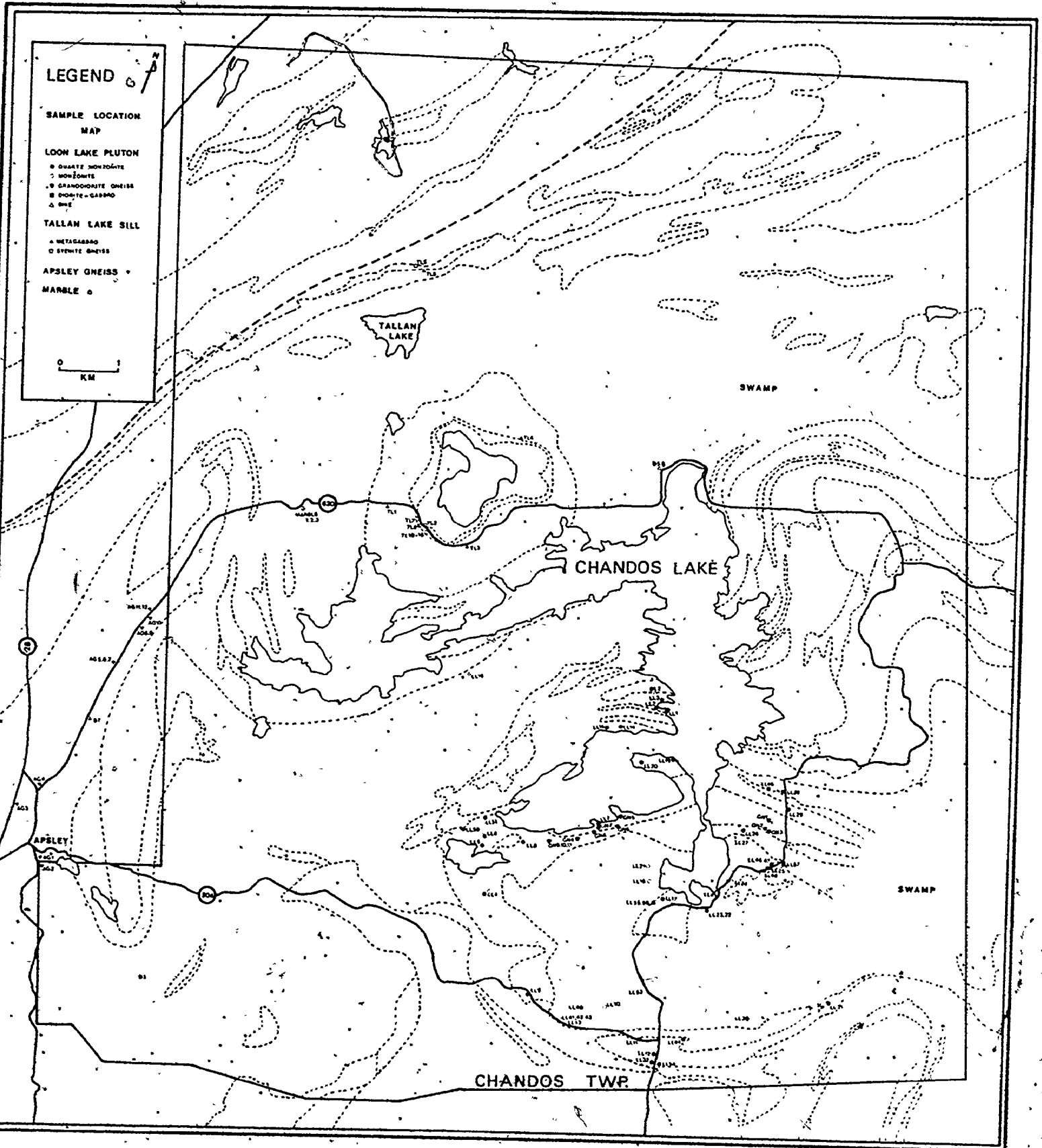


FIGURE A.1